ALTERNATIVE DECOUPLINGS OF THE ELECTRON PROPAGATOR

By

GREGORY J. BORN

A DISSERTATION PRESENTED TO THE GRADUATE COUNCIL OF
THE UNIVERSITY OF FLORIDA
IN PARTIAL FULFILLMENT OF THE REQUIREMENTS FOR THE
DEGREE OF DOCTOR OF PHILOSOPHY

UNIVERSITY OF FLORIDA

1979

ACKNOWLEDGMENTS

After twenty-one years of formal education which is culminating with this dissertation, it is impossible to individually thank every teacher who assisted me in this pursuit. The largest debt of gratitude however, is owed to my dissertation supervisor, Professor Yngve Öhrn, whose constructive criticism and constant encouragement has guided the direction of this research and my graduate education. His generous financial assistance over the years has also been greatly appreciated.

I would like to thank Professor Per-Olov Löwdin for his stimulating series of lectures in quantum theory as well as the national and international contacts he has made available to me and the other members of the Quantum Theory Project through the invitation of visiting scientists and the organization of the Sanibel Symposia. My attendance at the Summer School in Quantum Theory held in Uppsala, Sweden, and Dalseter, Norway (August 1976), was made possible by monetary awards secured by Prof. Löwdin for which I am also greatly appreciative.

Next I would like to thank Professor Jack Sabin, who supervised me during some preliminary investigations, and the other members of my supervisory committee for contributing their time and for occasional letters of recommendation.

Without the friendships and intellectual stimulation of other members of the Quantum Theory Project whom I have known, my graduate education would not have been as enjoyable or as rewarding. To several people I am indebted for the use of various computer subroutines which I gratefully acknowledge.

It is with regret that I must posthumously acknowledge my indebtedness to Professor Boris Muslin. Prof. Muslin supervised my undergraduate research in quantum theory at Southern Illinois University and was largely responsible for guiding me into this field.

I would finally like to thank my parents for their constant encouragement and financial assistance.

Special thanks are owed to Miss Brenda Foye for her painstaking efforts in typing this manuscript.

I also wish to take this opportunity to acknowledge the Northeast Regional Data Center of the State University System of Florida for the use of their facilities to obtain the numerical results presented here and the American Institute of Physics for permission to reproduce Figure 1 and Appendix 1 from the paper by G. Born, H. A. Kurtz, and Y. Öhrn in the Journal of Chemical Physics, Vol. 68, p. 74 (1978).

TABLE OF CONTENTS

TABLE OF CONTENTS (Continued)

LIST OF TABLES

LIST OF TABLES (Continued)

LIST OF FIGURES

Abstract of Dissertation Presented to the Graduate Council
of the University of Florida in Partial Fulfillment of the
Requirements for the Degree of Doctor of Philosophy

ALTERNATIVE DECOUPLINGS OF THE ELECTRON PROPAGATOR

By

Gregory J. Born

June 1979

Chairman: N. Yngve Öhrn
Major Department: Chemistry

Several alternative decouplings of the electron propagator are investigated in this dissertation in an attempt to derive more accurate and more tractable computational schemes for extracting the physical information contained in the electron propagator. When the electron propagator is defined as a single-time Green's function, the decoupling approximation and the choice of reference state average are shown to be independent approximations, and the use of uncorrelated, Hartree-Fock reference states is advocated. The derivation of each decoupling approximation utilizes the superoperator formalism and emphasizes elementary algebraic manipulations. In Chapter 1, operator product decouplings are reviewed and critically discussed. In Chapter 2, the moment conserving decouplings which consist of Pade' approximants to the propagator moment expansion are investigated. In Chapter 3, a partitioning of the superoperator Hamiltonian is invoked, and a perturbation expansion of the superoperator resolvent is developed. This

development leads straightforwardly to the derivation of the Dyson equation and permits an identification of wave and reaction superoperators. Two types of diagram conserving decouplings are then examined, and equivalences with the diagrammatic expansion method are demonstrated. Finally in Chapter 4, renormalized decouplings are considered, and the two particle-one hole, Tamm-Dancoff approximation is specifically derived and investigated. In each of the first four chapters, the decoupling approximations are evaluated on the basis of computational applications in which the propagator poles are compared to experimentally determined ionization energies for several molecules. In order to avoid a possible bias with this evaluation criterion, the quality of the Feynman-Dyson amplitudes is examined in Chapter 5 via the calculation of relative photoionization intensities. The four decoupling approximations are finally summarized as various approximations to the wave and reaction superoperators, and several extensions of these investigations are proposed.

INTRODUCTION

Since subatomic particles are beyond the limit of human sensory perception, our knowledge of atomic structure is based on the interpretation of measurements with auxiliary probes. The accumulation and interpretation of data from these types of measurements have led to the conception and axiomatization of quantum theory. Using the calculus of this theory, quantum mechanics, there is evidence to believe that it is possible, at least in principle, to calculate the statistical result of any experimental measurement. Unfortunately, the mathematical complexity of this calculus precludes exact solutions for all but a few, relatively trivial applications; consequently, the predictive value of the theory is limited. Owing to this limitation, one aspect of current theoretical research involves the formulation and evaluation of accurate mathematical approximations which are relevent to the interpretation of specific experiments.

With the development of photoelectron spectroscopy (Turner et al., 1970, Siegbahn et al., 1969), photoionization has become an extremely useful probe of atomic and molecular structure and has stimulated much theoretical interest (Cederbaum and Domcke, 1977, and references therein). In the photoionization experiment, light is shone on an atomic or molecular sample and the kinetic energy of the ionized electrons or photoelectrons which are ejected is then analyzed. From energy conservation, the binding energies of the photoelectrons may be deduced.

An ab initio, theoretical interpretation of photoelectron spectra requires the calculation of ionization energies. These calculations reflect fundamental assumptions about the complex nature of the many-electron interactions that occur in atoms and molecules and may be performed at various levels of sophistication. One conceptually simple scheme is the Hartree-Fock self-consistent field (HF-SCF) method (see e.g. Pilar, 1968). In this method, an orbital energy is calculated for each electron in an N-electron system by assuming that that electron interacts only with an average electron density formed by the remaining N-1 electrons. By thus averaging out the instantaneous electron-electron interactions, the original N-electron problem is reduced to N one-electron problems. The negative of the orbital energies obtained in this calculation can then be related to ionization energies via Koopmans' theorem (Koopmans, 1933).

Ionization energies obtained at the Hartree-Fock level of approximation are rarely accurate and occasionally predict even the wrong sequence of ionization. In order to obtain more accurate ionization energies, the electron-electron interactions must be treated more realistically. In the Hartree-Fock approximation, the N-1 electrons of the ion state are assumed to be "frozen" at the same energies they had in the ground state. Conceptually, each electron screens to some extent the electrostatic attraction between the positively charged nuclei and all the other electrons in the system. As can be easily rationalized, this screening is most effective for deep-lying or core electrons which have a high probability density near the nucleus than for more diffuse, valence electrons. Nevertheless, if one electron is ionized, all the others should experience a stronger nuclear attraction and will contract

producing a lower total energy. This rearrangement defines the relaxation energy, and it may be easily incorporated in the ionization energy calculation. Performing separate Hartree-Fock calculations for both the ground and ion states and obtaining a total energy by adding orbital energies with corrections for the overcounting of interelectronic repulsions, an improved ionization energy can be obtained by subtracting total energies. This level of approximation is known as the ΔE(SCF) method (Bagus, 1965) and generally yields reliable core electron ionization energies.

The remaining discrepency between the ΔE(SCF) ionization energies and the ionization energies obtained from the exact solution of a nonrelativistic, many-electron formulation can be defined as the correlation energy. This correction arises from the tendency of any pair of electrons in an atom or molecule to correlate their motion so as to minimize the electron-electron repulsion. Electron correlation can be conceptualized as various virtual scattering events between bound electrons in both the N- and (N-1)-electron systems. The simplest of these virtual processes is a particle-hole excitation in which one bound electron absorbs a virtual photon emitted by another electron and is excited from its original Hartree-Fock orbital to a more diffuse orbital of higher energy. A hole or vacancy is simultaneously created and propagates in the system. At some later time, the excited electron may decay reemitting the virtual photon which may then be reabsorbed by the first electron. Adopting the convention that holes propagate backwards in time while electrons propagate forward in time, a particle-hole excitation in the (N-1)-electron ion state can be diagrammatically represented as

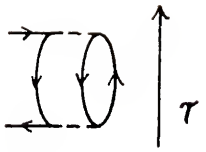

where the dotted lines represent the virtual photon exchanges. Although diagrams of this type represent quasi-classical, virtual processes which are not experimentally observable, they do provide a conceptual model and, as we will later see in Chapter 3, categorize specific algebraic expressions that will be derived to calculate correlation energy corrections. Finally, it should be noted that since the electron motions will be correlated to different extents in the N-electron ground state and (N-1)-electron ion states, it is not possible to predict, a priori, the effect of this correction on the ionization energies (see Fig. 1).

One many-electron formulation which provides a systematic procedure for incorporating both relaxation and correlation corrections into the calculation of ionization energies and which is the basis of this investigation, is the non-relativistic, single-particle Green's function or electron propagator (Linderberg and Öhrn, 1973). This method has the advantage of yielding ionization energies directly unlike other many-electron formulations which necessitate the total energy calculation for both ground and ion states and which yield the ionization energy as the difference. In the latter methods, significant loss of accuracy is inherent in the subtraction of two, nearly equal total energies to obtain a much smaller, ionization energy. Care must also be taken to avoid disparate levels of approximating electron correlation in the calculation of each different state.

Figure 1. The relaxation error (r) and the correlation error (c) for each of the principal ionizations in the water molecule. The numbers are estimated from the experimental results of Siegbahn *et al.* (1969) and from the ΔE(SCF) results reported by Goscinski *et al.* (1975).

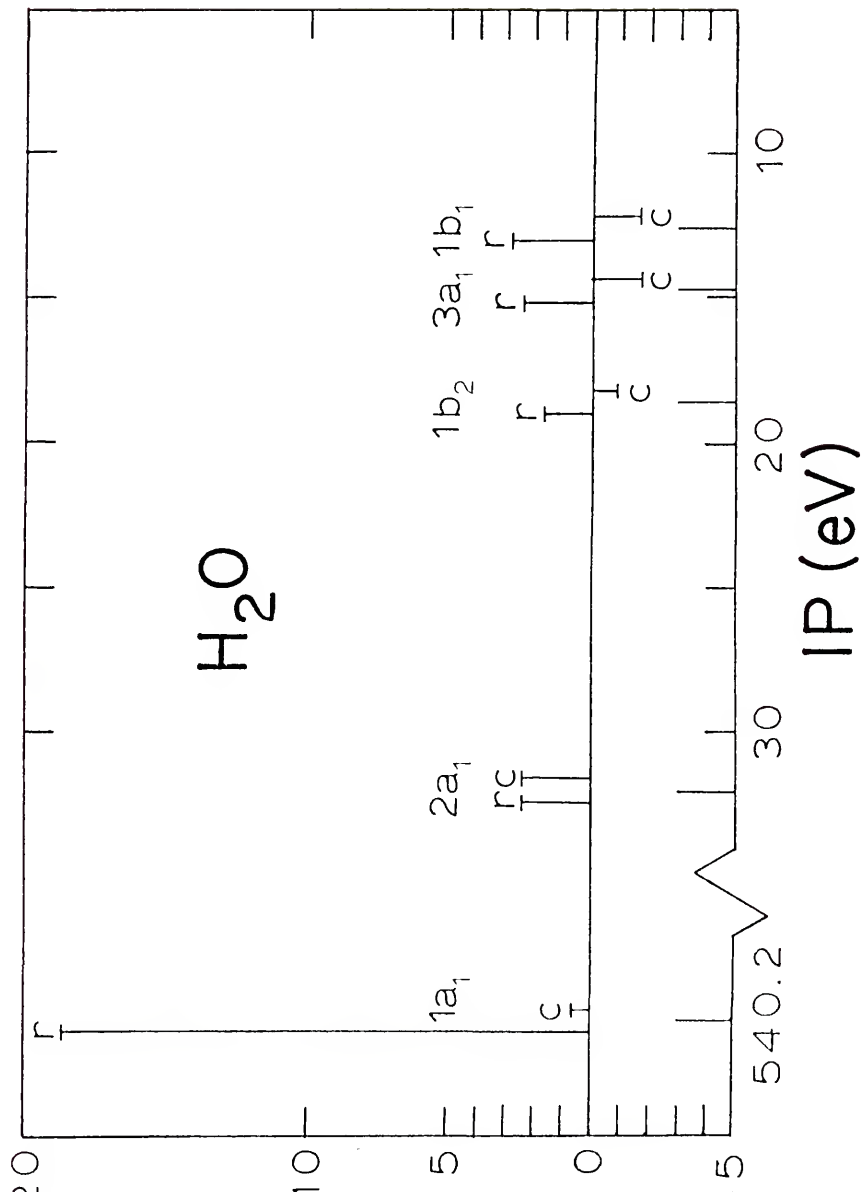
H2O
ERROR (eV)
IP (eV)
20
10
5
0
-5
10
20
30
540.2
1a1
2a1
1b2
3a1
1b1
r
c
rc

The electron propagator can be written as a function of the space and spin coordinates of one electron and of a complex energy variable. For each bound electron, this function describes mathematically all of the complicated many-electron interactions between that electron and the remaining N-1 electrons. This function also contains information about the interaction of an additional electron with the N bound electrons if this electron were to be added to the system in any of several possible orbitals. In a discrete basis representation of the electron propagator, this information manifests itself as simple poles or singularities at those values along the real energy axis which correspond to electron ionization energies or electron affinities, that is, electron detachment or attachment, respectively. The residues at these poles yield the single-particle reduced density matrix from which the N-electron ground state average of any one-electron operator may be calculated or which may be related to transition probabilities for electron detachment or attachment provided some description of the removed or added electron is included.

The electron propagator can be calculated in several ways. The procedure adopted here is derived from the electron propagator equation of motion, but one aspect of this investigation will demonstrate the formal equivalence between this method and the diagrammatic expansion technique. The equation of motion relates the electron propagator to the more complicated two-particle propagator. This two-particle propagator also satisfies an equation of motion which relates it to the three-particle propagator, and so on. This hierarchy of equations finally terminates with the N-particle propagator, but in order to make any practical calculation, this hierarchy must be approximated at some lower level, generally by expressing an M-particle propagator in terms of an

(M-1)-particle propagator. This approximation is called decoupling the equations of motion and is not unique. The accuracy of calculated ionization energies and the computational effort in obtaining them depend critically on the decoupling. This investigation proposes and evaluates several alternative methods.

In Chapter 1, the electron propagator is formally defined, and its equation of motion is derived. After an introduction of the superoperator formalism, the electron propagator is approximated by an inner projection, and the decoupling problem is studied in terms of the selection of an inner projection manifold. The remainder of this chapter discusses the computational procedure for solving the propagator equations and presents a critical evaluation of the operator product decoupling.

Chapter 2 describes some general aspects of the Pade' approximant method and its application to the calculation of the electron propagator. Owing to the conservation of various moment matrices in the propagator equation of motion these decouplings are known as moment conserving decouplings (Goscinski and Lukman, 1970). Numerical results obtained from the [1,0] and [2,1] Pade' approximants are presented and discussed.

A partitioning of the superoperator Hamiltonian and a perturbation expansion of the superoperator resolvent in the operator space is developed in Chapter 3. A superoperator Dyson equation is derived and wave and reaction superoperators are identified in analogy with ordinary resolvent operator techniques. Truncations of the wave superoperator operating on simple annihilation and creation operators are shown to yield inner projection manifolds that result in Pade' approximants to the self-energy. These Pade' approximants conserve various orders of the perturbation expansion for the self-energy and are therefore

categorized as diagram conserving decouplings. Two approximations based on this decoupling scheme are discussed and evaluated.

Chapter 4 is devoted to renormalized decouplings. These decouplings sum certain types of self-energy diagrams to all orders. The two-particle, one-hole Tamm-Dancoff approximation (2p-h TDA), which sums all ring and ladder diagrams, is explicitly derived and discussed in terms of the superoperator formalism. The diagonal 2p-h TDA previously proposed by other authors (Cederbaum, 1974, Purvis and Öhrn, 1974) is re-examined and is shown to neglect certain diagonal contributions. Both approximations are analyzed diagrammatically, and numerical results are presented and discussed.

The evaluation of each decoupling approximation in the first four chapters is ultimately based on a comparison of propagator poles to experimental ionization energies. Chapter 5, on the other hand, attempts to corroborate this evaluation criterion by an examination of the quality of the Feynman-Dyson amplitudes. This is indirectly accomplished via the calculation of relative photoionization intensities and their comparison with experimental data. The requisite equations for the photoionization cross-section are derived in terms of the Feynman-Dyson amplitudes, and the most critical approximations are discussed. Finally, numerical results are presented and are also discussed.

CHAPTER 1
OPERATOR PRODUCT DECOUPLINGS

1.1 Definition, Spectral Representation, and Equation of Motion of the Electron Propagator

The electron propagator is most commonly defined as a double-time Green's function which involves an exact N-electron ground state average of a time-ordered product of electron field operators, $\psi(x,t)$ and $\psi^{\dagger}(x',t')$ (Linderberg and Öhrn, 1973). These field operators are generally expressed in the Heisenberg representation,

$$\psi(x,t) = \exp(iHt)\ \psi(x,0)\exp(-iHt) \tag{1.1}$$

and are functions of the combined space-spin and time coordinates of the electrons. The operator, H, in the exponentials is the N-electron Hamiltonian. The field operators $\psi(x,t)$ and $\psi^{\dagger}(x',t')$ have the property of annihilating and creating, respectively, an electron at the space-spin and time coordinates, x,t (x',t'). Letting $|\Psi_i^N\rangle$ denote an exact eigenstate of the N-electron Hamiltonian, $|\Psi_i^{N-1}\rangle$ and $|\Psi_i^{N+1}\rangle$ denoting exact eigenstates of the (N-1)- and (N+1)-electron, ion Hamiltonians, these properties are expressed as

$$\psi(x,t)|\Psi_i^N\rangle = \sum_j c_j \exp\{-i(E_i^N - E_j^{N-1})t\}|\Psi_j^{N-1}\rangle \tag{1.2}$$

and

$$\psi^{\dagger}(x',t')|\Psi_i^N\rangle = \sum_j c_j \exp\{-i(E_j^{N+1} - E_i^N)t'\}|\Psi_j^{N+1}\rangle\ . \tag{1.3}$$

If the N-electron Hamiltonian is time independent, it is easy to show that the double-time Green's function depends only on the time difference, t-t' (Fetter and Walecka, 1971). In all practical calculations, however, this definition proves to be a severe restriction since the exact N-electron ground state is rarely known and an approximate ground state average is usually employed. With an inexact ground state average, the electron propagator will depend on both t and t'. To avoid this restriction, it is possible to define the electron propagator as a single-time Green's function by choosing t' equal to zero (Simons, 1976),

$$\begin{aligned} \langle\langle \psi^{\dagger}(x',0);\, \psi(x,t) \rangle\rangle &= -i\theta(t)\langle \psi(x,t)\, \psi^{\dagger}(x',0)\rangle \\ &\quad + i\theta(-t)\langle \psi^{\dagger}(x',0)\, \psi(x,-t)\rangle \, . \end{aligned} \tag{1.4}$$

This definition insures the dependence on only the time difference even when the ground state average is inexact. The brackets, $< \ldots >$, in Eq.(1.4) represent an average which may be either a pure-state average or an ensemble average,

$$< \ldots > = \sum_{\kappa} P_{\kappa} \langle \kappa | \ldots | \kappa \rangle \, . \tag{1.5}$$

To elucidate the analytic properties of the electron propagator, it is convenient to derive the spectral or Lehman representation (Linderberg and Öhrn, 1973). This representation is obtained by first expanding the eigenstates, $|\kappa>$, in terms of the exact N-electron eigenstates, $|\Psi_i^N>$,

$$|\kappa\rangle = \sum_{i} c_{\kappa i} |\Psi_i^N\rangle \, . \tag{1.6}$$

Using resolutions of the identity in terms of the exact (N-1)- and (N+1)-electron eigenstates, Eq.(1.4) can be written:

$$\langle\langle\psi^{\dagger}(x',0);\ \psi(x,t)\rangle\rangle = \sum_{\kappa}\ \sum_{i,j,k} P_{\kappa}\ c_{\kappa i}\ c_{\kappa j}\ \{-i\theta(t)\langle\Psi_i^N|\psi(x,t)|\Psi_k^{N+1}\rangle$$

$$\times\ \langle\Psi_k^{N+1}|\psi^{\dagger}(x',0)|\Psi_j^N\rangle + i\theta(-t)\langle\Psi_i^N|\psi^{\dagger}(x',0)|\Psi_k^{N-1}\rangle\langle\Psi_k^{N-1}|\psi(x,-t)|\Psi_j^N\rangle\}\ . \quad (1.7)$$

Explicitly introducing the time dependence of the field operators, Eq.(1.7) becomes

$$\langle\langle\psi^{\dagger}(x',0);\ \psi(x,t)\rangle\rangle = \sum_{\kappa}\ \sum_{i,j,k} P_{\kappa}\ c_{\kappa i}\ c_{\kappa j}$$

$$\times\ \{-i\theta(t)\langle\Psi_i^N|\psi(x,0)|\Psi_k^{N+1}\rangle\langle\Psi_k^{N+1}|\psi^{\dagger}(x',0)|\Psi_j^N\rangle\exp[-i(E_k^{N+1}-E_i^N)t]$$

$$+\ i\theta(-t)\langle\Psi_i^N|\psi^{\dagger}(x',0)|\Psi_k^{N-1}\rangle\langle\Psi_k^{N-1}|\psi(x,0)|\Psi_j^N\rangle\exp[i(E_j^N-E_k^{N-1})t]\}\ . \quad (1.8)$$

Since the calculation of ionization energies (electron affinities) from the electron propagator will be treated as a transition between stationary states of the N-electron ground state and N-1 (N+1)-electron ion states, it is convenient to Fourier transform Eq.(1.8) into an energy representation,

$$\langle\langle\psi^{\dagger}(x');\ \psi(x)\rangle\rangle_E = \int_{-\infty}^{\infty}\langle\langle\psi^{\dagger}(x',0)\psi(x,t)\rangle\rangle\exp(iEt)dt \quad (1.9)$$

which yields the spectral representation:

$$\langle\langle\psi^{\dagger}(x');\ \psi(x)\rangle\rangle_E = \lim_{\eta\to 0^+}\ \sum_{\kappa}\ \sum_{i,j,k} P_{\kappa}\ c^*_{\kappa i}\ c_{\kappa j}\left\{\frac{f_{ik}(x)f^*_{kj}(x')}{E-(E_k^{N+1}-E_i^N)+i\eta}\right.$$

$$\left.+\ \frac{g_{ik}(x)g^*_{kj}(x')}{E-(E_j^N-E_k^{N-1})-i\eta}\right\} \quad (1.10)$$

where $$f_{ik}(x) = \langle \Psi_i^N | \psi(x,0) | \Psi_k^{N+1} \rangle \tag{1.11}$$

and $$g_{ik}(x') = \langle \Psi_i^N | \psi^\dagger(x',0) | \Psi_k^{N-1} \rangle \tag{1.12}$$

are referred to as the Feynman-Dyson amplitudes. From Eq.(1.10) it is observed that the electron propagator has simple poles along the real energy axis corresponding to the difference between exact eigenvalues of the N-electron Hamiltonian and the $(N\pm1)$-electron Hamiltonians. The poles of this function, therefore, have a physical interpretation as ionization energies and electron affinities.

Since atomic and molecular computations are most conveniently performed in a Hilbert space, we introduce a complete, orthonormal set of one-electron spin orbitals, $\{u_i(x)\}$. In this basis, the electron field operators are represented by the expansion,

$$\psi(x,t) = \sum_i a_i(t) u_i(x) \tag{1.13}$$

which, with the expansion of the adjoint, defines the spin orbital annihilation and creation operators, $a_i(t)$ and $a_j^\dagger(0)$. At equal times, these operators satisfy the usual anti-commutation relations,

$$[a_i, a_j^\dagger]_+ = \delta_{ij} \tag{1.14}$$

$$[a_i^\dagger, a_j^\dagger]_+ = [a_i, a_j]_+ = 0 \tag{1.15}$$

In this discrete representation, the causal electron propagator can be written

$$\langle\langle \psi^\dagger(x',0);\ \psi(x,t) \rangle\rangle = \sum_{i,j} u_j^*(x') \langle\langle a_j^\dagger(0);\ a_i(t) \rangle\rangle u_i(x) \tag{1.16}$$

where

$$\langle\langle a_j^\dagger(0);\ a_i(t)\rangle\rangle = -i\theta(t)\langle a_i(t)a_j^\dagger(0)\rangle + i\theta(-t)\langle a_j^\dagger(0)a_i(-t)\rangle\ . \qquad (1.17)$$

Although a computational scheme for obtaining ionization energies and electron affinities could now be established from the spectral resolution, it is more convenient to develop a scheme based on the equation of motion (Linderberg and Öhrn, 1973),

$$i\frac{\partial}{\partial t}\langle\langle a_j^\dagger(0);\ a_i(t)\rangle\rangle = \delta(t)\langle a_i(t)a_j^\dagger(0)+a_j^\dagger(0)a_i(-t)\rangle + \langle\langle a_j^\dagger(0);\ [a_i(t),H]_-\rangle\rangle, \qquad (1.18)$$

which follows directly from Eq.(1.17). The quantity $\langle\langle a_j^\dagger(0);\ [a_i,H]_-\rangle\rangle$ is a two-particle propagator, and the N-electron Hamiltonian appearing in the commutator has the following Hilbert space representation:

$$H = \sum_{r,s} h_{rs}a_r^\dagger a_s + \tfrac{1}{4}\sum_{r,r',s,s'}\langle rr'||ss'\rangle\, a_r^\dagger a_{r'}^\dagger a_{s'}a_s \qquad (1.19)$$

where

$$h_{rs} = \int u_r^*(1)[-\tfrac{1}{2}\nabla^2(1) - \sum_\alpha \frac{Z\alpha}{r_{1\alpha}}]u_s(1)d\tau_1 \qquad (1.20)$$

and

$$\langle rr'||ss'\rangle = \iint u_r^*(1)u_{r'}^*(2)r_{12}^{-1}(1-P_{12})u_s(1)u_{s'}(2)d\tau_1 d\tau_2 \qquad (1.21)$$

With a notation similar to that used in Eq.(1.9), the energy transforms of the various quantities in Eq.(1.18) can be defined, e.g.

$$\langle\langle a_j^\dagger;\ a_i\rangle\rangle_E = \int_{-\infty}^{\infty}\langle\langle a_j^\dagger(0);\ a_i(t)\rangle\rangle \exp(iEt)dt\ . \qquad (1.22)$$

Substituting the inverse transforms:

$$i\frac{\partial}{\partial t}\langle\langle a_j^\dagger(0);a_i(t)\rangle\rangle = \frac{1}{2\pi}\int_{-\infty}^{\infty} E\langle\langle a_j^\dagger;\ a_i\rangle\rangle_E \exp(-iEt)dE, \qquad (1.23)$$

$$\delta(t)\langle a_i(t)a_j^\dagger(0)+a_j^\dagger(0)a_i(-t)\rangle = \frac{1}{2\pi}\int_{-\infty}^{\infty}\langle[a_i,a_j^\dagger]_+\rangle\exp(-iEt)dE, \qquad (1.24)$$

and

$$\langle\langle a_j^\dagger(0);\ [a_i(t),H]_-\rangle\rangle = \frac{1}{2\pi}\int_{-\infty}^{\infty}\langle\langle a_j^\dagger(0);\ [a_i(t),H]_-\rangle\rangle_E\exp(-iEt)dE, \qquad (1.25)$$

into Eq.(1.18), we obtain

$$\frac{1}{2\pi}\int_{-\infty}^{\infty}\{E\langle\langle a_j^\dagger;a_i\rangle\rangle_E - \langle[a_i,a_j^\dagger]_+\rangle - \langle\langle a_j^\dagger;[a_i,H]_-\rangle\rangle_E\}\exp(-iEt)dE = 0. \qquad (1.26)$$

From the general properties of Fourier transforms, it can be shown (Morse and Feshbach, 1953) that Eq.(1.26) implies

$$E\langle\langle a_j^\dagger,a_i\rangle\rangle_E = \langle[a_i,a_j^\dagger]_+\rangle + \langle\langle a_j^\dagger;[a_i,H]_-\rangle\rangle_E . \qquad (1.27)$$

which represents the energy transform of the equation of motion. The iteration of this equation yields N coupled equations relating the single-particle (electron) propagator to each of the higher-particle propagators. Successive substitution of these more complicated propagators back into Eq.(1.27) yields

$$\langle\langle a_j^\dagger;a_i\rangle\rangle_E = E^{-1}\langle[a_i,a_j^\dagger]_+\rangle + E^{-2}\langle[[a_i,H]_-,a_j^\dagger]_+\rangle + E^{-3}\langle[[[a_i,H]_-,H]_-,a_j^\dagger]_+\rangle + \ldots . \qquad (1.28)$$

1.2 The Superoperator Notation and Inner Projection Technique

The use of superoperators has antecedents in the work of Zwanzig (1961) and Banwell and Primas (1963) in statistical physics and was introduced into atomic and molecular propagator theory by Goscinski and Lukman (1970). As a notational simplification, the definition of a superoperator

Hamiltonian and identity, $\hat{H}$ and $\hat{I}$, provides a convenient representation of the nested commutators appearing in Eq.(1.28). More formally, this notation provides a connection with the time-independent resolvent methods introduced into many-body theory by Hugenholtz (1957).

The superoperator Hamiltonian and identity are defined to operate on the spin orbital annihilation and creation operators through the relations

$$\hat{H}a_i = [a_i,H]_- \tag{1.29}$$

and

$$\hat{I}a_i = a_i \ . \tag{1.30}$$

Powers of the superoperator Hamiltonian are defined by successive application of this superoperator, i.e.

$$\hat{H}^2a_i = \hat{H}[a_i,H]_- = [[a_i,H]_-,H]_- , \tag{1.31}$$

and will always yield linear combinations of odd (Fermion-like) products of the simple field operators, a_i and $a_j^\dagger$. This set of all Fermion-like operator products, $\{X_i\}$, forms a linear space and supports a scalar product defined by

$$(X_j|X_i) = \mathrm{Tr}\{\rho[X_i,X_j^\dagger]_+\} \tag{1.32}$$

where ρ is a normalized, but otherwise arbitrary, density operator corresponding to the N-electron ground state average of the electron propagator.

Using the preceding definitions and notation, Eq.(1.28) can be rewritten as

$$\langle\langle a_j^\dagger; a_i \rangle\rangle_E = G(E)_{ij} = E^{-1}(a_j|a_i) + E^{-2}(a_j|\hat{H}a_i) + E^{-3}(a_j|\hat{H}^2a_i) + \ . \ . \ . \ . \tag{1.33}$$

Collecting all annihilation operators in a row matrix and all creation operators in a column and formally summing the expansion in Eq. (1.33), the matrix equation of motion for the electron propagator becomes:

$$\underline{G}(E) = (\underline{a}|(E\hat{I}-\hat{H})^{-1}\underline{a}). \tag{1.34}$$

The superoperator resolvent in Eq. (1.34) can now be represented in closed form by a matrix inverse using the inner projection technique (Löwdin, 1965, Pickup and Goscinski, 1973). Introducing a projection operator,

$$\hat{0} = |\underline{f})(\underline{f}|\underline{f})^{-1}(\underline{f}| \ , \tag{1.35}$$

where $\hat{0}^2 = \hat{0}$ and $\hat{0}^+ = \hat{0}$, the inner projection of a positive definite, self-adjoint operator, A, is given by

$$A' = A^{\frac{1}{2}}\,\hat{0}\,A^{\frac{1}{2}} \ ; \quad A > 0 \ . \tag{1.36}$$

Making the substitution

$$|\underline{f}) = A^{-\frac{1}{2}}|\underline{h}) \ , \tag{1.37}$$

the inner projection of Eq. (1.36) becomes (Bazley, 1960)

$$A' = |\underline{h})(\underline{h}|A^{-1}\underline{h})^{-1}(\underline{h}| \tag{1.38}$$

and satisfies the operator inequalities (Löwdin, 1965)

$$0 < A' \leq A \ . \tag{1.39}$$

Since the superoperator resolvent in Eq. (1.34) is an indefinite operator, it is not valid to discuss an inner projection of the type in Eq. (1.36). Equation (1.38) however, which does not contain $A^{\frac{1}{2}}$, is still an acceptable definition of the inner projection provided A is nonsingular. Using this definition for an indefinite operator, the equality in Eq. (1.39) will still hold when $\underline{h}$ is complete, but the bounding properties will now be lost with incomplete manifolds. Using the Bazley inner

projection, the electron propagator has the following form

$$\underline{G}(E) \simeq (\underline{a}|\underline{h})(\underline{h}|(E\hat{I}-\hat{H})\underline{h})^{-1}(\underline{h}|\underline{a}) \tag{1.40}$$

in which the decoupling problem has now been transformed into the problem of choosing an appropriate inner projection manifold.

1.3 The Hartree-Fock Propagator

Before proceeding to formulate more sophisticated decoupling schemes, it is convenient at this point to recapitulate the approximations underlying all propagator calculations and to demonstrate the algebraic manipulations which are involved by examining one simple decoupling in some detail. Implicitly assuming the clamped nuclei and non-relativistic approximations, there are basically three additional approximations involved in any scheme for computing the electron propagator. The first is the truncation of the complete (infinite) set of spin orbitals, $\{u_i(x)\}$, to some finite subset. This approximation is also characteristic of the more conventional wavefunction formulations and has received considerable attention. Standard basis sets of various sizes and qualities are available in the literature (Roetti and Clementi, 1974, Huzinaga, 1965, Dunning, 1970, Dunning and Hay, 1977). The second approximation is the specification of the N-electron ground state average or equivalently, a density operator (Eq. (1.32)), in terms of which the electron propagator is defined. The final approximation is the specification of the inner projection manifold or the actual decoupling of the equations of motion.

The simplest approximation to the inner projection manifold, $\underline{h}$, in Eq. (1.40) is just the set, $\{a_i\}$, of simple field operators. With this choice, Eq. (1.40) simplifies to

$$\underline{G}(E) = (\underline{a}|(E\hat{\underline{I}}-\hat{\underline{H}})\underline{a})^{-1} \tag{1.41}$$

since

$$(\underline{a}|\underline{a}) = \underline{1} \tag{1.42}$$

which can be verified by evaluating a specific matrix element:

$$(a_j|a_i) = Tr\{\rho[a_i,a_j^\dagger]_+\} = \delta_{ij}Tr\{\rho\} = \delta_{ij} \ . \tag{1.43}$$

One particularly convenient density operator, which corresponds to an independent particle, ensemble average, is the grand canonical density operator (Abdulnur *et al.*, 1972, Linderberg and Öhrn, 1973),

$$\rho = \prod_k [1 - \langle n_k\rangle + (2\langle n_k\rangle - 1)\, a_k^\dagger a_k]. \tag{1.44}$$

This density operator yields the following results for various operator averages:

$$Tr\{\rho a_r^\dagger a_s\} = \delta_{rs}\langle n_r\rangle \tag{1.45}$$

$$Tr\{\rho a_r^\dagger a_{r'}^\dagger a_{s'} a_s\} = [\delta_{rs}\delta_{r's'} - \delta_{rs'}\delta_{sr'}]\langle n_r\rangle\langle n_{r'}\rangle \tag{1.46}$$

and reduces to a pure state average when occupation numbers, $\langle n_k\rangle$, of zero or one are chosen.

Considering the i,j-th matrix element of the electron propagator,

$$G(E)_{ij} = [E\delta_{ij} - (a_j|\hat{H}a_i)]^{-1}, \tag{1.47}$$

the remaining operator scalar product, $(a_j|\hat{H}a_i)$, can be evaluated by first operating with the superoperator Hamiltonian (Eq. 1.29)

$$\hat{H}a_i = [a_i,H]_- = \sum_s h_{is}a_s + \tfrac{1}{2}\sum_{r',s,s'} \langle ir'||ss'\rangle a_{r'}^\dagger a_{s'} a_s, \tag{1.48}$$

then anti-commuting with $a_j^\dagger$ (Eq. 1.32)

$$(a_j|\hat{H}a_i) = h_{ij} + \sum_{r',s'} \langle ir'||js'\rangle \mathrm{Tr}\{\rho a^{\dagger}_{r'} a_{s'}\}. \tag{1.49}$$

Using the grand canonical density operator to evaluate the trace (Eq. 1.45), we obtain

$$(a_j|\hat{H}a_i) = h_{ij} + \sum_{s'} \langle is'||js'\rangle \langle n_{s'}\rangle. \tag{1.50}$$

The particular basis of simple field operators,

$$\tilde{a}_i = \sum_k x^*_{ik} a_k, \tag{1.51}$$

which satisfies the equation

$$\hat{H}\tilde{a}_i = \varepsilon_i \tilde{a}_i \tag{1.52}$$

diagonalizes the matrix, $(\underline{a}|\hat{H}\underline{a})$, and must be obtained self-consistently. This is an equivalent statement of the conventional Hartree-Fock procedure since the transformation in Eq. (1.51) also defines the canonical Hartree-Fock spin orbitals

$$\tilde{u}_i = \sum_k x^*_{ik} u_k. \tag{1.53}$$

The eigenvalues, ε_i, are the Hartree-Fock orbital energies.

Substituting these results into Eq. (1.47), we obtain

$$G(E)_{ij} = (E-\varepsilon_i)^{-1}\delta_{ij} \tag{1.54}$$

for this simple decoupling scheme. The poles of this function occurring at $E = \varepsilon_i$ correspond to the Koopmans' theorem (Koopmans, 1933) approximation to the ionization energies. Because of the analogy between this decoupling and the conventional Hartree-Fock procedure, Eq. (1.54) is referred to as the Hartree-Fock propagator and will constitute the starting point for more exact approximations.

1.4 Operator Product Decoupling

As was pointed out in the introduction, the Koopmans' theorem approximation to ionization energies is frequently unreliable and necessitates the incorporation of many-electron relaxation and correlation corrections. The simple decoupling scheme which yielded the Hartree-Fock propagator in the preceding section can be extended to incorporate relaxation and correlation by extending the inner projection operator manifold, $\underline{h}$, in Eq. (1.40). One extension of this manifold, proposed by Pickup and Goscinski (1973), is the union of all operator subspaces containing different Fermion-like products of simple field operators:

$$\underline{h} = \{a_k\}U\{a_k^+ a_l a_m\}U\{a_j^+ a_k^+ a_l a_m a_n\}U \ldots . \tag{1.55}$$

In terms of the equations of motion, Eq. (1.28), this type of decoupling is equivalent to expressing a higher-particle Green's function in terms of lower ones and was originally discussed in the context of atomic and molecular theory by Linderberg and Öhrn (1967).

The formulation of explicit electron propagator approximations with this extended operator product manifold is simplified by the use of the partitioning technique (Löwdin, 1962). Having already derived an expression for the Hartree-Fock propagator with a manifold consisting of simple field operators, it is convenient to make the partition

$$\underline{h} = \underline{a}U\underline{f} \tag{1.56}$$

where $\underline{a}$ is the subspace of simple field operators and $\underline{f}$ represents the orthogonal complement containing all higher, Fermion-like operator products. This partitioning is imposed through the relations

$$(\underline{a}|\underline{a}) = (\underline{f}|\underline{f}) = \underline{1} \ , \tag{1.57}$$

$$(\underline{a}|\underline{f}) = (\underline{f}|\underline{a}) = \underline{0} \tag{1.58}$$

and leads to a blocked matrix equation for the electron propagator:

$$\underline{G}(E) = (\underline{1}\ \underline{0}) \begin{pmatrix} (\underline{a}|(E\hat{I}-\hat{H})\underline{a}) & -(\underline{a}|\hat{H}\underline{f}) \\ -(\underline{f}|\hat{H}\underline{a}) & (\underline{f}|(E\hat{I}-\hat{H})\underline{f}) \end{pmatrix}^{-1} \begin{pmatrix} \underline{1} \\ \underline{0} \end{pmatrix} \ . \tag{1.59}$$

Solving for the upper left block of the inverse matrix, an equation for $\underline{G}^{-1}(E)$ is easily obtained

$$\underline{G}^{-1}(E) = (\underline{a}|(E\hat{I}-\hat{H})\underline{a}) - (\underline{a}|\hat{H}\underline{f})(\underline{f}|(E\hat{I}-\hat{H})\underline{f})^{-1}(\underline{f}|\hat{H}\underline{a}) \ . \tag{1.60}$$

The first term on the right hand side of Eq. (1.60) is the inverse of the Hartree-Fock propagator and the second term represents the relaxation and correlation corrections to the Koopmans' theorem ionization energies. Based on the resemblance of Eq. (1.60) with the Dyson equation derived in quantum electrodynamics (Dyson, 1949), the Hartree-Fock propagator can be identified as a zeroth order, i.e. uncorrelated, approximation to $\underline{G}(E)$ while the remaining term is identified as the self-energy,

$$\underline{G}^{-1}(E) = \underline{G}_0^{-1}(E) - \underline{\Sigma}(E) \ . \tag{1.61}$$

A number of approximations to $\underline{G}(E)$, based on different choices of the operator manifold in Eq. (1.55), have been reported in the literature. Pickup and Goscinski (1973) chose their manifold to consist of single- and triple-operator products and replaced the superoperator Hamiltonian in the self-energy by the Fock superoperator defined by

$$\hat{F}X = [X,F]_- \quad ; \ F = \sum_k \epsilon_k a_k^\dagger a_k \ . \tag{1.62}$$

This approximation was applied to the calculation of ionization energies for helium and nitrogen by Purvis and Öhrn (1974) and was later extended to include the full superoperator Hamiltonian (Purvis and Öhrn, 1975a). Redmon et al. (1975) have derived an approximation which includes single-, triple-, and quintuple-operator products in $\underline{h}$ and have computed the ionization energies of neon. Finally, several approximations have been reported using an inner projection manifold of single and triple products in conjunction with correlated reference states. (Purvis and Öhrn, 1975b, Jørgensen and Simons, 1975).

1.5 Method of Solution

The solution of Eq. (1.60) consists of finding the poles and Feynman-Dyson amplitudes of the electron propagator and writing a spectral representation similar to that of the exact propagator in Eq. (1.10). The procedure for obtaining the spectral representation from the Dyson equation has been discussed by Layzer (1963) and Csanak et al. (1971) and begins with a solution to the energy dependent eigenvalue problem:

$$\underline{L}(E)\underline{\phi}(E) = \underline{\phi}(E)\underline{W}(E), \tag{1.63}$$

where

$$\underline{L}(E) = (\underline{a}|\hat{H}\underline{a}) + \underline{\Sigma}(E) , \tag{1.64}$$

$$\underline{\phi}(E)\underline{\phi}^{\dagger}(E^{*}) = \underline{1} , \tag{1.65}$$

and $\underline{W}(E)$ is a diagonal eigenvalue matrix. Expanding in terms of the eigenfunctions, $\underline{\phi}(E)$, $\underline{G}(E)$ assumes the form

$$\underline{G}(E) = \underline{\phi}(E)[E\underline{1}-\underline{W}(E)]^{-1}\underline{\phi}^{\dagger}(E) , \tag{1.66}$$

and the poles are those values of E satisfying the equation,

$$E_k = W_k(E_k) \ . \tag{1.67}$$

The energy dependence of the eigenvalues, $W_k(E)$, is sketched in Fig. 2 which shows that the poles occur at the intersections of these curves with a line of unit slope passing through the origin. When the inner projection manifold is energy independent, the slopes of the $W_k(E)$ curves are always negative since

$$\frac{d}{dE}\underline{\Sigma}(E) = -(\underline{a}|\hat{H}\underline{f})(\underline{f}|(E\hat{I}-\hat{H})\underline{f})^{-2}(\underline{f}|\hat{H}\underline{a}) \ , \tag{1.68}$$

and the number of propagator poles between any pair of self-energy poles is equal to the number of basis functions in that symmetry (Purvis and Öhrn, 1974).

From the spectral representation, it was noted that the exact propagator has only simple poles, and it is easily shown that the residues at the poles are precisely the Feynman-Dyson amplitudes. Assuming that the approximate propagator in Eq. (1.60) also has only simple poles, the residues can be obtained from elementary residue calculus as

$$\lim_{E\to E_k} (E-E_k)G_{ij}(E) = \Gamma_k \phi_{ik}(E_k)\phi^*_{jk}(E_k) \tag{1.69}$$

where

$$\Gamma_k^{-1} = [1 - \frac{d}{dE} W_k(E)]_{E=E_k} \ . \tag{1.70}$$

According to the Mittag-Leffler theorem (Mittag-Leffler, 1880), the electron propagator can now be written as

Figure 2. A sketch of the energy dependence of the function $W_k(E)$ between self-energy poles (indicated by vertical dashed lines). Propagator poles occur at the intersections of these curves with a line of unit slope.

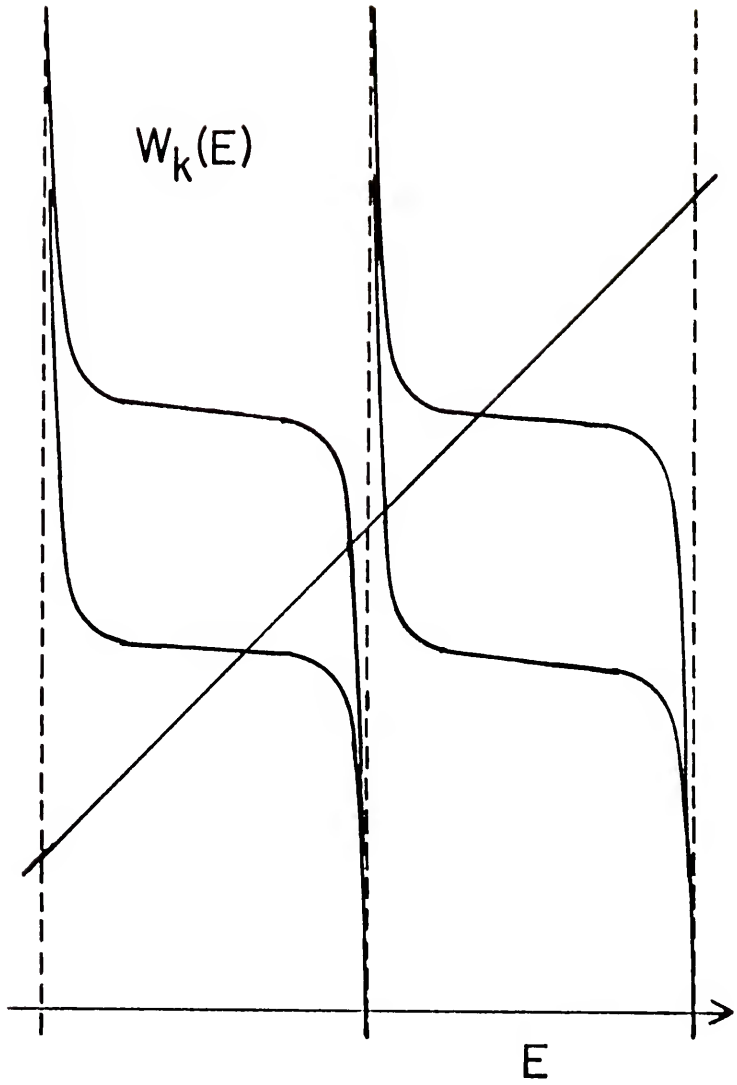
$W_k(E)$
E

$$G_{ij}(E) = \sum_k \frac{\Gamma_k \phi_{ik}(E_k)\phi^*_{jk}(E_k)}{(E-E_k)} \tag{1.71}$$

which has the form of the spectral representation.

1.6 Analysis and Limitations of the Operator Product Decoupling

In order to analyze approximate electron propagator expressions as obtained in Eq. (1.60), it is necessary to compare the propagator poles with the exact energy differences between the corresponding N- and N-1 (N+1)-electron states. This analysis can be performed, in principle, in one of two ways. Since a full configuration interaction (CI) calculation will yield the exact total energy to any finite dimensional, model problem, the total energies of the N- and N-1 (N+1)-electron state could be calculated and then subtracted to yield the ionization energy (electron affinity). A full CI, however, is not practical except for systems well described by small basis sets ($\lesssim$10) because the number of configurations in the CI expansion, given by Weyl's formula (Shavitt, 1977), increases roughly as $N^{-2}(2Me/N)^N$ where N is the number of electrons, M is the size of the spin orbital basis, and e is the constant 2.718. Furthermore, the CI solution, which is expressed as a determinental expansion, is not readily amenable to detailed analysis. On the other hand, a perturbation expansion of the N- and N-1 (N+1)-electron total energies also yields the exact solution (in a non-zero region of convergence), but in addition, allows an order by order analysis of the total energy contributions in terms of orbital energies and two-electron integrals.

Using Rayleigh-Schrödinger perturbation theory (RSPT) to represent the N- and (N-1)-electron states through second order, Pickup and

Goscinski (1973) derived a second-order electron propagator expression for the energy difference. Since a Hartree-Fock self-consistent field solution was assumed as the unperturbed problem, the orbital basis sets of the N- and (N-1)-electron states are different. Before the total energy expressions may be subtracted, therefore, the orbitals of the (N-1)-electron problem must be expanded in terms of the N-electron orbitals. This procedure has been extended by Born et al. (1978) through third order, and the resulting third-order self-energy is listed in Appendix 1. Each third-order term in Appendix 1 is characterized by a diagram and may be alternatively obtained using diagrammatic techniques, but for pedagogic reasons this discussion will be deferred until Chapter 3.

Although the results of Purvis and Öhrn (1974, 1975a) and Redmon et al. (1975) represent significant improvements to the Koopmans' theorem and $\Delta E(SCF)$ approximations for the ionization energies they computed, the operator product decoupling was demonstrated to have certain computational and formal limitations or ambiguities. Computationally, the most severe limitation is the dimension of the inverse matrix in the matrix product of Eq. (1.42). The dimension of this matrix increases rapidly with the size of the spin orbital basis and prohibits an exact inversion for all but the smallest basis sets. In contrast to the CI matrix where only the lowest few eigenvalues of each symmetry are usually computed, the inversion of this matrix requires all the eigenvalues and eigenvectors. As an illustration of the size problem, when $\underline{f}$ consists of only triple products, the dimension is roughly proportional to $NM(M-N)$ where N is the number of electrons and M is the size of the spin orbital basis. This limitation necessitates the approximation of the inverse matrix in diagonal or near-diagonal form (Purvis and Öhrn, 1974).

The formal limitations of the operator product manifolds involve certain ambiguities when extending the decoupling approximation and the difficulty in performing an order analysis. Although Manne (1977) has proven that the set of all Fermion-like operator products forms a complete set, the extension to higher operator products is not consistent with an order by order extension of the perturbation analysis. In fact, Redmon et al. (1975) have suggested that perhaps some quintuple products should be preferentially included before all triple products. This, they felt, was particularly important in describing shake-up processes, i.e. ionization plus a simultaneous excitation of the (N-1)-electron ion. This observation has recently been confirmed by Herman et al. (1978) in calculations employing the closely related equation of motion (EOM) method (Rowe, 1968, Simons and Smith, 1973).

As mentioned in Section 1.3, correlation corrections may be included in either the density operator or the inner projection manifold. This dichotomy leads to another ambiguity: should larger operator products be chosen to extend the decoupling or a more highly correlated reference state? It has been shown by Jørgensen and Simons (1975) that in order to obtain a decoupling approximation correct through third order, an inner projection manifold consisting of single and triple products must be chosen as well as a reference state which includes all single and double excitations. Unfortunately, this combination of approximations makes the order analysis unnecessarily complicated, as we will later show in Chapter 3.

Finally, the Hermiticity problem should be mentioned. With a density operator that commutes with the Hamiltonian, the Hermiticity of the superoperator Hamiltonian can be expressed as

$$(X_i|\hat{H}X_j) = (\hat{H}X_i|X_j) = (X_j|\hat{H}X_i)^* \quad . \tag{1.72}$$

With density operators that do not commute with the Hamiltonian, however, Eq. (1.72) is generally not satisfied and leads to both computational and formal complications. This problem has been studied by Nehrkorn et al. (1976) who observed computationally that the non-Hermitian terms which arise when the density operator is correlated to first and second order in RSPT are cancelled when the reference state was improved to second and third order respectively. A general proof was given by Linderberg* which states that the Hermiticity error is of order n+1 when the reference state is correlated through order n.

In the following chapters, alternative decoupling procedures will be proposed and investigated with the intention of remedying the various limitations inherent in the operator product decoupling as discussed here, yet which retain a quantitative description of ionization processes.

---

*See Ref. (14) in Nehrkorn et al. (1976).

CHAPTER 2
MOMENT CONSERVING DECOUPLINGS

2.1 Pade' Approximants and the Extended Series of Stieltjes

The evaluation of special functions assumes a central role in applied mathematics. A large number of these functions, from the simple trigonometric and exponential functions to the more complex, hypergeometric functions and Green's functions, have power series expansions. Their evaluation, therefore, consists of summing the corresponding series expansion. When the series is slowly convergent or when only a limited number of expansion coefficients are known (as e.g. through perturbation theory), it may not be practical, or even possible, to evaluate the series term by term until a desired accuracy has been achieved. In these cases, optimal approximations based on a limited number of expansion coefficients are sought. This general problem was first studied by Tchebychev (1874) and Stieltjes (1884) for the series which bear their names and is referred to as the problem of moments. (For more recent reviews of this problem see e.g. Wall, 1948, Shohat and Tamarkin, 1963, or Vorobyev, 1965). A general solution of this problem was given by Pade' (1892) and is known as the Pade' approximant method (Baker, 1975).

Given a function, f(z), (z complex) which admits the formal, but not necessarily convergent, power series expansion

$$f(z) = \sum_{k=0}^{\infty} a_k z^k \ , \qquad (2.1)$$

the [N,M] Pade' approximant is defined as a rational fraction of the form P(z)/Q(z) where P(z) is a polynomial of degree M and Q(z) is a polynomial of degree N. The coefficients of these polynomials are uniquely determined by equating like powers of z in the equation

$$f(z)Q(z)-P(z)=0 \text{ (through order } z^{N+M}) \tag{2.2}$$

with the auxiliary condition Q(0)=1. The expansion of P(z)/Q(z), therefore, coincides with Eq. (2.1) through the (N+M)-th power of z and provides an approximation to the remaining terms.

The term by term convergence of Eq. (2.1) is replaced by the convergence of sequences of approximants (such as [N,N], N=1, 2, 3, . . .) in the Pade' approximant method, and although general convergence theorems are difficult to prove for arbitrary series, there exist several extensive special cases for which convergence has been proven. For these series, the Pade' approximant can often be shown to extend the natural region of convergence (Baker, 1975) and may be viewed as a method of approximate analytic continuation. A sequence of Pade' approximants, therefore, may converge rapidly when the original series expansion converges slowly or not at all.

Two series which have been extensively studied in the problem of moments and for which sequences of Pade' approximants have been proven to converge are the series of Stieltjes (Stieltjes, 1894) and the extended series of Stieltjes (Hamburger, 1920, 1921a, 1921b, also known as the Hamburger moment problem). A series is of the Stieltjes type if and only if the coefficients, a_k in Eq. (2.1), can be identified as moments of a distribution

$$a_k = \int_0^\infty x^k d\psi(x) \tag{2.3}$$

where $\psi(x)$ is a bounded, non-decreasing function with infinitely many points of increase in the interval $[0,\infty)$. The extended series of Stieltjes is defined similarly for the extended interval $(-\infty,\infty)$.

The extended series of Stieltjes has particular significance owing to its intimate relationship with resolvents of Hermitian operators. For any operator, A, we can define the operator function

$$R(zA) = (1-zA)^{-1} \tag{2.4}$$

which is trivially related to the resolvent of A. When A is Hermitian, the spectral theorem (Riesz and Sz.-Nagy, 1955) insures a unique integral representation of R(zA) having the form

$$R(zA) = \int_{-\infty}^{\infty} \frac{dE(\lambda)}{1-z\lambda} \quad . \tag{2.5}$$

The operator $E(\lambda)$ is called an orthogonal resolution of the identity, and when A has only a discrete spectrum, it can be written

$$E(\lambda) = \sum_k \theta(\lambda-a_k)|\phi_k\rangle\langle\phi_k| \quad , \tag{2.6}$$

where a_n and ϕ_n are the eigenvalues and eigenfunctions of A. For any vector f in the domain of A^n for all n, the function

$$\langle f|R(zA)f\rangle = R_f(z) = \int_{-\infty}^{\infty} \frac{dE_f(\lambda)}{1-z\lambda} \tag{2.7}$$

represents either an extended series of Stieltjes or a rational fraction

depending on whether $E_f(\lambda)$ has an infinite or finite number of points of increase (Masson, 1970).

In view of possible applications of the Pade' approximant method to the superoperator resolvent, we state two theorems regarding the extended series of Stieltjes and discuss some properties of two particular sequences of Pade' approximants to these series.

Theorem 1: (Wall, 1948, theorem 86.1) A necessary and sufficient condition for f(z) to be an extended series of Stieltjes is

$$\det \begin{pmatrix} a_0 & a_1 & \cdots & a_n \\ a_1 & a_2 & \cdots & a_{n+1} \\ \vdots & & & \\ a_n & a_{n+1} & \cdots & a_{2n} \end{pmatrix} > 0 \quad ; \; n=0, 1, 2, \ldots \tag{2.8}$$

Theorem 2: (Masson, 1970, theorem 4) If f(z) is an extended series of Stieltjes and the associated moment problem is determinant*, then, for fixed $j=0,\pm1,\pm2, \ldots \pm m$, the sequence [N,N+2j+1] of Pade' approximants converges to f(z) for Im $(z) \neq 0$. The convergence is uniform, i.e.

$$\lim_{N\to\infty} ||[N,N+2j+1]-f(z)|| = 0 , \tag{2.9}$$

with respect to z in any compact region in the upper or lower half-z plane.

In addition to being uniformly convergent, sequences of [N,N] and [N,N-1] Pade' approximants to extended series of Stieltjes have two other features which make them particularly attractive for computational applications. First, these approximants are closely related to

---

*The moment problem is said to be determinant if there is a unique, bounded, non-decreasing function $\psi(x)$ satisfying the moment conditions in Eq. (2.3) and the supplementary conditions $\psi(-\infty)=0$ and

$$\psi(x) = \lim_{\varepsilon\to 0} \tfrac{1}{2}\{\psi(x+\varepsilon) + \psi(x-\varepsilon)\} .$$

variational methods (Nuttall, 1970, 1973). When the operator R(zA) (defined in Eq. (2.5)) is positive definite, the [N,N] and [N,N-1] approximants provide the following bounds to $R_f(z)$ (Goscinski and Brändas, 1971):

$$[N,N] \geq R_f(z) \geq [N,N-1] \ . \tag{2.10}$$

For resolvent operators such as the superoperator resolvent which are indefinite, bounding properties are more difficult to establish. Vorobyev (1965) has shown, however, that the inverse poles of the [N,N-1] approximant to $R_f(z)$ are equivalent to the eigenvalues obtained from the usual Rayleigh-Ritz variational problem

$$\text{extr} \ \frac{\langle\psi|A|\psi\rangle}{\langle\psi|\psi\rangle} \tag{2.11}$$

where $\psi = c_0 f + c_1 Af + \ . \ . \ . \ c_{N-1} A^{N-1} f$, and the coefficients $\{c_i\}$ are variationally determined. In this sense, the poles of [N,N-1] to $R_f(z)$ are variationally optimum, but they have no definite bounding properties.

The second attractive feature of the [N,N] and [N,N-1] approximants is the ease with which they may be computed. Rather than solving Eq. (2.2) to obtain the coefficients of the polynomials P(z) and Q(z), these approximants may be expressed directly in terms of the series coefficients $\{a_k\}$ using matrix formulae derived by Nuttall (1967) and Goscinski and Brändas (1971). For the [N,N-1] approximant, we have

$$[N,N-1] = \underline{a}_0^{\dagger}[\underline{A}_0 - z\underline{A}_1]^{-1}\underline{a}_0 \ , \tag{2.12}$$

where, in general, $\underline{a}_i$ is a column vector with the elements a_i, a_{i+1}, . . . a_{i+N-1}, and $\underline{A}_i$ is an N x N square matrix with the columns $\underline{a}_i$, $\underline{a}_{i+1}$, . . . $\underline{a}_{i+N-1}$. Similarly for the [N,N] approximant we can write

$$[N,N] = a_0 + z\underline{a}_1^{\dagger}[\underline{A}_1 - z\underline{A}_2]^{-1}\underline{a}_1 \ . \tag{2.13}$$

2.2 Moment Conserving Decoupling

Expanding the superoperator resolvent in Eq. (1.34) and multiplying both sides of the equation by E, the electron propagator can be expressed as the moment expansion

$$\underline{EG}(E) = \sum_{k=0}^{\infty} E^{-k}(\underline{a}|\hat{H}^k\underline{a}) \ . \tag{2.14}$$

Before the Pade' approximant method may be applied to this equation, however, the conventional definition of the Pade' approximant must be generalized to matrix Pade' approximants (Baker, 1975). This generalization is achieved by replacing the moment coefficients by the corresponding moment matrices and noting that these matrices do not commute when performing subsequent algebraic manipulations. Using Eq. (2.12) to represent the [N,N-1] approximant to $\underline{EG}(E)$, we obtain

$$\underline{EG}(E) = \underline{m}_0^{\dagger}(\underline{M}_0 - E^{-1}\underline{M}_1)^{-1}\underline{m}_0 \ , \tag{2.15}$$

or multiplying each side of this equation by E^{-1}, Eq. (2.15) becomes

$$\underline{G}(E) = \underline{m}_0^{\dagger}(E\underline{M}_0 - \underline{M}_1)^{-1}\underline{m}_0 \tag{2.16}$$

where $\underline{m}_0$ is now a column matrix with block elements

$$\underline{m}_0 = \begin{pmatrix} \underline{c}_0 \\ \underline{c}_1 \\ \cdot \\ \cdot \\ \cdot \\ \underline{c}_{N-1} \end{pmatrix} \quad ; \quad \underline{c}_i = (\underline{a}|\hat{H}^i\underline{a}) \ . \tag{2.17}$$

If $\underline{c}_i$ has the dimensions M x M, $\underline{M}_i$ is an NM x NM square matrix with columns $\underline{m}_i$, $\underline{m}_{i+1}$, . . . $\underline{m}_{i+N-1}$.

There is a close relationship between Eq. (2.16) and the inner projection of the superoperator resolvent

$$\underline{G}(E) = (\underline{a}|\underline{h})(\underline{h}|(E\hat{I}-\hat{H})\underline{h})^{-1}(\underline{h}|\underline{a}) \ . \tag{2.18}$$

Goscinski and Lukman (1970) have shown that if the inner projection manifold is chosen to consist of

$$\underline{h} = \{a_k\}U\{\hat{H}a_k\}U \ . \ . \ . \ U\{\hat{H}^{N-1}a_k\} \ , \tag{2.19}$$

the inner projection and the [N,N-1] Pade' approximant are equal. Since, in general, the [N,M] Pade' approximant conserves the first N+M+1 moments in the moment expansion, this choice of inner projection manifolds for the superoperator resolvent is called a moment conserving decoupling of the equation of motion.

An examination of the [N,N-1] approximant to the electron propagator shows that its poles are given by the eigenvalues of

$$\underline{M}_1\underline{c} = \underline{M}_0\underline{cd} \ . \tag{2.20}$$

The matrix $\underline{M}_0$ corresponds to a metric matrix and by virtue of the operator scalar product, is always positive definite

$$\underline{M}_0 = (\underline{h}|\underline{h}) = Tr\{\rho[\underline{hh}^{\dagger}+\underline{h}^{\dagger}\underline{h}]\}>0 \ . \tag{2.21}$$

The determinants of the metric matrices corresponding to various truncations of the moment conserving inner projection manifold, i.e.

$$\det\ (\underline{h}_0|\underline{h}_0) > 0 \qquad \underline{h}_0 = \{\underline{a}\} \tag{2.22}$$

$$\det\ (\underline{h}_1|\underline{h}_1) > 0 \qquad \underline{h}_1 = \{\underline{a}\}U\{\hat{H}\underline{a}\} \ , \tag{2.23}$$

. . .

provide the necessary and sufficient conditions of Theorem 1 to prove that the electron propagator is an extended series of Stieltjes. Consequently, the sequence of [N,N-1] Pade' approximants to the electron propagator should be uniformly convergent and should have variationally optimum properties.

The spectral representation of the electron propagator (Eq. (1.10)) consists of two summations, one which has poles in the lower half of the complex E-plane corresponding to ionization energies and one which has poles in the upper half plane corresponding to electron affinities. Based on the physical argument that the removal of an electron from a stable atomic or molecular system always requires energy, we might suspect a separation of the superoperator resolvent which yields a negative definite operator for these processes. If this were possible, the poles of the [N,N-1] approximants would then be upper bounds to the exact ionization energies obtainable with a given basis. This separation has not been explicitly demonstrated but an overwhelming amount of numerical data seemsto substantiate this conjecture. In particular, the [1,0] approximant, which is easily verified to be the Hartree-Fock propagator, generally yields poles larger in absolute value than experimental ionization energies. One possible exception to this rule may be the near Hartree-Fock limit calculation of Cade *et al.* (1966) on diatomic nitrogen. In this calculation, the magnitude of the $1\pi_u$ orbital energy is slightly (0.2 eV) smaller than the experimental $1\pi_u$ ionization energy. If on the other hand, the $X^2\pi_u$ ion state was fortuitously better described than the ground state with their extended basis, this result may still be an upper bound to the exact ionization energy *in that basis*.

Relaxation and correlation corrections are incorporated in any [N,N-1] Pade' approximant beyond the [1,0] or Hartree-Fock approximant. In particular, we have studied the [2,1] approximant in some detail. This approximant corresponds to the truncation

$$\underline{h} = \{\underline{a}\}U\{\hat{H}\underline{a}\} \tag{2.24}$$

of the inner projection manifold and conserves the first four moment matrices. The operators $\{f_i | f_i = \hat{H}a_i\}$, which were evaluated in Eq. (1.48), consist of a sum over all triple products of simple field operators with each operator product in the sum weighted by an antisymmetrized, two-electron integral. These linear combinations provide a significant reduction in the subspace of triple operators thus overcoming one major limitation of the operator product decoupling.

Another type of moment conserving decoupling of the electron propagator equations of motion has been analyzed by Babu and Ratner (1972). This decoupling is achieved by truncating the moment expansion after the m-th moment and replacing the m-th moment matrix with

$$\underline{c}_m = \underline{c}_m\underline{G}(E) \quad . \tag{2.25}$$

Solving the truncated moment expansion for $\underline{G}(E)$ yields

$$(E^{m+1}\underline{1} - \underline{c}_m)\underline{G}(E) = \sum_{k=0}^{m-1} E^{m-k}\underline{c}_k \tag{2.26}$$

or

$$\underline{G}(E) = (E^{m+1}\underline{1} - \underline{c}_m)^{-1} \sum_{k=0}^{m-1} E^{m-k}\underline{c}_k \tag{2.27}$$

These rational approximants formally conserve m moments but are not of the Pade' type (as Babu and Ratner incorrectly identify them) since the

auxiliary equation, $Q(0)=1$, is not satisfied, i.e.

$$\underline{Q}(0) = -\underline{c}_m \neq \underline{1} \quad . \tag{2.28}$$

The auxiliary equation guarantees the uniqueness of the Pade' approximants: only one [N,N-1] Pade' approximant will conserve exactly m moments. The nonuniqueness of Babu and Ratner's decoupling scheme is easily demonstrated by replacing Eq. (2.25) with

$$\sum_{k=n}^{m} E^{-k}\underline{c}_k = \sum_{k=n}^{m} E^{-k}\underline{c}_k \, \underline{G}(E) \qquad 0 < n \leq m \; . \tag{2.29}$$

Solving for $\underline{G}(E)$,

$$[E\underline{1} - \sum_{k=n}^{m} E^{-k}\underline{c}_k] \, \underline{G}(E) = \sum_{l=0}^{n-1} E^{-l}\underline{c}_l \tag{2.30}$$

$$\underline{G}(E) = [E^m\underline{1} - \sum_{k=n}^{m} E^{m-k}\underline{c}_k]^{-1} \sum_{l=0}^{n-1} E^{m-l}\underline{c}_l \; , \tag{2.31}$$

we obtain m rational approximants (n=1, . . . m) which formally conserve m moments. Because these approximants are not uniquely defined, we will only consider Pade' approximants in this chapter.

2.3 Method of Solution

The first step in obtaining the spectral representation of the electron propagator with the moment conserving decoupling is the evaluation of the necessary moment matrices. The first four moment matrices which are necessary to construct the [2,1] approximant have been evaluated by Redmon (1975) using the grand canonical density operator (Eq. (1.44)).

An independent check of these derivations, however, revealed an error in the matrix elements of $(\underline{a}|\hat{H}^3\underline{a})$ (Redmon, 1975, Eq. (11.30)). The correct result has subsequently been verified by Redmon (1977) and appears in Appendix 2.

Once the moment matrices have been evaluated, the matrices $\underline{M}_0$ and $\underline{M}_1$ are constructed and the corresponding eigenvalue problem, Eq. (2.20), must be solved. In general, the dimension of the eigenvalue problem increases linearly with the size of the inner projection manifold, i.e. the [N,N-1] approximant presents an eigenvalue problem of dimension NM where M is the size of the spin orbital basis. For the [2,1] approximant, therefore, the dimension of this problem is only twice the size of the spin orbital basis. This means that for even rather large basis sets, standard matrix eigenvalues techniques may be employed to solve this problem in nonpartitioned form. As a consequence, all the poles and the spectral density of the electron propagator are obtained from a single matrix diagonalization thus avoiding the energy-dependent pole search.

Denoting the eigenvectors by $\underline{c}$, where

$$\underline{cc}^{\dagger} = \underline{M}_0^{-1} \ , \tag{2.32}$$

and the eigenvalues by the diagonal matrix $\underline{d}$, the spectral representation of the electron propagator can be derived,

$$\underline{G}(E) = \underline{m}_0^{\dagger}\ \underline{cc}^{-1}[E\underline{M}_0-\underline{M}_1]^{-1}\underline{M}_0\ \underline{cc}^{-1}\underline{M}_0^{-1}\underline{m}_0 \tag{2.33}$$

$$= \underline{m}_0^{\dagger}\ \underline{c}[E\underline{1}-\underline{d}]^{-1}\underline{c}^{-1}\underline{M}_0^{-1}\underline{m}_0 \ . \tag{2.34}$$

Defining the matrix

$$\underline{x} = \underline{m}_0^{\dagger}\ \underline{c} \ , \tag{2.35}$$

which is rectangular with the dimensions M x NM, Eq. (2.34) becomes

$$\underline{G}(E) = \underline{x}(E\underline{1}-\underline{d})^{-1}\underline{x}^{\dagger} \quad . \tag{2.36}$$

This equation conserves the first 2N moment matrices of the moment expansion which implies, in particular,

$$\underline{x}\underline{x}^{\dagger} = (\underline{a}|\underline{a}) = \underline{1} \tag{2.37}$$

from the conservation of the first moment.

The complete solution of the electron propagator which is conveniently obtained with this decoupling can be used to determine a self-consistent, single-particle reduced density matrix (1-matrix). The i, j-th element of the 1-matrix can be computed from the contour integral (Linderberg and Öhrn, 1973)

$$\langle a_i^{\dagger} a_j \rangle = (2\pi_i)^{-1} \int_c G(E)_{ij} dE \quad . \tag{2.38}$$

The contour, c, runs from $-\infty$ to ∞ along the real axis and encloses only poles of $G(E)_{ij}$ that lie below the chemical potential (μ) when finally closed in the upper half of the complex E-plane. The integral is then evaluated using the Cauchy residue theorem (Morse and Feshbach, 1953)

$$\langle a_i^{\dagger} a_j \rangle = \sum_{k \leq \mu} \lim_{E \to d_k} (E-d_k) G(E)_{ij} \tag{2.39}$$

$$= \sum_{k \leq \mu} x_{ik} x_{jk}^{*} \quad . \tag{2.40}$$

Owing to the orthonormality of the spectral density elements (Eq. (2.37))

$$x_{ik} x_{jk}^{*} = \delta_{ij} |x_{ik}|^2 \quad , \tag{2.41}$$

it follows that the 1-matrix is diagonal with occupation numbers determined by

$$\langle n_i \rangle = \sum_{k \leq \mu} |x_{ik}|^2 \quad . \tag{2.42}$$

Using pure state occupation numbers of zero and one in the grand canonical density operator for the initial computation of $\underline{G}(E)$, then occupation numbers determined from Eq. (2.42) on subsequent computations, a self-consistent set of occupation numbers can be sought.

2.4 Computational Considerations and Applications

The most time consuming step in the construction of the [2,1] Pade' approximant to the electron propagator is the construction of the moment matrices. The fourth moment matrix (given in Appendix 2) is particularly difficult since it involves five unrestricted orbital summations plus another two symmetry restricted, orbital summations of two-electron integrals. Using direct summation techniques, the time needed to construct this matrix is roughly proportional to N^7. This is a formidable computational problem, but one that must be accepted in favor of the more manageable matrix dimensions.

Fortunately, the N^7 problem is not as intimidating as it might seem on first appearance. The "brute-force" summation of two-electron integrals in the moment matrices resums certain partial sums which may appear in more than one term or matrix element. These redundant summations can be avoided with considerable savings in computer time by computing the partial sums once and reusing them. Two specific partial sums we have employed are

$$[ij|kl] = \sum_{s,s'} \langle ij||ss'\rangle\langle ss'||kl\rangle \tag{2.43}$$

$$\{ij|kl\} = \sum_{s,s'} \langle is||js'\rangle\langle ks'||ls\rangle \quad . \tag{2.44}$$

Since these partial sums contain a double summation which is performed only once, the original N^7 problem is effectively reduced to N^5. The construction of the moment matrices is now comparable in difficulty to the transformation of the two-electron integrals from the primitive basis to the computational (usually Hartree-Fock) basis which is also roughly proportional to N^5.

When the number of two-electron integrals is too large to be held in core, their random access from peripheral storage becomes relatively time consuming. The partial sums are much more efficiently constructed from ordered lists of two-electron integrals which can be read into primary (core) storage when needed. For the partial sums defined above, the two-electron integrals must be sorted into ordered lists of the type $\langle ij|**\rangle$ and $\langle i*|j*\rangle$ where * indicates all orbital indices which yield a non-zero integral for the corresponding i,j-th distribution.

The integral sorts are performed using the Yoshimine sorting technique (Yoshimine, 1973). Briefly summarized, this technique involves a partition of available core into a number of buffers. Each buffer holds integrals corresponding to a specific i,j distribution, e.g. $\langle ij|**\rangle$. (When the number of distributions is large, several may be held in each buffer.) Reading through the two-electron integral list, integrals are then sorted into the appropriate buffers. As each buffer fills, it is written to direct access, peripheral storage and assigned a record number. All record numbers corresponding to integrals from the same buffer are saved in a "chaining" array for that buffer. After the entire integral list has been processed and all buffers have been dumped, it is then

possible to chain back through the direct access records, copying integrals of the same distribution back into core. These integrals may then be further sorted within distributions, e.g. k<1 for each i,j, and finally saved sequentially on a peripheral storage device.

Diatomic nitrogen was the first molecule to be studied with the [2,1] Pade' approximant. Owing to its abundance in the atmosphere, nitrogen has great chemical interest and has been extensively investigated both experimentally and theoretically. It is an ideal test case for calculating ionization energies from a correlated, many-electron formalism such as propagator theory since both the Hartree-Fock and ΔE(SCF) approximations incorrectly predict the order of the $3\sigma_g$ and $1\pi_u$ ionizations (Cade et al., 1966). Only when correlation corrections are included is the correct ordering obtained (Cederbaum and Domcke, 1977 and references therein).

A double zeta, contracted basis of Gaussian type orbitals (GTO's) was employed in this calculation. This basis consisted of Huzinaga's 9s,5p set of primitive orbitals (Huzinaga, 1965) which was contracted to 4s,2p (Dunning, 1970). This basis has been optimized by Dunning on the nitrogen atom and is listed in Table 1. The corresponding one- and two-electron integrals were calculated at the experimental internuclear separation, R=2.068 a.u. (Herzberg, 1955), using the MOLECULE integral program (Almlöf, 1974).

The Hartree-Fock calculation and the two-electron integral transformation were performed with the program GRNFNC (Purvis, 1973). The Hartree-Fock total energy with this basis was E(HF)= -108.8782 a.u. which is about 3 eV higher than the result of Cade et al. (1966). There is also a discrepancy in the Hartree-Fock orbital energies. While

Table 1. Contracted Gaussian Basis for Nitrogen.

Nitrogen s orbitals

Exponents	Contraction Coefficients
5909.4400	0.002001
887.4510	0.015310
204.7490	0.074293
59.8376	0.253364
19.9981	0.600576
2.6860	0.245111
7.1927	1.000000
0.7000	1.000000
0.2133	1.000000

Nitrogen p orbitals

Exponents	Contraction Coefficients
26.7860	0.018257
5.9564	0.116407
1.7074	0.390111
0.5314	0.637221
0.1654	1.000000

the calculation of Cade et al. (incorrectly) predicted the $1\pi_u$ orbital energy to be 0.53 eV below the $3\sigma_g$, this calculation predicts the $1\pi_u$ energy to be 0.05 eV higher. The correct ordering of the $3\sigma_g$ and $1\pi_u$ ionizations with this basis is merely fortuitous, since based on a total energy criterion, the basis of Cade et al. is more accurate.

The next step of the calculation involved the integral sorts, partial summations, and the construction of the moment matrices. The poles and spectral density were finally computed as outlined in the previous section and are presented along with the [1,0] results in Table 2. The ionization energies of both approximants seem to be upper bounds to the experimental results of Siegbahn et al. (1969), but without exception, the results of the [2,1] approximant are worse than the [1,0] approximant. In an attempt to incorporate some ground state correlation into the grand canonical density operator, new occupation numbers were computed from the spectral density and the [2,1] approximant was recalculated. This calculation, however, yielded no significant improvements in the ionization energies.

In order to ascertain whether the poor results from the [2,1] approximant for nitrogen are representative of other calculations or just the consequence of a pathological test case, the water molecule was chosen for a second application. Similarly to the calculation for nitrogen, a double zeta contracted basis of GTO's was also employed in this calculation. Huzinaga's 9s,5p primitive basis for oxygen and 4s primitive basis for hydrogen were contracted with Dunning's coefficients to 4s,2p and 2s, respectively. The orbital exponents for the hydrogen atoms were scaled by 1.14 to more realistically represent the effective nuclear charge in the molecule, and the final basis appears in Table 3. Again,

Table 2. Principal Ionization Energies for the Nitrogen Molecule Resulting from the [1,0] and [2,1] Propagator Approximants.

Orbital	[1,0]	[2,1]	Exp.[a]
$1\sigma_g$	427.7	472.4	409.9
$2\sigma_g$	41.6	46.5	37.3
$3\sigma_g$	17.0	30.4	15.5
$1\pi_u$	17.0	23.1	16.8
$1\sigma_u$	427.6	478.8	409.9
$2\sigma_u$	21.0	30.9	18.6

E(HF) = -108.8782 H.

[a] Siegbahn *et al.* (1969).

Table 3. Contracted Gaussian Basis for Water.

Hydrogen s sets

Exponents	Contraction Coefficients
13.3615	0.032828
2.0133	0.231208
0.4538	0.817238
0.1233	1.000000

Oxygen s sets

Exponents	Contraction Coefficients
7816.5400	0.002031
1175.8200	0.015436
273.1880	0.073771
81.1696	0.247606
27.1836	0.611832
3.4136	0.241205
9.5322	1.000000
0.9398	1.000000
0.2846	1.000000

Oxygen p sets

Exponents	Contraction Coefficients
35.1832	0.019580
7.9040	0.124189
2.3051	0.394727
0.7171	0.627375
0.2137	1.000000

the integrals were computed with the MOLECULE program at the equilibrium internuclear geometry, R(OH)= 1.809 a.u., ∢HOH = 104.5^{0} (Benedict et al., 1956). A total energy of E(HF)= -76.0082 a.u. was computed with the Hartree-Fock portion of GRNFNC and was followed by the two-electron integral transformation. Finally, the integral sorts and partial sums were performed, the moment matrices constructed, and the poles and spectral density obtained for the [2,1] approximant. The results for both the [1,0] and [2,1] approximants are presented in Table 4 and appear to be upper bounds to the experimental ionization energies. Once more, the [2,1] results are consistently worse than the [1,0] results. A few iterations on the occupation numbers yielded no significant improvements.

2.5 Evaluation of the Moment Conserving Decoupling

Formally, the moment conserving decoupling is an attractive decoupling procedure. Being closely related to the Pade' approximant method, this decoupling allows the application of numerous results from the classical moment problem to propagator theory. In particular, it was proven that the sequence of [N,N-1] approximants converge uniformly to the exact electron propagator in a given basis, and it was shown that these approximants represent a variationally optimum choice of the inner projection manifold. Why then are the results of the [2,1] approximant so much worse than the results of the [1,0] approximant? To answer this question, it is necessary to analyze the three approximations identified in Section 1.3, namely: basis quality, density operator, and decoupling procedure.

First of all, since computational economy and not high accuracy was the criterion for the test calculations on nitrogen and water, polarization

Table 4. Principal Ionization Energies for Water Resulting from the [1,0] and [2,1] Propagator Approximants.

Orbital	[1,0]	[2,1]	Exp.[a]
$1a_1$	559.4	619.2	540.2
$2a_1$	37.0	44.7	32.2
$3a_1$	15.4	29.7	14.7
$1b_1$	13.8	32.6	12.6
$1b_2$	19.5	29.6	18.6

E(HF) = -76.0082 H.

[a]Siegbahn *et al.* (1969).

functions were intentionally excluded from the basis sets. Polarization functions are diffuse, virtual orbitals which can be very important in describing electron relaxation and correlation (Purvis and Öhrn, 1974, Cederbaum and Domcke, 1977). It is reasonable to expect that the addition of polarization functions will improve both the [1,0] and [2,1] approximants to varying degrees; however, with the same basis and with the same density operator, the larger inner projection manifold (if judiciously chosen) should yield a more accurate decoupling. Since this was not the situation in these test calculations, any improvements in the basis sets did not seem worthwhile.

Second, it is possible that significant ground state correlation may have been neglected with our choice of the grand canonical density operator. With the spin orbital annihilation and creation operators expanded in the Hartree-Fock basis and using pure state occupation numbers of zero or one, this density operator yields the uncorrelated, Hartree-Fock ground state average. Rather than explicitly correlating the density operator (as e.g. through perturbation theory), an attempt was made to estimate the effect of correlation through the self-consistent determination of the occupation numbers as described in Section 2.3. This procedure was not pursued to true self-consistency since each iteration required a complete recalculation of the [2,1] approximant. It was obvious, however, after the first few iterations that no significant improvements had been obtained.

Based on the preceding implications, the third approximation--the inner projection manifold truncation--seems to be primarily responsible for the poor numerical results. Owing to the complicated operator sums in this manifold, an order analysis (as discussed in Section 1.6) is not

readily possible. Consequently, it is extremely difficult to identify the problem with this decoupling procedure. It can only be concluded that the number of moments conserved is not a useful criterion for decoupling.* This conclusion is consistent with the uniform convergence of the [N,N-1] sequence since uniform convergence is not necessarily monotonic, but it suggests that more accurate decouplings require the incorporation of more information about the moment expansion than just the moment matrices. The additional information needed is indeed available and, in the next chapter, we will demonstrate how it may be extracted using perturbation theory.

---

*Babu and Ratner (1972) reported the same conclusion which was based on an application of their rational approximants to the Hubbard model.

CHAPTER 3
DIAGRAM CONSERVING DECOUPLINGS

3.1 The Diagrammatic Expansion Method

The superoperator formalism which is employed in the previous two chapters is by no means the only formalism available to formulate decoupling approximations for the electron propagator. Two commonly used, alternative methods are the functional differentiation method (see e.g. Csanak *et al.*, 1971) and the diagrammatic expansion method (see e.g. Mattuck, 1967, Fetter and Walecka, 1971, or Cederbaum and Domcke, 1977). Of these latter two methods, the diagrammatic expansion method has proven to be particularly effective. This method avoids some of the algebraic tedium involved in deriving propagator decoupling approximations by establishing certain rules for constructing and manipulating diagrams which represent the underlying algebraic structure.

The diagrammatic expansion of the electron propagator is usually derived using time-dependent perturbation theory. The N-electron Hamiltonian is partitioned into an unperturbed part plus a time-dependent perturbation

$$H = H_0 + \exp(-\varepsilon|t|)V \ , \tag{3.1}$$

where ε is a small positive quantity. The unperturbed Hamiltonian, H_0, is chosen to yield an exactly solvable, eigenvalue problem

$$H_0|\Phi_0\rangle = E_0|\Phi_0\rangle \ , \tag{3.2}$$

and the time dependence of the unperturbed eigenstates is given by

$$|\Phi_0(t)\rangle = \exp(-iH_0t)|\Phi_0\rangle \quad . \tag{3.3}$$

In order to simplify the remaining problem of finding the fully perturbed eigenstates $|\Psi(t)\rangle$, it is convenient to introduce the "interaction representation" (Fetter and Walecka, 1971) by the transformation

$$|\Psi_I(t)\rangle = \exp(iH_0t)|\Psi(t)\rangle \ . \tag{3.4}$$

In this representation, the Schrödinger equation has the form

$$i \frac{\partial}{\partial t} |\Psi_I(t)\rangle = \exp(-\varepsilon|t|)V(t)|\Psi_I(t)\rangle \tag{3.5}$$

where

$$V(t) = \exp(iH_0t)V\exp(-iH_0t) \quad . \tag{3.6}$$

The time dependence of the interaction eigenstates can be expressed as

$$|\Psi_I(t)\rangle = U_\varepsilon(t,t_0)|\Psi_I(t_0)\rangle \tag{3.7}$$

where $U_\varepsilon(t,t_0)$ is the time-evolution operator. Substituting Eq. (3.7) into Eq. (3.5), the evolution operator is found to satisfy the differential equation

$$i \frac{\partial}{\partial t} U_\varepsilon(t,t_0) = \exp(-\varepsilon|t|)V(t)U_\varepsilon(t,t_0) \tag{3.8}$$

with the initial condition

$$U_\varepsilon(t_0,t_0) = 1 \ . \tag{3.9}$$

It is more convenient to solve for $U_\varepsilon(t,t_0)$ by first transforming Eq. (3.8) into an integral equation

$$U_\varepsilon(t,t_0) = 1 - i \int_{t_0}^{t} dt_1 \exp(-\varepsilon|t|)V(t_1)U_\varepsilon(t_1,t_0) \ . \qquad (3.10)$$

This integral equation has the form of the Volterra equation of the second kind (Löwdin, 1967) and is solved iteratively

$$U_\varepsilon(t,t_0) = 1 - i \int_{t_0}^{t} dt_1 \exp(-\varepsilon|t|)V(t_1)$$

$$+ (-i)^2 \int_{t_0}^{t} dt_1 \int_{t_0}^{t_1} dt_2 \exp\{-\varepsilon(|t_1|+|t_2|)\}V(t_1)V(t_2)U_\varepsilon(t_2,t_0) \qquad (3.11)$$

$$= \sum_{n=0}^{\infty} (-i)^n \int_{t_0}^{t} dt_1 \int_{t_0}^{t_1} dt_2 \ . \ . \ . \int_{t_0}^{t_{n-1}} dt_n \exp\{-\varepsilon(|t_1|+|t_2|+ \ . \ . \ . |t_n|)\}$$

$$x \ V(t_1)V(t_2) \ . \ . \ . \ V(t_n) \qquad t \geq t_1 \geq t_2 \geq \ . \ . \ . \geq t_n \ . \qquad (3.12)$$

Eq. (3.12) can be generalized slightly by modifying the limits of integration and introducing the time ordering operator, T,

$$U_\varepsilon(t,t_0) = \sum_{n=0}^{\infty} (-i)^n \frac{1}{n!} \int_{t_0}^{t} dt_1 \int_{t_0}^{t} dt_2 \ . \ . \ . \int_{t_0}^{t} dt_n$$

$$x \exp\{-\varepsilon(|t_1|+|t_2|+ \ . \ . \ . |t_n|)\} \ T[V(t_1)V(t_2) \ . \ . \ . \ V(t_n)] \ . \qquad (3.13)$$

The time ordering operator rearranges the product of perturbation operators such that the left-most term is the latest in chronological order.

The perturbed eigenstates $|\Psi_I(t_0)\rangle$ can now be expressed in terms of the unperturbed eigenstates by noting that as $t_0 \to \pm\infty$, $|\Psi_I(t_0)\rangle \to |\Phi_0\rangle$, and as t_0 increases from $-\infty$ to zero, the perturbation is "adiabatically switched on"

$$|\Psi_I(0)\rangle = U_\varepsilon(o,-\infty)|\Phi_0\rangle \quad . \tag{3.14}$$

According to a theorem of Gell-Mann and Low (1951), if

$$\lim_{\varepsilon\to 0} \frac{U_\varepsilon(o,-\infty)|\Phi_0\rangle}{\langle\Phi_0|U_\varepsilon(o,-\infty)|\Phi_0\rangle} \equiv \frac{|\Psi_I(0)\rangle}{\langle\Phi_0|\Psi_I(0)\rangle} \tag{3.15}$$

exists, then it is an eigenstate of H

$$\frac{H|\Psi_I(0)\rangle}{\langle\Phi_0|\Psi_I(0)\rangle} = \frac{E|\Psi_I(0)\rangle}{\langle\Phi_0|\Psi_I(0)\rangle} \quad . \tag{3.16}$$

These results can now be used to determine the electron propagator. In Chapter 1, the propagator was defined as the ground state average of a time-ordered product of field operators in the Heisenberg representation

$$iG_{ij}(t) = \frac{\langle\Psi_H|T[a_i(t)a_j^\dagger(0)]|\Psi_H\rangle}{\langle\Psi_H|\Psi_H\rangle} \quad . \tag{3.17}$$

Using Eq. (3.15) and the fact that $|\Psi_H\rangle=|\Psi_I(0)\rangle$, this average can be expressed in the interaction representation as

$$iG_{ij}(t) = \frac{\langle\Phi_0|U_\varepsilon(\infty,t)T[a_i(t)a_j^\dagger(0)]U_\varepsilon(t,-\infty)|\Phi_0\rangle}{\langle\Phi_0|U_\varepsilon(-\infty,\infty)|\Phi_0\rangle} \quad . \tag{3.18}$$

Using the expansion of the evolution operator (Eq. (3.13)) and taking the limit $\varepsilon\to 0$, it can be shown (Fetter and Walecka, 1971) that

$$iG_{ij}(t) = \sum_{n=0}^{\infty} (-i)^n \frac{1}{n!} \int_{-\infty}^{\infty} dt_1 \ . \ . \ . \int_{-\infty}^{\infty} dt_n$$

$$\times \frac{\langle\Phi_0|T[V(t_1) \ . \ . \ . \ V(t_n)a_i(t)a_j^\dagger(0)]|\Phi_0\rangle}{\langle\Phi_0|U(-\infty,\infty)|\Phi_0\rangle} \tag{3.19}$$

The final step in the diagrammatic expansion method is to expand the numerators of each term in Eq. (3.19) using Wick's theorem (Wick, 1950) and to represent them diagrammatically (e.g. Fetter and Walecka, 1971). The denominator of Eq. (3.19) must also be expanded and diagrammed, and when this is done, all disconnected diagrams arising from the expansion of the numerator will cancel (Abrikosov et al., 1965).

Formally, the diagrammatic expansion method and the superoperator formalism appear strikingly dissimilar. The diagrammatic method is formulated in the causal representation while the superoperator formalism utilizes the energy representation. The diagrammatic method employs a pictorial representation of the algebraic structure while the superoperator formalism emphasizes the algebraic structure directly. Yet the primary goal of each formalism is the same: an accurate prediction of ionization energies and electron affinities. Therefore, the two formalisms are inherently equivalent. It is our desire in this chapter to explicitly demonstrate the equivalence between these two formalisms and to re-examine the superoperator decoupling approximations in terms of a diagrammatic analysis.

3.2 Perturbation Theory

The unifying feature of the diagrammatic expansion method and the superoperator formalism is perturbation theory (Born and Öhrn, 1978). Since the commutator product is distributive with respect to addition, we can define a partitioning of the superoperator Hamiltonian into an unperturbed part plus a perturbation,

$$\hat{H} = \hat{H}_0 + \hat{V} \ . \tag{3.20}$$

One convenient partitioning, which will be shown to readily yield the Hartree-Fock propagator as the unperturbed electron propagator, is the Møller-Plesset partitioning (Møller and Plesset, 1934). With this partitioning, H_0 has the form

$$H_0 = \sum_r \varepsilon_r a_r^\dagger a_r - \tfrac{1}{2} \sum_{r,r'} \langle rr'||rr'\rangle \langle n_r\rangle \langle n_{r'}\rangle \tag{3.21}$$

and the perturbation is expressed as

$$V = \sum_{r,r',s,s'} \langle rr'||ss'\rangle [\tfrac{1}{4} a_r^\dagger a_{r'}^\dagger a_{s'} a_s - \delta_{r's'} \langle n_{r'}\rangle a_r^\dagger a_s] + \tfrac{1}{2} \sum_{r,r'} \langle rr'||rr'\rangle \tag{3.22}$$

Of course, when the commutator product is formed for the superoperators, the constant term in these definitions will cancel.

Other partitionings of the Hamiltonian may also be assumed and may lead to superior convergence properties (Claverie *et al.*, 1967). One alternative partitioning which has been employed in the perturbation calculation of correlation corrections to the total energy is the Epstein-Nesbet partitioning (Epstein, 1926, Nesbet, 1955a, 1955b). In propagator applications, the work of Kurtz and Öhrn (1978) may be roughly interpreted in terms of a partitioning where the unperturbed Hamiltonian incorporates all relaxation contributions to the ionization energy. It is difficult to define this unperturbed Hamiltonian explicitly, but it formally satisfies the eigenvalue equation

$$\hat{H}_0' a_k = \Delta E_k(\mathrm{SCF}) a_k \tag{3.23}$$

in contrast to

$$\hat{H}_0 a_k = \varepsilon_k a_k \tag{3.24}$$

for the Møller-Plesset partitioning. The method of Kurtz and Öhrn yields

excellent ionization energies and electron affinities with a simple second-order self-energy, however it has not been formally analyzed in detail.

Corresponding to the partitioning of the superoperator Hamiltonian, we can introduce a partitioning of the operator space defined by the projection superoperators $\hat{O}$ and $\hat{P}$,

$$\hat{O} = \sum_k |a_k)(a_k| = |\underline{a})(\underline{a}| \tag{3.25}$$

$$\hat{P} = \hat{I} - \hat{O} \tag{3.26}$$

These superoperators operate on elements of the operator space through the relations

$$\hat{O}X_i = \sum_k |a_k)(a_k|X_i) \tag{3.27}$$

$$\hat{P}X_i = X_i - \hat{O}X_i \tag{3.28}$$

and are idempotent ($\hat{O}^2 = \hat{O}$, $\hat{P}^2 = \hat{P}$), self-adjoint ($\hat{O}^\dagger = \hat{O}$, $\hat{P}^\dagger = \hat{P}$), and mutually exclusive ($\hat{O}\hat{P}=\hat{P}\hat{O}=0$). The superoperator $\hat{O}$ projects from an arbitrary operator product that part which lies in the model subspace, i.e. that part which is spanned by the eigenelements of $\hat{H}_0$. The superoperator $\hat{P}$ projects onto the orthogonal complement of the model subspace, i.e. that part which we have no *a priori* knowledge about.

To obtain a perturbation expansion of the superoperator resolvent, we consider its outer projection (Löwdin, 1965) onto the model subspace,

$$\hat{G}(E) = \hat{O}(E\hat{I}-\hat{H})^{-1}\hat{O} \tag{3.29}$$

$$= \hat{O}(E\hat{I}-\hat{H}_0-\hat{V})^{-1}\hat{O} \tag{3.30}$$

By iterating the identity

$$(A-B)^{-1} = A^{-1} + A^{-1}B(A-B)^{-1} , \tag{3.31}$$

the inverse in Eq. (3.30) can be expanded as

$$\hat{G}(E) = (E\hat{I}-\hat{H}_0)^{-1}\hat{O} + (E\hat{I}-\hat{H}_0)^{-1}\hat{O}\hat{V}(E\hat{I}-\hat{H}_0)^{-1}\hat{O}$$

$$+ (E\hat{I}-\hat{H}_0)^{-1}\hat{O}\hat{V}(E\hat{I}-\hat{H}_0)^{-1}\hat{V}(E\hat{I}-\hat{H}_0)^{-1}\hat{O} + \ldots \tag{3.32}$$

where the property

$$[\hat{H}_0,\hat{O}]_- = 0 \tag{3.33}$$

has been used. Now since $\hat{O}$ plus $\hat{P}$ form a resolution of the identity, each resolvent of $\hat{H}_0$ occurring between perturbation superoperators, $\hat{V}$, can be rewritten as a sum of its projections on the model subspace and the orthogonal complement,

$$(E\hat{I}-\hat{H}_0)^{-1} = (E\hat{I}-\hat{H}_0)^{-1}\hat{O} + (E\hat{I}-\hat{H}_0)^{-1}\hat{P} \tag{3.34}$$

$$= \hat{G}_0(E) + \hat{T}_0(E) . \tag{3.35}$$

With this notation, Eq. (3.32) becomes

$$\hat{G}(E) = \hat{G}_0(E) + \hat{G}_0(E)\hat{V}\hat{G}_0(E) + \hat{G}_0(E)\hat{V}[\hat{G}_0(E) + \hat{T}_0(E)]\hat{V}\hat{G}_0(E)$$

$$+ \hat{G}_0(E)\hat{V}[\hat{G}_0(E) + \hat{T}_0(E)]\hat{V}[\hat{G}_0(E) + \hat{T}_0(E)]\hat{V}\hat{G}_0(E) + \ldots \tag{3.36}$$

and can be resummed to yield

$$\hat{G}(E) = \hat{G}_0(E) + \hat{G}_0(E)[\hat{V} + \hat{V}\hat{T}_0(E)\hat{V} + \hat{V}\hat{T}_0(E)\hat{V}\hat{T}_0(E)\hat{V} + \ldots]\hat{G}(E) \tag{3.37}$$

Defining the reduced resolvent of the full superoperator Hamiltonian as

$$\hat{T}(E) = \hat{P}[\alpha\hat{O} + \hat{P}(E\hat{I}-\hat{H})\hat{P}]^{-1}\hat{P} \qquad (\alpha\neq 0) \tag{3.38}$$

$$= \hat{T}_0(E) + \hat{T}_0(E)\hat{V}\hat{T}(E) , \tag{3.39}$$

Eq. (3.37) can be written in closed form

$$\hat{G}(E) = \hat{G}_0(E) + \hat{G}_0(E)[\hat{V} + \hat{V}\hat{T}(E)\hat{V}]\hat{G}(E) \ . \tag{3.40}$$

Alternatively, we can define wave and reaction superoperators through the equations (cf. Löwdin, 1962, or Brandow, 1967)

$$\hat{W}(E) = \hat{I} + \hat{T}(E)\hat{V} \tag{3.41}$$

$$\hat{t}(E) = \hat{V}\hat{W}(E) \ . \tag{3.42}$$

The reduced resolvent, wave, and reaction superoperators introduced in this section are functions of the superoperators $\hat{I}$, $\hat{H}_0$, and $\hat{V}$ and as a consequence, operate in a more complicated way. To apply a superoperator function to an operator in the operator space, it must first be expanded in terms of the superoperators $\hat{I}$, $\hat{H}_0$, and $\hat{V}$ which are then successively applied to the operator. For example,

$$\hat{W}(E)X_i = [\hat{I} + \hat{T}(E)\hat{V}]X_i \tag{3.43}$$

$$= [\hat{I} + \hat{T}_0(E)\hat{V} + \hat{T}_0(E)\hat{V}\hat{T}_0(E)\hat{V} + \ . \ . \ . \ ]X_i \tag{3.44}$$

where

$$\hat{T}_0(E)\hat{V}X_i = [E^{-1}\hat{I} + E^{-2}\ \hat{H}_0 + E^{-3}\ \hat{H}_0^2 + \ . \ . \ . \ ]\hat{P}\hat{V}X_i \ , \tag{3.45}$$

etc.

3.3 Equivalence of the Superoperator Formalism and the Diagrammatic Expansion Method

Eqs. (3.37) and (3.40) represent the superoperator form of the Dyson equation (Dyson, 1949), and the reaction superoperator (Eq. (3.42)) can be identified as the self-energy. To demonstrate that Eq. (3.37)

corresponds term by term with the diagrammatic propagator expansion, we must first form the operator average of $\hat{G}(E)$ to obtain the matrix Dyson equation, next evaluate all necessary operator averages, and finally diagram the resulting algebraic formulae. Owing to the complicated operator averages that must be evaluated in third and higher orders of the perturbation superoperator, the equivalence between these two formalisms has only been explicitly demonstrated through third order and is assumed in all higher orders.

The matrix Dyson equation is obtained by forming the operator average of $\hat{G}(E)$ with respect to the basis elements of our model subspace

$$\underline{G}(E) = (\underline{a}|\hat{G}(E)\underline{a}) \tag{3.46}$$

$$= \underline{G}_0(E) + \underline{G}_0(E)\underline{\Sigma}(E)\underline{G}(E) \ , \tag{3.47}$$

where

$$\underline{\Sigma}(E) = (\underline{a}|\hat{V}\underline{a}) + (\underline{a}|\hat{V}\hat{T}_0(E)\hat{V}\underline{a})$$

$$+ (\underline{a}|\hat{V}\hat{T}_0(E)\hat{V}\hat{T}_0(E)\hat{V}\underline{a}) + \ . \ . \ . \ . \tag{3.48}$$

Since $\hat{H}_0$ was chosen to be the Fock superoperator, the appropriate density operator to employ in the evaluation of the operator averages is the Hartree-Fock density operator. Realizing that the grand canonical density operator (Eq. (1.44)) reduces to the Hartree-Fock density operator when pure state occupation numbers of zero or one are chosen, we shall employ this density operator.

Beginning with the evaluation of matrix elements for the unperturbed propagator, $\underline{G}_0(E)$, the Hartree-Fock propagator is easily obtained (cf. Section 1.3)

$$G_0(E)_{ij} = (a_j|(E\hat{I}-\hat{H}_0)^{-1}a_i) \tag{3.49}$$

$$= E^{-1}(a_j|a_i) + E^{-2}(a_j|\hat{H}_0 a_i) + E^{-3}(a_j|\hat{H}_0^2 a_i) + \ldots \tag{3.50}$$

$$= E^{-1}\delta_{ij} + E^{-2}\varepsilon_i\delta_{ij} + E^{-3}\varepsilon_i^2\,\delta_{ij} + \ldots \tag{3.51}$$

$$G_0(E)_{ij} = (E-\varepsilon_i)^{-1}\delta_{ij} \tag{3.52}$$

The evaluation of each term in the self-energy expansion requires the initial evaluation of $\hat{V}a_i$,

$$\hat{V}a_i = \tfrac{1}{4}\sum_{r,r',s,s'} \langle rr'||ss'\rangle [a_i, a_r^\dagger a_{r'}^\dagger a_{s'} a_s]_- - \sum_{r,s,s'} \langle rs'||ss'\rangle [a_i, a_r^\dagger a_s]_- \tag{3.53}$$

$$= \tfrac{1}{2}\sum_{r,s,s'} \langle ir||ss'\rangle a_r^\dagger a_{s'} a_s - \sum_{s,s'} \langle is'||ss'\rangle \langle n_{s'}\rangle a_s \,. \tag{3.54}$$

With this result, the first-order term $(a_j|\hat{V}a_i)$ is obtained without much additional effort

$$\Sigma^{(1)}(E)_{ij} = (a_j|\hat{V}a_i) \tag{3.55}$$

$$= \tfrac{1}{2}\sum_{r,s,s'} \langle ir||ss'\rangle \mathrm{Tr}\{\rho[a_r^\dagger a_{s'} a_s, a_j^\dagger]_+\} - \sum_{s,s'} \langle is'||ss'\rangle \langle n_{s'}\rangle \mathrm{Tr}\{\rho[a_s, a_j^\dagger]_+\} \tag{3.56}$$

$$= \sum_{r,s} \langle ir||js'\rangle \langle n_{s'}\rangle \delta_{rs'} - \sum_{s} \langle is'||js'\rangle \langle n_{s'}\rangle \tag{3.57}$$

$$\Sigma^{(1)}(E)_{ij} = 0 \,. \tag{3.58}$$

When the effective, single-particle potential used in the unperturbed problem is the Hartree-Fock self-consistent field potential, all single-particle corrections vanish (Bartlett and Silver, 1975a).

The evaluation of the second- and higher-order self-energy matrices requires the evaluation of $\hat{T}_0(E)\hat{V}a_i$ and $\hat{V}\hat{T}_0(E)\hat{V}a_i$. The first of these quantities can be expanded as

$$\hat{T}_0(E)\hat{V}a_i = (E\hat{I}-\hat{H}_0)^{-1}\hat{P}\hat{V}a_i \tag{3.59}$$

$$= (E\hat{I}-\hat{H}_0)^{-1}\hat{V}a_i - \sum_k (E\hat{I}-\hat{H}_0)^{-1}|a_k)(a_k|\hat{V}a_i) \tag{3.60}$$

using Eq. (3.26). It follows from the previous result for $(a_j|\hat{V}a_i)$ that the second term in Eq. (3.60) vanishes. The first term can now be evaluated by expanding the resolvent of $\hat{H}_0$ and realizing that any operator product is an eigenelement to $\hat{H}_0$, i.e.

$$\hat{H}_0 a_r^+ a_{s'} a_s = (\varepsilon_r-\varepsilon_{s'}-\varepsilon_s)a_r^+ a_{s'} a_s \quad . \tag{3.61}$$

Consequently, we obtain

$$\hat{T}_0(E)\hat{V}a_i = \tfrac{1}{2}\sum_{r,s,s'}(E+\varepsilon_r-\varepsilon_s-\varepsilon_{s'})^{-1}\langle ir||ss'\rangle\, a_r^+ a_{s'} a_s$$

$$- \sum_{s,s'}(E-\varepsilon_s)^{-1}\langle is'||ss'\rangle\langle n_{s'}\rangle a_s \tag{3.62}$$

with the help of Eq. (3.45). The remaining application of $\hat{V}$ and the average value evaluation is straightforward and yields

$$\Sigma^{(2)}(E)_{ij} = (a_j|\hat{V}\hat{T}_0(E)\hat{V}a_i) \tag{3.63}$$

$$= \sum_{r,s,s'}\frac{\langle ir||ss'\rangle\langle ss'||jr\rangle}{(E+\varepsilon_r-\varepsilon_s-\varepsilon_{s'})}\left[\tfrac{1}{2}\langle n_r\rangle+\tfrac{1}{2}\langle n_s\rangle\langle n_{s'}\rangle-\langle n_r\rangle\langle n_{s'}\rangle\right] \tag{3.64}$$

for the matrix elements of the second-order self-energy.

The Hartree-Fock average is now obtained by choosing occupation numbers of zero and one. An examination of the occupation number factor in Eq. (3.64) reveals that with this restriction, it will be non-vanishing

only when the summation index r runs over occupied spin orbitals and s and s' run over unoccupied spin orbitals or when r runs over unoccupied spin orbitals and s and s' run over occupied spin orbitals. Denoting a, b, c, . . . as summation indices over occupied spin orbitals; p, q, r, . . . for unoccupied spin orbitals; and i, j, k, . . . for unspecified spin orbitals, Eq. (3.64) can now be written as two terms which involve restricted spin orbital summations

$$\Sigma^{(2)}(E)_{ij} = \tfrac{1}{2} \sum_{a,p,q} \frac{\langle ia||pq\rangle\langle pq||ja\rangle}{(E+\epsilon_a-\epsilon_p-\epsilon_q)} + \tfrac{1}{2} \sum_{p,a,b} \frac{\langle ip||ab\rangle\langle ab||jp\rangle}{(E+\epsilon_p-\epsilon_a-\epsilon_b)} \quad . \tag{3.65}$$

The conversion of Eq. (3.65) into diagrams is a straightforward procedure for which we shall use the rules and diagram convention of Brandow (1967) and Bartlett and Silver (1975b). This convention represents the synthesis of the antisymmetrized vertices of the Hugenholtz (1957) or Abrikosov (1965) diagrams with the extended interaction lines of the Goldstone (1957) diagrams, and the rules for constructing these diagrams are given in Table 5. The application of these rules to the terms in Eq. (3.65) yields the following diagrams:

$$\tfrac{1}{2} \sum_{a,p,q} \frac{\langle ia||pq\rangle\langle pq||ja\rangle}{(E+\epsilon_a-\epsilon_p-\epsilon_q)} \tag{3.66}$$

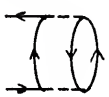

$$\tfrac{1}{2} \sum_{p,a,b} \frac{\langle ip||ab\rangle\langle ab||jp\rangle}{(E+\epsilon_p-\epsilon_a-\epsilon_b)} \tag{3.67}$$

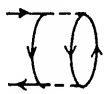

These diagrams are precisely the same as those obtained in the second-order diagrammatic expansion after a Fourier transformation into the energy representation (Cederbaum and Domcke, 1977).

Table 5. Rules for Constructing Self-Energy Diagrams.

1. Each antisymmetrized two-electron integral factor in the numerator is represented by an interaction line with a vertex (dot) at both ends. The number of interaction lines denotes the order of the term.

2. Using the Dirac bra-ket notation, both indices in the bra are represented by lines leaving a vertex while those of the ket are represented by lines entering a vertex. There must be only one outgoing and one incoming line per vertex, therefore, assign the index of electron coordinate one to the left vertex and the index of electron coordinate two to the right vertex of each interaction line.

3. Summation indices running over hole states (occupied orbitals) are directed downward, indices running over particle states (unoccupied orbitals) are directed upward, and external indices (not summed) are drawn horizontally.

To Check Diagrams:

4. The energy denominator of the diagrammed expression should be obtained by first connecting the external lines and assigning a factor of E to this directed segment. Second, imagine horizontal lines drawn between each pair of interaction lines. Each horizontal line corresponds to a multiplicative, denominator factor obtained by summing the orbital energies of each hole (downgoing) line that intersects it minus the sum of orbital energies for particle (upgoing) lines that intersect it. Treat the factor E of the connected external lines as an orbital energy.

5. Numerical factors should be obtained by assigning a factor of $\frac{1}{2}$ for each pair of equivalent internal lines. Equivalent internal lines are two lines which begin on the same interaction line, end on the same interaction line, and go in the same direction.

6. The overall sign factor should be obtained by assigning a factor of minus one to each internal hole line segment and a minus one to each closed loop.

The evaluation of the third-order self-energy matrix is similar to the second-order matrix but much more tedious and the result is presented in Appendix 3. As was done for the second-order expression, the occupation numbers must again be restricted to zero and one to obtain the Hartree-Fock average. When this restriction is made, the unrestricted spin orbital summations in Appendix 3 will reduce to summations involving occupied, unoccupied, and unspecified spin orbitals. Using the algebraic identity

$$\frac{A}{(E-a)(E-b)} = \frac{A}{(a-b)} \left[\frac{1}{(E-a)} - \frac{1}{(E-b)} \right] \tag{3.68}$$

it is possible to combine terms in such a way that expressions involving only occupied and unoccupied spin orbital summations are obtained. These expressions are presented in Appendix 1. The corresponding diagrams in Appendix 1 again are precisely those occurring in the third-order, diagrammatic self-energy expansion.

3.4 Diagram Conserving Decoupling

The wave and reaction superoperators identified with the help of perturbation theory in Section 3.2 have special importance in the development of decoupling approximations for the electron propagator. As we have already seen, the reaction superoperator generates the diagrammatic self-energy expansion. A truncation of this expansion offers one viable decoupling scheme. The wave superoperator, on the other hand, has the property of generating eigenelements to the full superoperator Hamiltonian from the eigenelements of the unperturbed superoperator Hamiltonian

$$(E\hat{I}-\hat{H})\hat{W}(E)\underline{a} = 0 \quad . \tag{3.69}$$

This property is easily proven by first using Eq. (3.41) to expand $\hat{W}(E)$ and then premultiplying both sides of Eq. (3.69) by $\hat{P}$

$$(E\hat{I}-\hat{H})\hat{W}(E)\underline{a} = (E\hat{I}-\hat{H})\underline{a} + (E\hat{I}-\hat{H})\hat{T}(E)\hat{V}\underline{a} \tag{3.70}$$

$$\hat{P}(E\hat{I}-\hat{H})\hat{W}(E)\underline{a} = \hat{P}(E\hat{I}-\hat{H})\underline{a} + \hat{P}(E\hat{I}-\hat{H})\hat{T}(E)\hat{V}\underline{a} \quad . \tag{3.71}$$

Using the identity

$$\hat{P}(E\hat{I}-\hat{H})\hat{T}(E) = \hat{P} \tag{3.72}$$

and the property $\hat{P}\underline{a} = 0$, Eq. (3.71) simplifies to

$$\hat{P}(E\hat{I}-\hat{H})\hat{W}(E)\underline{a} = -\hat{P}\hat{V}\underline{a} + \hat{P}\hat{V}\underline{a} = 0 \tag{3.73}$$

which implies the validity of Eq. (3.69)

It is of interest at this point to show a connection between the superoperator formalism and the Equations of Motion (EOM) method for determining ionization energies (Simons and Smith, 1973). In this method, one seeks solutions of the equation

$$[H,Q]_{-} = \omega Q \tag{3.74}$$

which is precisely Eq. (3.69). Here the operator Q is interpreted as a correlated ionization operator that generates, in principle, the exact (N-1)-electron ion states from the exact N-electron reference state. One approach to solving Eq. (3.74) involves the application of Rayleigh-Schrödinger perturbation theory (Dalgaard and Simons, 1977). By partitioning the Hamiltonian operator, expanding both the ionization operator, Q, and the ionization energy, ω, in terms of a perturbation parameter, and collecting terms of the same order, a set of perturbation theory equations are obtained. The solution of these equations yields an expansion for Q which is analogous to the superoperator equation

$$\underline{h} = \hat{W}(E)\underline{a} \quad . \tag{3.75}$$

The only difference is that E is replaced by ω_0 which is a consequence of using Rayleigh-Schrödinger rather than Brillioun-Wigner perturbation theory.

Returning now to the inner projection of the superoperator resolvent,

$$\underline{G}(E) = (\underline{a}|\underline{h})(\underline{h}|(EI-H)\underline{h})^{-1}(\underline{h}|\underline{a}) \tag{3.76}$$

we may view Eq. (3.75) as an alternative prescription for choosing the inner projection operator manifold. Recalling from Section 1.6 that since the density operator describing the unperturbed (model) problem does not commute with the full Hamiltonian, the operator scalar product will not in general exhibit Hermitian symmetry. Consequently, we define

$$(\underline{h}| = (\underline{a}|\hat{W}^{\dagger}(E) \tag{3.77}$$

and note that

$$(\underline{a}|\hat{W}^{\dagger}(E) \neq (\hat{W}(E)\underline{a}| \quad . \tag{3.78}$$

Approximate electron propagator decouplings can now be obtained by truncating the expansion of the wave superoperator,

$$\hat{W}(E) = \hat{I} + \hat{T}_0(E)\hat{V} + \hat{T}_0(E)\hat{V}\hat{T}_0(E)\hat{V} + \ldots . \tag{3.79}$$

Truncation of this expansion, with only the superoperator identity, trivially yields the Hartree-Fock propagator, therefore we next consider

$$\hat{W}(E) = \hat{I} + \hat{T}_0(E)\hat{V} \quad . \tag{3.80}$$

Noting that the subspaces $\{a_k\}$ and $\{f_k | f_k = \hat{T}_0(E)\hat{V}a_k\}$ are mutually orthogonal, Eq. (3.76) can be readily solved for $\underline{G}^{-1}(E)$

$$\underline{G}^{-1}(E) = \underline{G}_0^{-1}(E) - \underline{\Sigma}(E) \ , \tag{3.81}$$

where

$$\underline{\Sigma}(E) = (\underline{a}|\hat{\hat{V}}\hat{\hat{T}}_0(E)\hat{V}\underline{a})(\underline{a}|\hat{\hat{V}}\hat{\hat{T}}_0(E)(E\hat{I}-\hat{H})\hat{T}_0(E)\hat{V}\underline{a})^{-1}(\underline{a}|\hat{\hat{V}}\hat{\hat{T}}_0(E)\hat{V}\underline{a}) \tag{3.82}$$

Making the following identifications from Section 3.3:

$$(\underline{a}|\hat{\hat{V}}\hat{\hat{T}}_0(E)\hat{V}\underline{a}) = \Sigma^{(2)}(E) \ , \tag{3.83}$$

$$(\underline{a}|\hat{\hat{V}}\hat{\hat{T}}_0(E)(E\hat{I}-\hat{H}_0)\hat{T}_0(E)\hat{V}\underline{a}) = \underline{\Sigma}^{(2)}(E) \ , \tag{3.84}$$

and

$$(\underline{a}|\hat{\hat{V}}\hat{\hat{T}}_0(E)\hat{\hat{V}}\hat{\hat{T}}_0(E)\hat{V}\underline{a}) = \underline{\Sigma}^{(3)}(E) \ , \tag{3.85}$$

Eq. (3.82) can be rewritten

$$\underline{\Sigma}(E) = \underline{\Sigma}^{(2)}(E)[\underline{\Sigma}^{(2)}(E) - \underline{\Sigma}^{(3)}(E)]^{-1}\underline{\Sigma}^{(2)}(E) \ . \tag{3.86}$$

Expanding the inverse of Eq. (3.86), we easily see that this self-energy approximant coincides with the diagrammatic expansion through third order but additionally yields contributions to all higher orders. If the exact self-energy is rewritten as a moment expansion in terms of a perturbation parameter, λ,

$$\lambda^{-1}\underline{\Sigma}(E) = \sum_{k=0}^{\infty} \lambda^k(\underline{a}|\hat{V}(\hat{T}_0(E)\hat{V})^k\underline{a}) \ , \tag{3.87}$$

we see that Eq. (3.86) represents the [1,1] Pade' approximant to this expansion. Owing to the close connection between Pade' approximants and the inner projection technique as demonstrated in Chapter 2, this result is not surprising. These Pade' approximants to the self-energy, however, will have entirely different convergence properties than those studied in Chapter 2.

3.5 Approximations and Applications

Computational applications of the [1,1] Pade' approximant to the self-energy require the evaluation of the second- and third-order self-energy matrices. The second-order matrix is relatively easy to evaluate. The third-order matrix, on the other hand, is exceedingly more difficult and can presently be only approximately calculated without excessive computational effort. An examination of the formulae in Appendix 3 reveals that unlike the fourth moment matrix in the moment conserving decoupling, the third-order self-energy matrix is energy dependent. This additional complication makes the partial summation technique used in the moment conserving decoupling ineffectual since the third-order self-energy matrix will generally need to be resummed with different values of E hundreds of times in the search for poles of the propagator.

The first approximation that we will examine is the complete neglect of the third-order self-energy matrix. With this approximation, the [1,1] approximant in Eq. (3.86) reduces to a second-order truncation of the diagrammatic self-energy expansion,

$$\underline{\Sigma}(E) = \underline{\Sigma}^{(2)}(E) \ . \tag{3.88}$$

This second-order self-energy approximation is interesting not only because it contains the most important relaxation and correlation corrections to Koopmans' theorem (in a perturbation theoretical sense), but also because it exhibits the same analytic form as the exact self-energy (Hedin and Lundqvist, 1969, Cederbaum and Domcke, 1977). Furthermore, since several second-order, ionization energy calculations have been reported in the literature, this approximation will afford both a convenient check of new computer code and the computational experience necessary to implement more refined approximations.

The first computational application of this decoupling approximation was to the water molecule using the same basis and internuclear geometry as described in Section 2.4. The results of this calculation are presented in Table 6 along with the Koopmans' theorem, $\Delta E(SCF)$, and experimental values for the ionization energies. Two ionization energies have been tabulated for the $2a_1$ ionization with their corresponding pole strength (Γ_k of Eq. (1.70)) in parentheses. The occurence of two, relatively strong propagator poles for this ionization represents a breakdown in the quasi-particle description of inner valence ionizations (Cederbaum, 1977) and makes assignments of principal and shake-up ionizations ambiguous.* In general, the second-order ionization energies are quite encouraging and represent significant improvements to each of the Koopmans' values. Furthermore, these results are comparable in accuracy to the $\Delta E(SCF)$ results but possess the convenience of being obtained in a single calculation whereas the $\Delta E(SCF)$ results required six separate Hartree-Fock calculations.

The relatively poor agreement of the $3a_1$ and $1b_1$ ionization energies with the experimental values in Table 6 seems attributable to basis incompleteness. Despite the lack of polarization functions, this suspicion is supported by the facts that the $3a_1$ orbital is the highest occupied orbital in that symmetry and that this basis contains only two contracted Gaussian orbitals of b_1 symmetry. In order to study the basis dependence of the second-order self-energy approximation, two additional calculations

---

*The ESCA spectrum of the water molecule (Siegbahn et al., 1969) substantiates this phenomenon since the $2a_1$ peak is quite broad and asymmetric. Experimentally, it appears that the lower energy ionization should have a larger pole strength (in contrast with the results of Table 5) since the peak is skewed to higher binding energies.

Table 6. Principal Ionization Energies of Water Computed with the 14 CGTO Basis.

Orbital	Koopmans	$\Delta E(SCF)$[a]	$\Sigma^{(2)}(E)$	Exp.[b]
$1a_1$	559.4	540.8	539.4	540.2
$2a_1$	37.0	34.6	34.0 (.61) 32.6 (.28)	32.2
$3a_1$	15.4	13.0	12.9	14.7
$1b_1$	13.8	11.0	10.8	12.6
$1b_2$	19.5	17.8	18.1	18.6

[a]Goscinski *et al.* (1975).

[b]Siegbahn *et al.* (1969).

were performed with larger basis sets. The first of these calculations employed a 26 contracted orbital basis which augmented the original 14 orbitals (Table 3) with a set of p-orbitals on the hydrogen atoms and a set of d-orbitals on oxygen--all with unit exponents. The Hartree-Fock total energy obtained with this basis was E(HF)= -76.0459 H. The second calculation employed a 38 contracted orbital basis which included all of the orbitals in the 26 orbital basis plus an additional set of diffuse p-orbitals on the hydrogen atoms (α = 0.25) and a set of diffuse d-orbitals on oxygen (α = 0.40). This basis yielded a Hartree-Fock total energy of E(HF)= -76.0507 H.

The most significant propagator poles calculated in the valence region (0~40 eV) with each of the three water basis sets are presented in Table 7 along with the second-order results of Cederbaum (1973a). The inclusion of polarization functions not only improves the $3a_1$ and $1b_1$ ionization energies, it also reverses the relative pole strengths of the two dominant $2a_1$ poles bringing the theoretical results into better agreement with experimental observations (see footnote on page 73). Cederbaum's second-order results were obtained with a basis comparable in size and quality to the 26 orbital basis in Table 7. He deletes several virtual orbitals from this basis before computing the ionization energies, however. This approximation may account for the small discrepancies between his results and those reported here.

The formaldehyde molecule was chosen for a second application of the second-order self-energy approximation. Ionization energies were calculated using two basis sets. The first consisted of Huzinaga's 9s, 5p primitive basis sets for oxygen and carbon (Huzinaga, 1965) contracted to 4s and 2p functions with Dunning's contraction coefficients (Dunning,

Table 7. Basis Set Effects on the Ionization Energies of Water Computed with a Second-Order Self-Energy Approximation.

Symmetry	14 CGTO's	26 CGTO's	38 CGTO's	Ced.[a]
a_1	36.5 (.005)	37.1 (.003)		
	34.0 (.607)	33.4 (.288)	33.2 (.231)	
	32.6 (.279)	32.1 (.592)	31.9 (.628)	32.9
	12.9 (.913)	13.4 (.908)	13.5 (.903)	13.2
b_1	34.9 (.005)	35.1 (.005)		
	10.8 (.909)	11.1 (.904)	11.2 (.900)	10.9
b_2	40.6 (.003)	40.8 (.004)		
	18.1 (.931)	18.0 (.922)	18.0 (.919)	17.7
E(HF)	-76.0082	-76.0459	-76.0507	-76.0419

[a]Cederbaum (1973a).

1970). The orbital exponents of Huzinaga's 4s primitive basis for hydrogen were scaled by a factor of 1.2, and the resultant orbitals were contracted to 2s functions as recommended by Dunning. The complete basis appears in Table 8. The second basis augmented the first by the addition of one set of p-orbitals on the hydrogen atoms and one set of d-orbitals on both the oxygen and carbon atoms. Unit exponents were chosen for the p-orbitals on hydrogen while exponents of 0.8 were chosen for the d-orbitals. One- and two-electron integrals were computed with the MOLECULE program (Almlöf, 1974) at the experimental equilibrium geometry: R(CO)= 2.2825 a.u., R(CH)= 2.1090 a.u., and ∢(HCH)= 116.52^{o} (Oka, 1960, Takagi and Oka, 1963), and the Hartree-Fock calculations and two-electron integral transformations were performed with GRNFNC (Purvis, 1973). The Hartree-Fock total energy for the smaller, 24 orbital basis (no polarization) was E(HF)= -113.8257 H., and for the larger, 42 orbital basis (with polarization) E(HF)= -113.8901 H. The Hartree-Fock orbital energies and second-order self-energy results for both basis sets are presented in Table 9 for the principal ionizations along with the second-order results of Cederbaum et al. (1975) and the experimental values.

The results in Table 9 typify two general features of ionization energy calculations. The first is that Koopmans' theorem yields values which are usually higher than experimental ionization energies. Second, the inclusion of second-order relaxation and correlation corrections generally overcorrects the Koopmans' estimate and yields values which are usually lower than experiment. For several ionizations in Table 9, the second-order deviations from experiment are as large as the Koopmans' values only opposite in sign. Although it is possible that the larger, polarized basis used in the second calculation may still lack adequate

Table 8. Contracted Gaussian Basis for Formaldehyde.

Carbon s sets	
Exponents	Contraction Coefficients
4232.6100	0.002029
634.8820	0.015535
146.0970	0.075411
42.4974	0.257121
14.1892	0.596555
1.9666	0.242517
5.1477	1.000000
0.4962	1.000000
0.1533	1.000000

Oxygen s sets	
Exponents	Contraction Coefficients
7816.5400	0.002031
1175.8200	0.015436
273.1880	0.073771
81.1696	0.247606
27.1836	0.611832
3.4136	0.241205
9.5322	1.000000
0.9398	1.000000
0.2846	1.000000

Carbon p sets	
Exponents	Contraction Coefficients
18.1557	0.018534
3.9864	0.115442
1.1429	0.386206
0.3594	0.640089
0.1146	1.000000

Oxygen p sets	
Exponents	Contraction Coefficients
35.1832	0.019580
7.9040	0.124189
2.3051	0.394727
0.7171	0.627375
0.2137	1.000000

Hydrogen s sets	
Exponents	Contraction Coefficients
19.2406	0.032828
2.8992	0.231208
0.6535	0.817238
0.1776	1.000000

Table 9. Principal Ionization Energies for Formaldehyde.

	24		42			
Orbital	Koopmans	$\Sigma^{(2)}(E)$	Koopmans	$\Sigma^{(2)}(E)$	Ced.[a]	Exp.
$1a_1$	560.12	538.93	559.81	538.62	-	539.43[b]
$2a_1$	309.09	297.27	308.87	296.90	-	294.21[b]
$3a_1$	38.94	33.66	38.18	32.56	-	34.2[c]
$4a_1$	23.39	20.97	23.30	21.03	-	21.15[c]
$5a_1$	17.29	13.98	17.38	14.38	14.42	16.2[d]
$1b_1$	14.56	13.83	14.45	13.72	13.50	14.5[d]
$1b_2$	19.47	17.16	19.08	17.07	16.63	17.0[d]
$2b_2$	12.06	9.04	11.93	9.30	9.25	10.9[d]
E(HF)	-113.8257		-113.8901		-113.9012	

[a]Second order results of Cederbaum *et al.* (1975).

[b]Jolly and Schaaf (1976).

[c]Hood *et al.* (1976).

[d]Estimated center of gravity (Cederbaum and Domcke, 1977) from spectrum of Turner *et al.* (1970).

polarization functions, the rather large discrepancies between the second-order results and experiment more probably indicate that third- (and higher) order self-energy corrections are now sizable. The general conclusion that a second-order self-energy approximation is inadequate for an accurate calculation of ionization energies has been previously concluded by Cederbaum (1973b) and necessitates a re-examination of the approximation made in Eq. (3.88).

Rather than completely neglecting the third-order self-energy matrix, let us now consider an approximation that includes at least part of these contributions. Which third-order self-energy diagrams should be included? There are two well-established results that are relevant to this question: Studies of the electron gas model have shown that in the limit of high electron density, the so-called ring diagrams dominate the self-energy expansion (Pines, 1961), while in the limit of low electron density, the so-called ladder diagrams dominate (Galitskii, 1958). In order to determine whether atomic and molecular self-energies can be approximated by specific third-order diagrams (e.g. rings or ladders), we need to evaluate all third-order diagrams for some representative systems. Cederbaum (1975) has done this for several simple systems and has found that both ring and ladder diagrams dominate the third-order self-energy. This result implies that atoms and molecules lie somewhere between the high and low density extremes. It is therefore essential to include both ring and ladder diagrams in any third-order self-energy approximation. These diagrams are

rings ladders

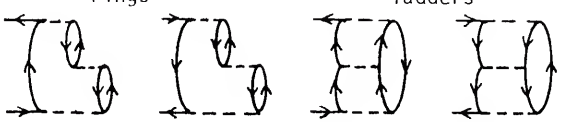

(3.89)

and correspond to the algebraic expressions labeled A, B, C, and D in Appendix 1.

We include six additional diagrams in our third-order self-energy approximation because of the computational efficiency with which they are evaluated. These diagrams are the energy independent diagrams

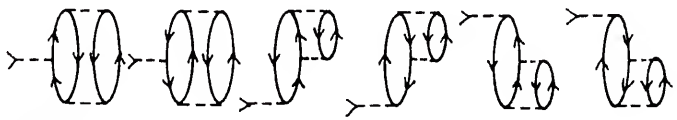

(3.90)

corresponding to expressions M-R in Appendix 1. For these six diagrams, it is feasible to employ the partial summation technique since they must be evaluated only once.

Approximating the full third-order self-energy matrix by only ring, ladder, and constant energy diagrams, let us now consider the solution of the Dyson equation with the [1,1] Pade' approximant to the self-energy expansion. Owing to the fact that the inner projection manifold from which the [1,1] approximant was derived is energy dependent (Eq. (3.80)), the simple analytic form of the self-energy eigenvalues, illustrated in Fig. 2, is lost. Furthermore, the self-energy poles are now given by

$$\det\left(\underline{\Sigma}^{(2)}(E) - \underline{\Sigma}^{(3)}(E)\right) = 0 \tag{3.91}$$

rather than by an eigenvalue problem and are consequently more difficult to obtain. For these reasons, the pole search described in Chapter 1 and used with the second-order self-energy approximation is no longer an efficient or reliable procedure. An alternative method of solution used in the following applications was to use the Hartree-Fock orbital energy as an initial guess to the propagator pole and to iterate Eq. (1.67) to convergence. When convergent, this procedure invariably yields

a principal propagator pole and its corresponding pole strength. Although the [1,1] self-energy approximant does not quarantee a positive pole strength, this was never a problem in any of the calculations reported here.

The principal ionization energies for the water molecule were calculated using both the 14 and 26 CGTO basis sets in order to evaluate the [1,1] Pade' approximant to the self-energy expansion, and the results appear in Table 10. The most significant feature of these results is that each ionization energy has been shifted from its second order value to higher energy and is now in better agreement with the experimental value. It is further noticed that the valence ionization energies are still smaller than the experimental values while the $1a_1$ (core) ionization energy is now larger than experiment. Apparently, the diagrams included in the third-order self-energy matrix overestimate the actual relaxation and correlation effects for this ionization.

Convergence difficulty was experienced for the $2a_1$ ionization energy using the 14 orbital basis. A schematic plot of $W_{2a_1}(E)$ is presented in Fig. 3 and reveals that there are no propagator poles in this energy region. This anomaly is no doubt a consequence of some quirk in the basis since the 26 orbital basis yields a very accurate $2a_1$ ionization energy.

3.6 Evaluation of the Diagram Conserving Decoupling

The algebraic structure of the superoperator formalism has been successfully exploited in this chapter to yield several new insights into the decoupling problem. The application of perturbation theory has demonstrated that the electron propagator equation of motion can be

Table 10. Comparison of Principal Ionization Energies for Water Obtained with the Second-Order and the [1,1] Self-Energies Using the 14 and 26 CGTO Basis Sets.

	14		26		
Orbital	$\Sigma^{(2)}(E)$	[1,1]	$\Sigma^{(2)}(E)$	[1,1]	Exp.[a]
$1a_1$	539.4	541.6	539.2	540.9	540.2
$2a_1$	34.0 (.607) 32.6 (.279)	no convergence (see text)	32.1	32.2	32.2
$3a_1$	12.9	13.4	13.4	13.6	14.7
$1b_1$	10.8	11.1	11.1	11.3	12.6
$1b_2$	18.1	18.4	18.0	no results	18.6

[a]Siegbahn *et al.* (1969).

Figure 3. A sketch of W_{2a_1} in the energy region of the $2a_1$ ionization obtained with the [1,1] self-energy approximant using the 14 CGTO basis.

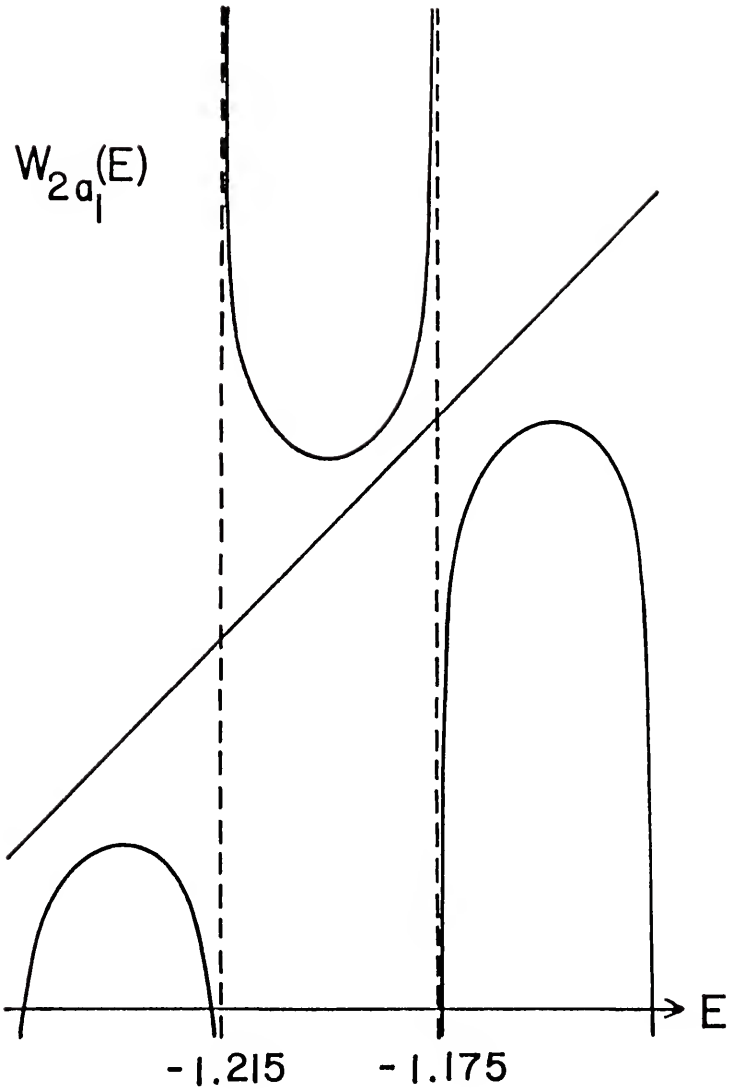
$W_{2a_1}(E)$
E
-1.215
-1.175

resummed to yield the equivalent of the diagrammatic expansion. This resummation also allows the identification of wave and reaction superoperators which have special importance in decoupling approximations. We have shown that when the inner projection manifold of the superoperator resolvent is chosen to consist of the first-order truncation of the wave superoperator, a [1,1] Pade' approximant to the self-energy expansion is obtained. This approximant is correct through third order and contains a geometric approximation to all higher orders. In general, the Nth-order truncation of the wave superoperator will yield an [N,N] Pade' approximant which is correct through the (2N+1)st order in the self-energy expansion. One final insight afforded by this decoupling is the realization that electron correlation can be described exclusively in the operator space. We argued in Chapter 1 that when the propagator was defined as a single-time Green's function, the density operator was arbitrary. We have now demonstrated in this chapter that any desired order in the self-energy expansion may be obtained using as a specific choice, the uncorrelated, Hartree-Fock density operator.

Computational applications of the diagram conserving decoupling have been encouraging. These applications have confirmed previous conclusions (Cederbaum, 1973b) that a second-order self-energy is generally inadequate for obtaining accurate ionization energies. It is important if not essential that third-order ring and ladder diagrams be included in any self-energy approximation although the errors arising from basis incompleteness may be of equal magnitude and hence cannot be ignored. The inclusion of the third-order ring, ladder, and constant energy diagrams in the [1,1] self-energy approximant has succeeded in improving the second-order results but even these results are not consistently better than the Koopmans' theorem values.

One important feature of the [1,1] self-energy approximant is that even though it is constructed from only the second- and third-order self-energy matrices, it contains a geometric approximation of all higher orders in the self-energy expansion. Certainly, some fourth- or higher-order terms may be just as important as third-order terms; therefore, this approximation is highly desirable. The fourth- and higher-order terms arising from the [1,1] self-energy approximant, however, are not readily analyzed diagrammatically. In fact, being a purely algebraic approximation, the [1,1] approximant may not yield any valid fourth- or higher-order diagrams. Given the fact that ring and ladder diagrams dominate the third-order self-energy matrix, one can argue that they may also dominate the higher orders of the self-energy expansion. An appropriate modification of this decoupling scheme might then allow the summation of these specific diagrams in all orders. Approximations of this type are referred to as renormalized decouplings and are examined within the superoperator formalism in the next chapter.

CHAPTER 4
RENORMALIZED DECOUPLINGS

4.1 Renormalization Theory

In Chapter 3, we tacitly assumed that the application of perturbation theory to the calculation of ionization energies and electron affinities was valid and that the resulting self-energy expansion was convergent. Historically however, it was discovered that in both the nuclear many-body problem and the electron gas model, the simple self-energy expansions are divergent. In order to remove these divergencies, it is necessary to sum certain appropriate classes of diagrams to all orders. This method of partial summations is known as renormalization theory (see e.g. Kumar, 1962 or Mattuck, 1967) and may be viewed as an analytic continuation of the perturbation expansion. Although a variety of renormalization procedures exist, such as propagator renormalizations, interaction renormalizations, and vertex renormalizations, the distinctions mainly depend on the types of diagrams included in the partial summation and are not particularly important for our consideration.

One renormalization that we are already familiar with is the [1,1] self-energy approximant derived in the preceding chapter. In fact, any rational self-energy approximant may be regarded as a renormalization since its geometric expansion will approximate all orders of the perturbation expansion. One problem encountered with the [1,1] approximant and that occurs in general for rational approximants derived via purely algebraic considerations is that their geometric expansions may contain

no readily identifiable diagrams (at least beyond the lowest orders). Since specific diagrams often dominate the self-energy expansion (such as ring and ladder diagrams for atoms and molecules) it is valuable to investigate whether the superoperator formalism can be adapted to yield renormalized self-energy expressions that sum specific diagrams. The solution as we shall see is rather simple and involves a restriction in the types of operator products allowed to span the orthogonal complement of the model subspace. As a specific example, the two particle-one hole Tamm-Dancoff approximation (2p-h TDA), (Schuck et al., 1973, Schirmer and Cederbaum, 1978), is derived from an effective interaction which is logically obtained by a projection of the perturbation superoperator onto the subspace spanned by 2p-h type operators (Born and Öhrn, 1979). Finally, the diagonal approximation to the full 2p-h TDA self-energy previously derived and applied to the calculation of ionization energies is shown to neglect terms which, in fact, are diagonal and are necessary to prevent an overcounting of all diagrams containing diagonal ladder parts.

4.2 Derivation of the 2p-h TDA and Diagonal 2p-h TDA Equations

Recalling some of the results of the previous chapter, we had obtained the matrix Dyson equation

$$\underline{G}(E) = \underline{G}_0(E) + \underline{G}_0(E)\underline{\Sigma}(E)\underline{G}(E) \ , \tag{4.1}$$

where the self-energy matrix, $\underline{\Sigma}(E)$, had the following expansion

$$\underline{\Sigma}(E) = (\underline{a}|\hat{V}+\hat{V}\hat{\hat{T}}_0(E)\hat{V}+\hat{V}\hat{\hat{T}}_0(E)\hat{V}\hat{\hat{T}}_0(E)\hat{V}+ \ . \ . \ . \ |\underline{a}) \ . \tag{4.2}$$

Introducing the reduced resolvent of the full superoperator Hamiltonian, $\hat{T}(E)$, which is just a projection of the superoperator resolvent on the orthogonal complement

$$\hat{T}(E) = \hat{P}[\alpha\hat{O}+(E\hat{I}-\hat{H}_0)\hat{P}-\hat{P}\hat{V}\hat{P}]^{-1}\hat{P} \ , \tag{4.3}$$

the self-energy expansion was written in closed form

$$\underline{\Sigma}(E) = (\underline{a}|\hat{V}\underline{a}) + (\underline{a}|\hat{V}\hat{T}(E)\hat{V}\underline{a}) \ . \tag{4.4}$$

It was further shown that when the grand canonical density operator is used to evaluate the operator averages, the first-order term vanishes.

When $\hat{P}$ is the exact projector of the orthogonal complement,

$$\hat{P} = \hat{I} - \hat{O} \ , \tag{4.5}$$

the term $\hat{P}\hat{V}\hat{P}$ in Eq. (4.3) is responsible for generating the operator products that span this subspace. The expansion of this term from the inverse and its repeated application in each order of the perturbation expansion yields larger and larger operator products which are only limited by the number of electrons in the reference state. If instead of allowing all possible operator products, we restrict them to some simple types which occur in each order, it may be possible to identify and sum specific diagrams in all orders of the perturbation expansion.

The restriction of the operator products in the orthogonal complement is achieved by approximating the orthogonal projector as

$$\hat{P} = |\underline{f})(\underline{f}| \tag{4.6}$$

where the manifold $\{\underline{f}\}$ contains the desired operator products. The projector $\hat{P}$ now has the effect of projecting from the perturbation expansion

only those operator products which lie in the subspace spanned by $\{\underline{f}\}$. The approximation to $\hat{P}$ in Eq. (4.6) must of course preserve the properties of the exact projector and should be idempotent, self-adjoint, and orthogonal to $\hat{0}$.

Our previous experience with the operator product decouplings suggests that the set of triple operator products $\{a_k^\dagger a_l a_m\}$ be chosen as a first approximation to $\hat{P}$. There is a stronger motivation for using this operator product, however. If the third-order ring and ladder diagrams in Eq. (3.70) are examined, it can be seen that between any two interaction lines there occurs only two particle lines (upgoing) and one hole line (downgoing) or vice versa. This implies that the intermediate or virtual states that are represented by these diagrams consist of only 2p-h or 2h-p excitations of the reference state. Both of these excitations are described with the triple-operator products.

The set of triple products $\{a_k^\dagger a_l a_m\}$ is not orthogonal to the simple operators of the model subspace, hence these two subspaces must be orthogonalized. Using the Gram-Schmidt orthogonalization procedure (see e.g. Pilar, 1968), we define

$$f_{klm} = N_{klm}^{-\frac{1}{2}}[a_k^\dagger a_l a_m - \Sigma_n (a_n | a_k^\dagger a_l a_m) a_n] \tag{4.7}$$

$$= N_{klm}^{-\frac{1}{2}}[a_k^\dagger a_l a_m + \delta_{km}\langle n_k\rangle a_l - \delta_{kl}\langle n_k\rangle a_m] \tag{4.8}$$

where

$$N_{klm} = \langle n_k\rangle - \langle n_k\rangle\langle n_l\rangle - \langle n_k\rangle\langle n_m\rangle + \langle n_l\rangle\langle n_m\rangle \ . \tag{4.9}$$

The projector

$$\hat{P} = \sum_{k,l,m} |f_{klm})(f_{klm}| \quad , \quad l<m \tag{4.10}$$

is now idempotent, self-adjoint, and orthogonal to $\hat{0}$. The projection of the perturbation superoperator on the 2p-h subspace, $\hat{P}\hat{V}\hat{P}$, which occurs in Eq. (4.3) can now be regarded as an effective interaction. The expansion of Eq. (4.3) with $\hat{P}$ defined as in Eq. (4.10) should yield all diagrams containing 2p-h and 2h-p excitations of the reference state.

The necessary operator averages needed to evaluate $\hat{P}\hat{V}\hat{P}$ are:

$$(a_k^\dagger, a_l, a_m, |\hat{V}a_l) = (a_l|\hat{V}a_k^\dagger, a_l, a_m,)^* = N_{k'l'm'}\langle lk'||m'l'\rangle \tag{4.11}$$

and

$$\begin{aligned}(a_k^\dagger, a_l, a_m, |\hat{V}a_k^\dagger a_l a_m) = N_{k'l'm'}\{&\langle ml||m'l'\rangle\delta_{kk'}(1-\langle n_m\rangle-\langle n_l\rangle)\\
&-\langle k'm||km'\rangle\delta_{ll'}(\langle n_k\rangle-\langle n_m\rangle)-\langle k'l||kl'\rangle\delta_{mm'}(\langle n_k\rangle-\langle n_l\rangle)\\
&+\langle k'm||kl'\rangle\delta_{m'l}(\langle n_k\rangle-\langle n_m\rangle)+\langle k'l||km'\rangle\delta_{ml'}(\langle n_k\rangle-\langle n_l\rangle)\\
&+\langle k'm||l'm'\rangle\delta_{kl}\langle n_k\rangle+\langle k'l||m'l'\rangle\delta_{km}\langle n_k\rangle\}\\
&+N_{klm}\{\langle ml||kl'\rangle\delta_{m'k'}\langle n_{m'}\rangle+\langle ml||m'k\rangle\delta_{l'k'}\langle n_{l'}\rangle\}\end{aligned} \tag{4.12}$$

Substituting these expressions and performing some cancelation yields:

$$\begin{aligned}\hat{P}\hat{V}\hat{P} = &\sum_{\substack{k,l,m\\ l<m}}\sum_{\substack{k',l',m'\\ l'<m'}} N_{klm}^{-\frac{1}{2}}N_{k'l'm'}^{\frac{1}{2}}\langle ml||m'l'\rangle\delta_{kk'}(1-\langle n_m\rangle-\langle n_l\rangle)|f_{k'l'm'})(f_{klm}|\\
&-\sum_{\substack{k,l,m\\ l<m}}\sum_{\substack{k',l',m'\\ l'<m'}} N_{klm}^{-\frac{1}{2}}N_{k'l'm'}^{\frac{1}{2}}\langle k'm||km'\rangle\delta_{ll'}(\langle n_k\rangle-\langle n_m\rangle)|f_{k'l'm'})(f_{klm}|\\
&-\sum_{\substack{k,l,m\\ l<m}}\sum_{\substack{k',l',m'\\ l'<m'}} N_{klm}^{-\frac{1}{2}}N_{k'l'm'}^{\frac{1}{2}}\langle k'l||kl'\rangle\delta_{mm'}(\langle n_k\rangle-\langle n_l\rangle)|f_{k'l'm'})(f_{klm}|\\
&+\sum_{\substack{k,l,m\\ l<m}}\sum_{\substack{k',l',m'\\ l'<m'}} N_{klm}^{-\frac{1}{2}}N_{k'l'm'}^{\frac{1}{2}}\langle k'm||kl'\rangle\delta_{lm'}(\langle n_k\rangle-\langle n_m\rangle)|f_{k'l'm'})(f_{klm}|\\
&+\sum_{\substack{k,l,m\\ l<m}}\sum_{\substack{k',l',m'\\ l'<m'}} N_{klm}^{-\frac{1}{2}}N_{k'l'm'}^{\frac{1}{2}}\langle k'l||km'\rangle\delta_{ml'}(\langle n_k\rangle-\langle n_l\rangle)|f_{k'l'm'})(f_{klm}|\end{aligned} \tag{4.13}$$

Additional simplification can be achieved at this point by anti-commuting the operators $a_{l'}$ and $a_{m'}$ in $|f_{k'l'm'})$ of the last two terms in Eq. (4.13) with the appropriate change of sign,

$$|f_{k'l'm'}) = - |f_{k'm'l'}) \ . \tag{4.14}$$

After interchanging dummy indices $l' \leftrightarrow m'$, the fourth and fifth terms become equal to the second and third terms, respectively, and since the diagonal terms $l' = m'$ vanish, the summations with $l' < m'$ and $l' > m'$ can be combined as unrestricted summations over l' and m'. Since the first term in Eq. (4.13) is obviously symmetric in l' and m', the restriction $l' < m'$ in that term may be removed by multiplying the sum by a factor of $\frac{1}{2}$. The remaining restriction, $l < m$, may also be removed by introducing another factor of $\frac{1}{2}$ since

$$\hat{P}\hat{V}\hat{P} = \sum_{\substack{k,l,m \\ l<m}} \sum_{k',l',m'} N_{klm}^{-\frac{1}{2}} N_{k'l'm'}^{\frac{1}{2}} \{\tfrac{1}{2}\langle ml||m'l'\rangle \delta_{kk'}(1-\langle n_m\rangle-\langle n_l\rangle)$$

$$-\langle k'm||km'\rangle \delta_{ll'}(\langle n_k\rangle-\langle n_m\rangle)-\langle k'l||kl'\rangle \delta_{mm'}(\langle n_k\rangle-\langle n_l\rangle)\} |f_{k'l'm'})(f_{klm}| \tag{4.15}$$

is symmetric in these indices as can be verified by interchanging $l \leftrightarrow m$ and relabeling dummy indices $l' \leftrightarrow m'$. Expanding the ket-bra superoperator

$$\tfrac{1}{2} \sum_{k,l,m} \sum_{k',l',m'} |f_{k'l'm'})(f_{klm}| \tag{4.16}$$

out of the inverse, evaluating the remaining operator averages, and resumming the expansion yields the 2p-h TDA self-energy

$$\Sigma(E)_{ij}^{\text{2p-h TDA}} = \tfrac{1}{2} \sum_{k,l,m} \sum_{k',l',m'} N_{klm}^{\frac{1}{2}} N_{k'l'm'}^{\frac{1}{2}} \langle ik||lm\rangle$$

$$\times \{(\underline{f}|(E\hat{I}-\hat{H}_0)\underline{f})-(\underline{f}|\hat{V}\underline{f})\}^{-1}_{klm,k'l'm'} \langle l'm'||jk'\rangle \tag{4.17}$$

where

$$(f_{k'l'm'}|(E\hat{I}-\hat{H}_0)f_{klm}) = (E+\varepsilon_k-\varepsilon_l-\varepsilon_m)\delta_{kk'}\delta_{ll'}\delta_{mm'} ,$$

$$(f_{k'l'm'}|\hat{V}f_{klm}) = N^{-\frac{1}{2}}_{klm}N^{\frac{1}{2}}_{k'l'm'}\{\tfrac{1}{2}\langle ml||m'l'\rangle\delta_{kk'}(1-\langle n_m\rangle-\langle n_l\rangle)$$
$$-\langle k'm||km'\rangle\delta_{ll'}(\langle n_k\rangle-\langle n_m\rangle)-\langle k'l||kl'\rangle\delta_{mm'}(\langle n_k\rangle-\langle n_l\rangle)\} \qquad (4.18)$$

Although different in appearance, this self-energy expression is formally the same as that obtained by Purvis and Öhrn (1975a) using the operator product decoupling and by Cederbaum (1975) and Schirmer and Cederbaum (1978) using the diagrammatic method. The present derivation clearly illuminates the parallelism between the two formalisms.

Owing to the large dimension of the $\{f_{klm}\}$ operator subspace and the associated difficulty in diagonalizing $(\underline{f}|\hat{V}\underline{f})$, computational applications of the 2p-h TDA have usually involved additional approximations. One approximation which has facilitated computational applications is known alternatively as the shifted Born collision (SBC) approximation (Purvis and Öhrn, 1974, 1975a) or the diagonal 2p-h TDA (Cederbaum, 1974, 1975 and Cederbaum and Domcke, 1977). This purportedly "diagonal" approximation restricts the spin-orbital summation indices in Eq. (4.13) to $k' = k$, $l' = l$, and $m' = m$ thereby neglecting the last two summations and yielding the following self-energy expression

$$\Sigma(E)^{\text{2p-h TDA}}_{ij} = \tfrac{1}{2}\sum_{k,l,m} N_{klm}\frac{\langle ik||lm\rangle\langle lm||jk\rangle}{(E+\varepsilon_k-\varepsilon_l-\varepsilon_m)-\Delta} \qquad (4.19)$$

where

$$\Delta=\langle ml||ml\rangle(1-\langle n_m\rangle-\langle n_l\rangle)-\langle km||km\rangle(\langle n_k\rangle-\langle n_m\rangle)-\langle kl||kl\rangle(\langle n_k\rangle-\langle n_l\rangle). \qquad (4.20)$$

By neglecting the last two summations in Eq. (4.13), however, this approximation actually neglects some diagonal contributions to $(f_{k'l'm'}|\hat{V}f_{klm})$. As we have explicitly demonstrated in the derivation of Eq. (4.17) and

(4.18), the 2p-h TDA self-energy sums are symmetric in both l,m and l',m'; consequently, the last two summations in Eq. (4.13) contain precisely the same contributions as the second and third summations, respectively. If the diagonal approximation (k'=k, l'=l, m'=m) is made in Eqs. (4.17) and (4.18), this symmetry is properly accounted for and the resulting self-energy expression is

$$\Sigma(E)^{\text{2p-h TDA}}_{ij} = \tfrac{1}{2} \sum_{k,l,m} N_{klm} \frac{\langle ik||lm\rangle\langle lm||jk\rangle}{(E+\varepsilon_k-\varepsilon_l-\varepsilon_m)-\Delta} \tag{4.21}$$

where

$$\Delta=\tfrac{1}{2}\langle ml||ml\rangle(1-\langle n_m\rangle-\langle n_l\rangle)-\langle km||km\rangle(\langle n_k\rangle-\langle n_m\rangle)-\langle kl||kl\rangle(\langle n_k\rangle-\langle n_l\rangle). \tag{4.22}$$

Eq. (4.22) differs from Eq. (4.20) by the factor of $\frac{1}{2}$ in the first term. The inclusion of this factor in the diagonal 2p-h TDA is necessary to prevent an overcounting of diagrams with diagonal ladder parts (see next section) and typically shifts ionization energies 0.3-0.4 eV higher in energy (Born and Öhrn, 1979).

4.3 Diagrammatic Analysis

In order to determine precisely which self-energy diagrams are included in the 2p-h TDA self-energy, it is necessary to expand the effective interaction matrix, $(\underline{f}|\hat{\underline{V}}\underline{f})$, from the inverse in Eq. (4.17) and diagram the resulting algebraic expressions in each order. The expansion of Eq. (4.17) yields the following terms in lowest orders

$$\Sigma(E)^{\text{2p-h TDA}}_{ij} = \tfrac{1}{2} \sum_{k,l,m} \sum_{k',l',m'} N^{\frac{1}{2}}_{klm} N^{\frac{1}{2}}_{k'l'm'} \langle ik||lm\rangle$$

$$\times \left\{ \frac{\delta_{kk'}\delta_{ll'}\delta_{mm'}}{(E+\varepsilon_k-\varepsilon_l-\varepsilon_m)} + \frac{(f_{k'l'm'}|\hat{V}f_{klm})}{(E+\varepsilon_k-\varepsilon_l-\varepsilon_m)(E+\varepsilon_{k'}-\varepsilon_{l'}-\varepsilon_{m'})} \right.$$

$$+ \sum_{\kappa,\lambda,\mu} \frac{(f_{k'l'm'}|\hat{V}f_{\kappa\lambda\mu})(f_{\kappa\lambda\mu}|\hat{V}f_{klm})}{(E+\varepsilon_k-\varepsilon_l-\varepsilon_m)(E+\varepsilon_\kappa-\varepsilon_\lambda-\varepsilon_\mu)(E+\varepsilon_{k'}-\varepsilon_{l'}-\varepsilon_{m'})} + \ldots \Big\} \langle l'm'||jk'\rangle \ . \tag{4.23}$$

As was done in Section 3.3, the terms in Eq. (4.23) can be simplified by first restricting the summations over all spin orbitals to summations over occupied or unoccupied spin orbitals such that the occupation number factor $N^{\frac{1}{2}}_{klm}N^{\frac{1}{2}}_{k'l'm'}$ is nonvanishing. Doing this in the first term of Eq. (4.23) and then summing over the delta functions yields

$$\tfrac{1}{2} \sum_{a,p,q} \frac{\langle ia||pq\rangle\langle pq||ja\rangle}{(E+\varepsilon_a-\varepsilon_p-\varepsilon_q)} \tag{4.24}$$

$$+\tfrac{1}{2} \sum_{p,a,b} \frac{\langle ip||ab\rangle\langle ab||jp\rangle}{(E+\varepsilon_p-\varepsilon_a-\varepsilon_b)} \tag{4.25}$$

which are the same second-order self-energy diagrams as obtained in Eqs. (3.66) and (3.67).

Restricting and spin orbital summations in the second term of Eq. (4.23) yields the following expressions

$$\tfrac{1}{2} \sum_{a,p,q} \sum_{b,r,s} \frac{\langle ia||pq\rangle}{(E+\varepsilon_a-\varepsilon_p-\varepsilon_q)} (f_{brs}|\hat{V}f_{apq}) \frac{\langle rs||jb\rangle}{(E+\varepsilon_b-\varepsilon_r-\varepsilon_s)} \tag{4.26}$$

$$+\tfrac{1}{2} \sum_{a,p,q} \sum_{r,b,c} \frac{\langle ia||pq\rangle}{(E+\varepsilon_a-\varepsilon_p-\varepsilon_q)} (f_{rbc}|\hat{V}f_{apq}) \frac{\langle bc||jr\rangle}{(E+\varepsilon_r-\varepsilon_b-\varepsilon_c)} \tag{4.27}$$

$$+\tfrac{1}{2} \sum_{p,a,b} \sum_{d,q,r} \frac{\langle ip||ab\rangle}{(E+\varepsilon_p-\varepsilon_a-\varepsilon_b)} (f_{cqr}|\hat{V}f_{pab}) \frac{\langle qr||jc\rangle}{(E+\varepsilon_c-\varepsilon_q-\varepsilon_r)} \tag{4.28}$$

$$+\tfrac{1}{2} \sum_{p,a,b} \sum_{q,c,d} \frac{\langle ip||ab\rangle}{(E+\varepsilon_p-\varepsilon_a-\varepsilon_b)} (f_{qcd}|\hat{V}f_{pab}) \frac{\langle cd||jq\rangle}{(E+\varepsilon_q-\varepsilon_c-\varepsilon_d)} \tag{4.29}$$

Now substituting Eq. (4.18) for the effective interaction matrices, we find that the delta functions in Eq. (4.18) further restrict the spin

orbital summations in such a way that only expressions (4.26) and (4.29) are nonvanishing. After some simplification, the nonvanishing contributions are found to be

$$\tfrac{1}{4} \sum_{a} \sum_{p,q,r,s} \frac{\langle ia||pq\rangle\langle qp||sr\rangle\langle rs||ja\rangle}{(E+\varepsilon_a-\varepsilon_p-\varepsilon_q)(E+\varepsilon_a-\varepsilon_r-\varepsilon_s)} \qquad (4.30)$$

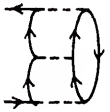

$$-\tfrac{1}{2} \sum_{a,b} \sum_{p,q,r} \frac{\langle ia||pq\rangle\langle bq||ar\rangle\langle pr||jb\rangle}{(E+\varepsilon_a-\varepsilon_p-\varepsilon_q)(E+\varepsilon_b-\varepsilon_p-\varepsilon_r)} \qquad (4.31)$$

$$-\tfrac{1}{2} \sum_{a,b} \sum_{p,q,r} \frac{\langle ia||pq\rangle\langle bp||ar\rangle\langle rq||jb\rangle}{(E+\varepsilon_a-\varepsilon_p-\varepsilon_q)(E+\varepsilon_b-\varepsilon_r-\varepsilon_q)} \qquad (4.32)$$

$$-\tfrac{1}{4} \sum_{a,b,c,d} \sum_{p} \frac{\langle ip||ab\rangle\langle ba||dc\rangle\langle cd||jp\rangle}{(E+\varepsilon_p-\varepsilon_a-\varepsilon_b)(E+\varepsilon_p-\varepsilon_c-\varepsilon_d)} \qquad (4.33)$$

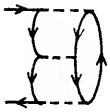

$$+\tfrac{1}{2} \sum_{a,b,c} \sum_{p,q} \frac{\langle ip||ab\rangle\langle qb||pc\rangle\langle ac||jq\rangle}{(E+\varepsilon_p-\varepsilon_a-\varepsilon_b)(E+\varepsilon_q-\varepsilon_a-\varepsilon_c)} \qquad (4.34)$$

$$+\tfrac{1}{2} \sum_{a,b,c} \sum_{p,q} \frac{\langle ip||ab\rangle\langle qa||pc\rangle\langle cb||jq\rangle}{(E+\varepsilon_p-\varepsilon_a-\varepsilon_b)(E+\varepsilon_q-\varepsilon_b-\varepsilon_c)} \qquad (4.35)$$

Expressions (4.30) and (4.33) are the only ones which represent valid third-order diagrams as written, however, by interchanging dummy indices $p \leftrightarrow q$ in Eq. (4.32) and $a \leftrightarrow b$ in Eq. (4.35), expressions (4.31) and (4.32) can be combined to yield

$$-\sum_{a,b} \sum_{p,q,r} \frac{\langle ia||pq\rangle\langle bq||ar\rangle\langle pr||jb\rangle}{(E+\varepsilon_a-\varepsilon_p-\varepsilon_q)(E+\varepsilon_b-\varepsilon_p-\varepsilon_r)} \qquad (4.36)$$

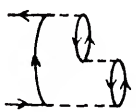

and expressions (4.34) and (4.35) combined to yield

$$\sum_{a,b,c} \sum_{p,q} \frac{\langle ip||ab\rangle\langle qb||pc\rangle\langle ac||jq\rangle}{(E+\varepsilon_p-\varepsilon_a-\varepsilon_b)(E+\varepsilon_q-\varepsilon_a-\varepsilon_c)} \qquad (4.37)$$

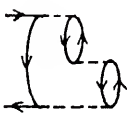

which now correspond to the two third-order ring diagrams as indicated. These results verify that one of our original objectives, which was to include all third-order ring and ladder diagrams, has been achieved.

The diagrammatic analysis of the third term in Eq. (4.23) proceeds in the same way as that of the first two terms, but since the effective interaction matrix appears twice, it involves considerably more algebra. For this reason, we simply display the resulting diagrams in Fig. 4. It is significant to realize that the fourth-order diagrams in Fig. 4 include not only ring and ladder diagrams but also mixed diagrams which consist of both ring and ladder parts. In the third-order analysis, the first term in Eq. (4.18) was responsible for yielding the ladder diagrams while the second and third terms yielded the ring diagrams. If we therefore denote the first term as a ladder part and the second and third terms as ring parts, the mixed diagrams in fourth order are found to arise from the product of a ladder part and a ring part. Inducing the results of the fourth-order analysis to higher orders, we conclude that our second objective, which was to sum all ring and ladder diagrams in all orders of the self-energy expansion, has been exceeded: not only are all ring and ladder diagrams included in the 2p-h TDA self-energy, but also the mixed diagrams which exhibit both ring and ladder parts.

The diagonal 2p-h TDA self-energy may also be analyzed diagrammatically. This analysis is even simpler than for the full 2p-h TDA since the denominator shifts are now scalars rather than matrices. A comparison of diagrams obtained with the denominator shift in Eq. (4.30) versus that in Eq. (4.22) will reveal the significance of the factor of $\frac{1}{2}$. Considering the approximation in Eqs. (4.21) and (4.22) first, we obtain the following third-order expressions

Figure 4. Fourth-order self-energy diagrams arising from the 2p-h TDA.

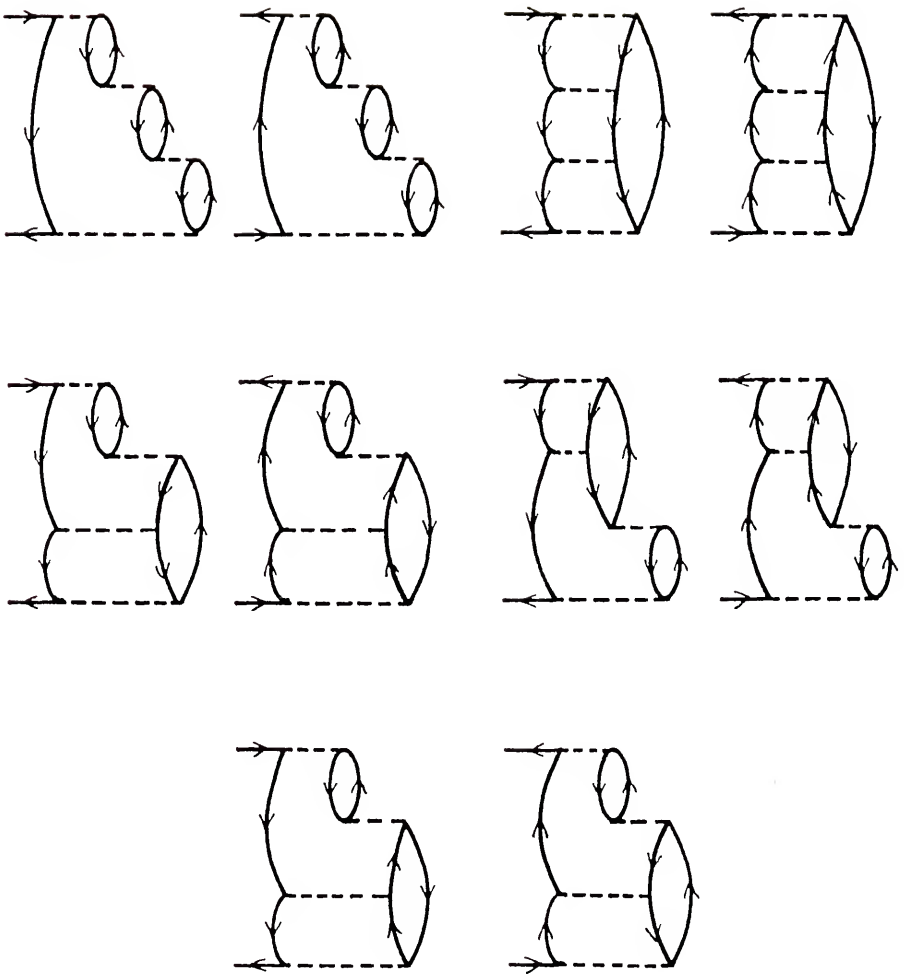

$$\tfrac{1}{4}\sum_{a,p,q}\frac{\langle ia||pq\rangle\langle pq||pq\rangle\langle pq||ja\rangle}{(E+\varepsilon_a-\varepsilon_p-\varepsilon_q)^2}$$

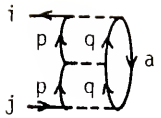

(4.38)

$$-\tfrac{1}{4}\sum_{a,b,p}\frac{\langle ip||ab\rangle\langle ab||ab\rangle\langle ab||jp\rangle}{(E+\varepsilon_p-\varepsilon_a-\varepsilon_b)^2}$$

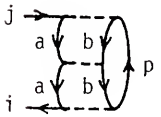

(4.39)

$$-\sum_{a,p,q}\frac{\langle ia||pq\rangle\langle ap||ap\rangle\langle pq||ja\rangle}{(E+\varepsilon_a-\varepsilon_p-\varepsilon_q)^2}$$

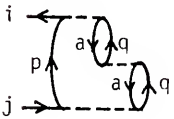

(4.40)

$$+\sum_{a,b,p}\frac{\langle ip||ab\rangle\langle pb||pb\rangle\langle ab||jp\rangle}{(E+\varepsilon_p-\varepsilon_a-\varepsilon_b)^2}$$

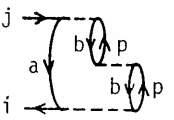

(4.41)

The only difference between these diagrams and the third-order diagrams of the full, 2p-h TDA is that the incoming lines on the middle interaction line have the same labels as the outgoing lines. Now analyzing the approximation in Eqs. (4.19) and (4.20), we obtain the following third-order expressions

$$\tfrac{1}{2}\sum_{a,p,q}\frac{\langle ia||pq\rangle\langle pq||pq\rangle\langle pq||ja\rangle}{(E+\varepsilon_a-\varepsilon_p-\varepsilon_q)^2} \tag{4.42}$$

$$-\tfrac{1}{2}\sum_{a,b,p}\frac{\langle ip||ab\rangle\langle ab||ab\rangle\langle ab||jp\rangle}{(E+\varepsilon_p-\varepsilon_a-\varepsilon_b)^2} \tag{4.43}$$

$$-\sum_{a,p,q}\frac{\langle ia||pa\rangle\langle ap||ap\rangle\langle pq||ja\rangle}{(E+\varepsilon_a-\varepsilon_p-\varepsilon_q)^2} \tag{4.44}$$

$$+\sum_{a,b,p}\frac{\langle ip||ab\rangle\langle pb||pb\rangle\langle ab||jp\rangle}{(E+\varepsilon_p-\varepsilon_a-\varepsilon_b)^2} \tag{4.45}$$

Expressions (4.44) and (4.45) are identical to (4.40) and (4.41) respectively; however, expressions (4.42) and (4.43) both differ by a factor of ½ from (4.38) and (4.39). This discrepancy is a direct consequence of the missing factor in the denominator shift, Eq. (4.20), and leads to an overcounting of these third-order diagonal ladder diagrams since, by rule 5 in Table 5, there should be a factor of ½ for each pair of equivalent lines. Similarly, it is rather easy to show that this approximation overcounts all higher order diagrams containing this diagonal ladder part.

4.4 Computational Applications and Evaluation of the Diagonal 2p-h TDA Self-Energy

The main attraction of the diagonal 2p-h TDA self-energy for the calculation of ionization energies and electron affinities is its pseudo second-order structure. Computational experience with the diagram conserving decouplings has taught us that the second-order self-energy approximant is both easily constructed and evaluated. The diagonal 2p-h TDA requires only the additional evaluation of Eq. (4.22) which merely shifts the second-order self-energy poles. As a consequence the diagonal 2p-h TDA self-energy mimics the exact self-energy by possessing only simple poles. Another consequence of the pseudo second-order structure is that the energy dependence will have the simple analytic form illustrated in Fig. 2. This property, which was absent in the [1,1] self-energy approximant, simplifies the pole search for the electron propagator. In spite of the simplicity of its pseudo second-order structure, however, the diagonal 2p-h TDA self-energy incorporates diagonal ring, ladder, and mixed diagrams in all orders of the self-energy expansion

as was shown in the previous section. This property encourages speculation that significantly more relaxation and correlation will be accounted for in this decoupling than with the second-order decoupling, but the accuracy of the corresponding ionization energies or electron affinities can only be evaluated via actual computational applications. As was done with the diagram conserving decouplings, ionization energies for the water and formaldehyde molecules were computed using the diagonal 2p-h TDA self-energy.

For the water molecule, calculations were performed with both the 14 and 26 contracted Gaussian orbital basis sets described in Chapters 2 and 3. The principal ionization energies computed with the diagonal 2p-h TDA and the diagonal 2p-h TDA plus third-order constant energy diagrams (denoted $\Sigma^{(2)}(E)_{SHIFT}$ and $\Sigma^{(2)}(E)_{SHIFT} + \Sigma^{(3)}(\infty)$) are presented in Table 11. Comparing these results with those in Table 9 for the second-order and [1,1] self-energy approximants reveals that each ionization has been shifted to higher energy. This shift has led to a significant improvement in the valence ionization energies ($3a_1$, $1b_1$, and $1b_2$) which are now within approximately 0.5 eV of the experimental results. For the inner valence ($2a_1$) and core ($1a_1$) ionizations, however, this energy shift leads to worse agreement. In addition, the diagonal 2p-h TDA results for the $1a_1$ ionization exhibit an enormous basis dependence. The addition of polarization functions in the 26 orbital basis has yielded nearly 13 eV in additional relaxation. The most probable explanation for this basis dependence is that the 2p-h TDA self-energy poles are determined by Hartree-Fock orbital energies and two-electron integrals rather than by orbital energies alone as with the second-order self-energy. The orbital energies are rather insentitive to basis changes, whereas the two-electron integrals are not.

Table 11. Water Results Obtained with the Diagonal 2p-h TDA and Diagonal 2p-h TDA plus Constant Third-Order Self-Energies.

	14 CGTO's			26 CGTO's			
	Koopmans	$\Sigma^{(2)}(E)_{SHIFT}$	$\Sigma^{(2)}(E)_{SHIFT} + \Sigma^{(3)}(\infty)$	Koopmans	$\Sigma^{(2)}(E)_{SHIFT}$	$\Sigma^{(2)}(E)_{SHIFT} + \Sigma^{(3)}(\infty)$	Exp.[a]
$1a_1$	559.45	554.91	556.04	559.40	542.78	543.51	540.2
$2a_1$	37.04	34.62	35.00	36.62	33.69	33.93	32.2
$3a_1$	15.43	13.61	13.95	15.66	14.12	14.31	14.7
$1b_1$	13.78	11.64	11.97	13.67	11.83	12.00	12.6
$1b_2$	19.52	18.51	18.80	19.34	18.46	18.61	18.6

[a]Siegbahn *et al.* (1969).

Calculations for the formaldehyde molecule were performed with the 24 and 42 orbital basis sets described in Chapter 3. Ionization energies were computed using the diagonal 2p-h TDA and are presented in Table 12. The third-order constant energy diagrams were not evaluated for this molecule. Similar to the water results, the diagonal 2p-h TDA results for formaldehyde are also consistently higher in energy than the second-order results (Table 9). This shift considerably improves the valence ionization energies; however, the average deviation from the experimental results remains approximately 0.8 eV. The core ionizations within the diagonal 2p-h TDA suffer a small deterioration in accuracy but do not exhibit the extreme basis dependence which was observed in the water calculations. Part of the discrepancies between the diagonal 2p-h TDA and the experimental results can certainly be eliminated by further basis saturation; however, in the next chapter, we will propose that even ionization energies of 1.0 eV accuracy are usually sufficient to unambiguously interpret photoelectron spectra if combined with a calculation of relative photoionization intensities.

Cederbaum and co-workers have recently developed computer programs which implement the full, nondiagonal 2p-h TDA to the self-energy and have reported several molecular applications (Cederbaum et al., 1977, Schirmer et al., 1977, Cederbaum et al., 1978, and Schirmer et al., 1978). In these calculations, they claim only a 1.0 eV accuracy and rely heavily on vibrational analyses to assist with the interpretation of photoelectron spectra. The off-diagonal matrix elements seem to have little importance in the valence region because the propagator poles are relatively well-separated. In the inner valence and core regions, however, where principal ionization poles and shake-up poles overlap and

Table 12. Formaldehyde Results Obtained with the Diagonal 2p-h TDA Self-Energy.

	24CGTO's		42 CGTO's		
	Koopmans	$\Sigma^{(2)}(E)_{SHIFT}$	Koopmans	$\Sigma^{(2)}(E)_{SHIFT}$	Exp.
$1a_1$	560.12	542.86	559.81	542.09	539.43[a]
$2a_1$	309.09	299.82	308.87	299.31	294.21[a]
$3a_1$	38.94	35.60	38.18	34.31	34.2[b]
$4a_1$	23.39	21.75	23.30	21.79	21.15[b]
$5a_1$	17.29	14.99	17.38	15.33	16.2[c]
$1b_1$	14.56	14.11	14.45	14.03	14.5[c,d]
$1b_2$	19.47	17.91	19.08	17.77	17.0[c]
$2b_2$	12.06	9.92	11.93	10.11	10.9[c]

[a] Jolly and Schaaf (1976).

[b] Hood *et al.* (1976).

[c] Estimated center of gravity (Cederbaum and Domcke, 1977) from spectrum of Turner *et al.* (1970).

[d] 14.38(8) VIP (Turner *et al.*, 1970).

interact, level shifts and intensity changes are observed. In these regions, even the nondiagonal 2p-h TDA is not fully satisfactory since ion-state relaxation and hole-hole interactions, neither of which are described by this self-energy approximation, may also be important (Wendin, 1979).

CHAPTER 5
PHOTOIONIZATION INTENSITIES

5.1 Introduction

The evaluation of each decoupling approximation in the preceding chapters was based on the comparison of propagator poles to experimental ionization energies. This criterion represents a particular bias since it does not reflect the quality of the Feynman-Dyson amplitudes (defined in Section 1.1). The Feynman-Dyson amplitudes determine the spectral density function (Linderberg and Öhrn, 1973)

$$A(x,x';E) = \begin{cases} \sum_k f_k(x)f^*(x')\delta(E-E_k) & E > \mu \\ \sum_k g_k(x)g^*(x')\delta(E-E_k) & E \leq \mu \end{cases} \qquad (5.1)$$

which contains a plethora of useful information. This is evidenced by the relation of the spectral density to the single-particle, reduced density matrix (Linderberg and Öhrn, 1973)

$$\gamma(x,x') = \int_C A(x,x';E)dE \ . \qquad (5.2)$$

It is important, therefore, to choose a decoupling approximation which not only yields accurate ionization energies but also an accurate spectral density. The quality of the spectral density is somewhat more difficult to evaluate since there are no experimental data with which it can be directly compared. One evaluation procedure, however, might involve the calculation of averages of specific one-electron operators from the reduced density matrix. The averages could then be compared with

experimental results. Another procedure which is more closely related to our goal of interpreting photoelectron spectra is the calculation of photoionization intensities or cross-sections. A theoretical prediction of relative photoionization intensities can simplify orbital assignments when the ionization energies are not accurately given. A theoretically predicted variation in relative intensities with photon energy is particularly useful if photoelectron spectra are available with different ionization sources (Katrib et al., 1973). In the following sections, we derive computational expressions which relate the Feynman-Dyson amplitudes to the total photoionization cross-section, discuss the major approximations assumed, and then present several applications.

5.2 Derivation of Computational Formulae for the Total Photoionization Cross-Section

The differential cross-section for photoionization derived from first-order, time-dependent perturbation theory using a semi-classical model for the interaction of radiation and matter is (Bethe and Salpeter, 1957, Kaplan and Markin, 1968, Smith, 1971)

$$\frac{d\sigma_s}{d\Omega_f} = \frac{4\pi^2|\vec{k}_f|}{c|A_0|^2\omega} \left| \langle N,s|\sum_k \vec{A}_k \cdot \vec{\nabla}_k |N\rangle \right|^2 . \tag{5.3}$$

In this equation, $\vec{k}_f$ is the momentum of the ejected photoelectron and $\vec{A} = \sum_k \vec{A}_k$ is the vector potential. For a closed-shell system, the initial state $|N\rangle$ can be represented by an antisymmetrized N-electron wavefunction

$$|N\rangle = \Phi_0(x_1,x_2, \ldots x_N) \tag{5.4}$$

and the final state $|N,s\rangle$ is represented by

$$|N,s> = (N/2)^{\frac{1}{2}} O_{AS} [v(\vec{k}_f,\vec{r})\alpha(\zeta)\Phi_{s\beta}(x_1,x_2, \ldots x_{N-1}) - v(\vec{k}_f,\vec{r})\beta(\zeta)\Phi_{s\alpha}(x_1,x_2, \ldots x_{N-1})] . \quad (5.5)$$

Here $\Phi_{s\alpha}$ and $\Phi_{s\beta}$ are the two, doublet spin components of the (N-1)-electron ion, $v(\vec{k}_f,\vec{r})$ denotes the wavefunction of the photoelectron, and O_{AS} is an antisymmetrizer

$$O_{AS} = N^{-1}[1 - \sum_{k=1}^{N-1} P_{kN}] . \quad (5.6)$$

The form of Eq. (5.5) guarantees that the singlet spin symmetry of the system is preserved.

Evaluating the matrix element in Eq. (5.3) yields (Purvis and Öhrn, 1975a)

$$<N,s|\sum_k \vec{A}_k \cdot \vec{\nabla}_k |N> = \sqrt{2} \int v^*(\vec{k}_f,\vec{r})\vec{A}_s \cdot \vec{\nabla}_s g_s(\vec{r})d\vec{r} + \sqrt{2} \int v^*(\vec{k}_f,\vec{r})\vec{p}_s(\vec{r})d\vec{r} \quad (5.7)$$

where

$$N^{-\frac{1}{2}}g_s(\vec{r})\chi(\zeta) = \int \Phi_s^* (x_1, \ldots x_{N-1})\Phi_0(x_1, \ldots x_{N-1};\vec{r},\chi(\zeta)) \times dx_1 \ldots dx_{N-1} \quad (5.8)$$

and

$$N^{-\frac{1}{2}}\vec{p}_s(\vec{r})\chi(\zeta) = (N-1) \int \Phi_s^* (x_1, \ldots x_{N-1})\vec{A}_1 \cdot \vec{\nabla}_1 \Phi_0(x_1, \ldots x_{N-1}; \vec{r},\chi(\zeta))dx_1 \ldots dx_{N-1} . \quad (5.9)$$

The first term in Eq. (5.7) relates the Feynman-Dyson amplitude $g_s(\vec{r})$ to the photoionization cross-section and the second term arises from the nonorthogonality of $v(\vec{k}_f,\vec{r})$ and Φ_0. When $v(\vec{k}_f,\vec{r})$ is strongly orthogonal to Φ_0, this term vanishes. Even when $v(\vec{k}_f,\vec{r})$ is not strongly orthogonal to Φ_0, the first term in Eq. (5.7) will dominate if the kinetic energy

of the photoelectron is much greater than its binding energy (Rabalais et al., 1974), therefore we shall neglect this term:

$$\frac{d\sigma_s}{d\Omega_f} = \frac{8\pi^2|\vec{k}_f|}{c|A_0|^2_\omega}\left|\int v^*(\vec{k}_f,\vec{r})\vec{A}_s\cdot\vec{\nabla}_s g_s(\vec{r})d\vec{r}\right|^2 . \tag{5.10}$$

Further simplification can be obtained by neglecting retardation of the photoelectron momentum by the photon momentum (also called the dipole approximation in analogy with photon induced transitions in the discrete spectrum, Bethe and Salpeter, 1957, Steinfeld, 1974). The vector potential $\vec{A}_s$ has the following plane wave decomposition in terms of the incident photon momentum $\vec{k}_\omega$ and polarization $\vec{n}$

$$\vec{A}_s = |\vec{A}_0| \exp(i\vec{k}_\omega\cdot\vec{r}_s)\vec{n} . \tag{5.11}$$

If the wavelength of the incident photon is large compared with molecular dimensions, the exponential may be approximated by the first term in its Taylor series expansion (unity)

$$\vec{A}_s \simeq |A_0|\vec{n} . \tag{5.12}$$

With this approximation, the differential photoionization cross-section becomes

$$\frac{d\sigma_s}{d\Omega_f} = \frac{8\pi^2|\vec{k}_f|}{c\omega}|\vec{n}\cdot\vec{P}|^2 . \tag{5.13}$$

where

$$\vec{P} \equiv \int v^*(\vec{k}_f,\vec{r})\vec{\nabla}g_s(\vec{r})d\vec{r} . \tag{5.14}$$

Owing to the random orientation of molecules in a gaseous sample, the experimentally observed photoionization intensities in the molecular reference frame represent an average over all incident photon directions. Furthermore, if the incident photon beam is unpolarized, we must also average over photon polarizations. Making the appropriate averages in Eq. (5.13) (Smith, 1971), we obtain

$$\frac{d\sigma_s}{d\Omega_f} = \left(\frac{8\pi^2|\vec{k}_f|}{c\omega}\right) \frac{1}{4\pi} \int \tfrac{1}{2} \{|\vec{n}_1 \cdot \vec{P}|^2 + |\vec{n}_2 \cdot \vec{P}|^2\} d\Omega_\omega \ . \tag{5.15}$$

Since the two polarization directions, $\vec{n}_1$ and $\vec{n}_2$, and the incident photon direction, $k_\omega/|k_\omega|$, form a right-handed system of axes, we can write

$$|\vec{P}|^2 = |\vec{n}_1 \cdot \vec{P}|^2 + |\vec{n}_2 \cdot \vec{P}|^2 + |\vec{k}_\omega \cdot \vec{P}|^2 \ / \ |\vec{k}_\omega|^2 \ . \tag{5.16}$$

and Eq. (5.15) becomes

$$\frac{d\sigma_s}{d\Omega_f} = \left(\frac{8\pi^2|\vec{k}_f|}{c\omega}\right) \frac{1}{8\pi} \int \{|\vec{P}|^2 - |\vec{k}_\omega \cdot \vec{P}|^2 \ / \ |\vec{k}_\omega|^2\} d\Omega_\omega \tag{5.17}$$

$$= \left(\frac{8\pi^2|\vec{k}_f|}{c\omega}\right) |\vec{P}|^2 \frac{1}{8\pi} \int \{1 - \cos^2 \theta_\omega\} d\Omega_\omega \tag{5.18}$$

$$\frac{d\sigma_s}{d\Omega_f} = \frac{8\pi^2|\vec{k}_f|}{c\omega} |\vec{P}|^2 \ . \tag{5.19}$$

In order to evaluate $|\vec{P}|^2$, some form for the photoelectron wavefunction $v(\vec{k}_f,\vec{r})$ must now be chosen. In principle, the photoelectron wavefunction could be obtained by the solution of the Bethe-Salpeter equation for the polarization propagator where the superoperator resolvent has been modified to include the time-dependent interaction of the radiation and matter fields (see e.g. Csanak et al., 1971). A solution

of this type would require the use of continuum functions as well as discrete functions in the molecular basis and is not yet feasible owing to several formal and practical difficulties. Alternatively, we seek a simple but accurate, analytic representation of the photoelectron wavefunction. For photoionization of atoms or molecules with high (tetrahedral or octahedral) symmetry, the electronic potential of the ion is nearly spherically symmetric, and $v(\vec{k}_f,\vec{r})$ may be asymptotically represented by a plane wave plus incoming Coulomb waves (see e.g. Smith, 1971). For molecules with lower symmetry, distortions of the electronic potential enormously complicate the nature of the incoming waves. In this derivation, the incoming waves are neglected, and the photoelectron is simply represented by the plane wave part

$$v(\vec{k}_f,\vec{r}) = (2\pi)^{-3/2} \exp(i\vec{k}_f \cdot \vec{r}) \ . \tag{5.20}$$

The applicability and implications of this approximation will be discussed in the following section. With this choice, Eq. (5.14) can be integrated by parts and yields

$$\vec{p} = (2\pi)^{-3/2} \int g_s(\vec{r}) \vec{\nabla} \exp(-i\vec{k}_f \cdot \vec{r}) d\vec{r} \tag{5.21}$$

$$= -i\vec{k}_f (2\pi)^{-3/2} \int \exp(-i\vec{k}_f \cdot \vec{r}) g_s(\vec{r}) d\vec{r} \ . \tag{5.22}$$

In our computational scheme, the Feynman-Dyson amplitudes in Eq. (5.22) are represented by a linear combination of Hartree-Fock orbitals. The Hartree-Fock orbitals can be decomposed into contracted Cartesian Gaussian functions on each atomic center, and each contracted Gaussian function can be further decomposed into a sum of primitive Gaussian functions. Ultimately therefore, the Feynman-Dyson amplitudes can be

represented as some linear combination of primitive Gaussian functions on each atomic center

$$g_s(\vec{r}) = \sum_{\alpha,k} c^s_{\alpha k}\, \phi_{\alpha k}\,(\vec{r} - \vec{R}_\alpha)\ . \tag{5.23}$$

Here α represents the sum over atomic centers and k the sum over primitive Gaussian functions on each center. Transforming the photoelectron position vector to the coordinate frames of each atomic center by the substitution $\vec{r}' = \vec{r} - \vec{R}_\alpha$, Eq. (5.22) can be re-expressed in terms of the primitive computational basis

$$\vec{P} = -i\vec{k}_f(2\pi)^{-3/2} \sum_{\alpha,k} \exp(-i\vec{k}_f \cdot \vec{R}\ )c^s_{\alpha k} \int \exp(-i\vec{k}_f \cdot \vec{r}')\phi_{\alpha k}(\vec{r}')d\vec{r}'\ . \tag{5.24}$$

The integral over $\vec{r}'$ in Eq. (5.24) represents a Fourier transform of each primitive Gaussian function, and formulae for its evaluation are derived by Kaijser and Smith (1977).

The final step in this derivation is to integrate the differential photoionization cross-section (Eq. (5.19)) over all photoelectron directions in the solid angle $d\Omega_f$

$$\sigma_s = \frac{8\pi^2 k_f}{3c\omega} \int |\vec{P}|^2 d\Omega_f\ . \tag{5.25}$$

Since $\vec{P}$ involves a sum over atomic centers, Eq. (5.25) will contain both one- and two-center contributions (Schweig and Thiel, 1974)

$$\sigma_s = \frac{8\pi^2 k_f^3}{3c\omega} \sum_{\alpha,k} \sum_{\beta,l} c^s_{\alpha k}\, c^s_{\beta l}\, Q^s_{\alpha k,\beta l} \tag{5.26}$$

The one-center terms (α=β) have the form

$$Q^{S}_{\alpha k,\alpha l} = \int \Phi^{*}_{\alpha k}(\vec{k}_f)\Phi_{\alpha l}(\vec{k}_f)d\Omega_f \tag{5.27}$$

where $\Phi_{\alpha k}(\vec{k}_f)$ represents the Fourier transform

$$\Phi_{\alpha k}(\vec{k}_f) = (2\pi)^{-3/2} \int \exp(-i\vec{k}_f \cdot \vec{r}')\phi_{\alpha k}(\vec{r}')d\vec{r}' \tag{5.28}$$

and the two-center terms ($\alpha \neq \beta$) are given by

$$Q^{S}_{\alpha k,\beta l} = \int \Phi^{*}_{\alpha k}(\vec{k}_f)\Phi_{\beta l}(\vec{k}_f)\exp(-i\vec{k}_f \cdot \vec{R}_{\alpha\beta})d\Omega_f \tag{5.29}$$

where $\vec{R}_{\alpha\beta} = \vec{R}_{\alpha} - \vec{R}_{\beta}$. Owing to the orthogonality of the spherical harmonics which describe the angular dependence of the Fourier transforms, the one-center terms are easily evaluated. The two-center terms are complicated slightly by the exponential factor, but these too can be evaluated analytically. For this purpose, it is convenient to define the integral

$$I(l_1m_1,l_2m_2) = \int Y_{l_1m_1}(\theta_f,\phi_f)Y_{l_2m_2}(\theta_f,\phi_f)\exp(-i\vec{k}_f \cdot \vec{R}_{\alpha\beta})d\Omega_f, \tag{5.30}$$

where $Y_{l_1m_1}$ and $Y_{l_2m_2}$ are real spherical harmonics (Harris, 1973) representing the angular dependence of the transforms $\Phi^{*}_{\alpha k}$ and $\Phi_{\beta l}$ respectively. Using the expansion

$$\exp(\pm i\vec{k}_f \cdot \vec{R}_{\alpha\beta}) = 4\pi \sum_{l=0}^{\infty} \sum_{m=-1}^{l} (\pm i)^{l} j_l(k_f R_{\alpha\beta}) Y_{lm}(\theta_f,\phi_f) Y_{lm}(\theta,\phi), \tag{5.31}$$

Eq. (5.30) becomes

$$I(l_1m_1,l_2m_2) = 4\pi \sum_{l=0}^{\infty} \sum_{m=-1}^{l} (-i)^{l} j_l(k_f R_{\alpha\beta}) C^{m_1 m_2 - m}_{l_1 l_2 l} Y_{lm}(\theta,\phi). \tag{5.32}$$

In these equations, (θ_f,ϕ_f) represents the photoelectron direction in the atomic reference frame, (θ,ϕ) represents the direction of $R_{\alpha\beta}$ in the molecular frame, $j_l(k_f R_{\alpha\beta})$ is a spherical Bessel function of l-th order, and $C^{m_1 m_2 - m}_{l_1 l_2 l}$ is a Clebsh-Gordan coefficient defined by (Harris, 1973)

$$C^{m_1 m_2 m}_{l_1 l_2 l} = \int Y_{l_1 m_1}(\theta_f,\phi_f) Y_{l_2 m_2}(\theta_f,\phi_f) Y_{lm}(\theta_f,\phi_f) d\Omega_f \ . \qquad (5.33)$$

When the distance vector $\vec{R}_{\alpha\beta}$ coincides with the molecular z-axis, the expansion in Eq. (5.31) simplifies to

$$\exp(\pm i\vec{k}_f \cdot \vec{R}_{\alpha\beta}) = (4\pi)^{\frac{1}{2}} \sum_l (\pm i)^l (2l+1)^{\frac{1}{2}} j_l(k_f R_{\alpha\beta}) Y_{l0}(\theta_f,\phi_f) \qquad (5.34)$$

and Eq. (5.30) becomes

$$I(l_1 m_1, l_2 m_2) = (4\pi)^{\frac{1}{2}} \delta_{m_1 m_2} \sum_{l=|l_1-l_2|}^{|l_1+l_2|} (-i)^l (2l+1)^{\frac{1}{2}} C^{m_1 m_2 0}_{l_1 l_2 l} \, j_l(k_f R_{\alpha\beta}) \qquad (5.35)$$

For arbitrary directions of $\vec{R}_{\alpha\beta}$ which do not coincide with the molecular z-axis, a new coordinate frame can be defined in which $\vec{R}_{\alpha\beta}$ does coincide with this axis, and the spherical harmonics can be transformed to this coordinate frame using the familiar rotation matrices (Schweig and Thiel, 1974). In this way, Eq. (5.35) can be used to evaluate all two-center integrals arising from any molecular geometry.

5.3 Discussion of Approximations

Relatively little work has been devoted to the theoretical calculation of photoionization cross-sections for molecules compared with that for atoms (see e.g. Marr, 1967, Steward, 1967, Kelly, 1976). The major impediments until recently have been a lack of sufficiently accurate molecular wavefunctions and an absence of accurate analytic representations for the photoelectron wavefunction (Kaplan and Markin, 1967, Schweig and Thiel, 1974). With the development of efficient, molecular integral and Hartree-Fock programs, Hartree-Fock wavefunctions are now readily available for a large number of molecules. This availability in turn has stimulated several theoretical calculations of molecular

photoionization cross-sections using the frozen orbital approximation (Rabalais et al., 1974, Dewar et al., 1975, Allison and Cavell, 1978, and Cavell and Allison, 1978).

In the frozen orbital approximation, the N-electron reference state is assumed to be the Hartree-Fock ground state, and the ion states are constructed by removing the orbital corresponding to the ionized electron. This approximation neglects both correlation corrections in the ground and ion states and ion state relaxation (see Introduction). Following Purvis and Öhrn (1975a), we have replaced the frozen orbital approximation by a many-electron treatment which incorporates both relaxation and correlation corrections. This treatment derives from the use of the Feynman-Dyson amplitudes obtained from the electron propagator to compute the photoionization cross-section.

The form of the photoelectron wavefunction is still a major problem in the calculation of molecular photoionization cross-sections and represents the most critical step in our derivation. The plane wave approximation was chosen for its simplicity, however, it has several serious limitations. The most serious limitation is its failure to correctly predict experimentally observed angular distributions (Bethe and Salpeter, 1957, Schweig and Thiel, 1974). This deficiency is not readily apparent when the differential cross-section is averaged over all photoelectron directions, and in our computational applications, we compute only spherically averaged, total cross-sections. Lohr (1972) has shown that by retaining the second term in Eq. (5.7), qualitatively correct angular distributions may be obtained. The retention of this term is equivalent to orthogonalizing the plane wave to every one-electron function in the N-electron ground state and is known as the orthogonalized plane wave (OPW) approximation.

A second limitation of the plane wave approximation is the implicit neglect of electrostatic interactions between the photoelectron and the molecular ion. For ionization processes near threshold where the photoelectron leaves with low kinetic energy, these interactions are especially important, and the wavefunction of the photoelectron exhibits a decrease in wavelength as $\vec{r} \to \vec{0}$. The OPW approximation again partially corrects this deficiency (Lohr, 1972) but exhibits a rather abrupt change in wavelength which is more characteristic of a short-range potential rather than the long-range Coulomb potential. Other representations of low energy photoelectrons, e.g. multicentered Coulomb wave expansions, have also been proposed (Tuckwell, 1970). As the kinetic energy of the photoelectron tends to higher energies, the effect of electrostatic interactions on the total cross-section becomes negligible, and the plane wave approximation becomes sufficiently accurate (Bethe and Salpeter, 1957).

Unfortunately, as the plane wave approximation becomes more suitable at high photoelectron energies, the dipole approximation (Eq. (5.12)) deteriorates and must be re-examined. Bethe and Salpeter (1957) have shown that when retardation effects are included in the calculation of differential photoionization cross-sections, the lowest order correction is proportional to $(|\vec{v}|/c)$, where $\vec{v}$ is the photoelectron velocity. This correction, however, only effects the angular distribution and vanishes when the differential cross-section is averaged over all incident photon directions. Higher-order corrections for retardation are proportional to $(|\vec{v}|/c)^2$ as are the relativistic corrections, but these are usually negligible even when the photon wavelength is comparable to the molecular dimensions.

5.4 Computational Applications

In this section, the relative photoionization intensities for the water and acetylene molecules are computed using the Feynman-Dyson amplitudes obtained in the second-order, diagram conserving and the diagonal 2p-h TDA, renormalized decoupling approximations. Comparative calculations corresponding to a Mg K_α photon source ($\hbar\omega$ = 1253.6 eV), for which the plane wave approximation is expected to be good, and a He (II) photon source ($\hbar\omega$ = 40.81 eV), for which the plane wave approximation is expected to be less accurate, are presented. These results are further compared with intensities obtained using the frozen orbital approximation in order to assess the magnitude of many-electron correlation and relaxation corrections. For acetylene, the dependence of intensity on photon energy for the valence orbitals is plotted, and orbital and density difference plots are presented and discussed.

The relative photoionization intensities for water corresponding to a Mg K_α photon source and a He (II) photon source are presented in Tables 13 and 14, respectively. These results were obtained using the 26 contracted Gaussian orbital basis at the experimentally determined equilibrium geometry as described in detail in Section 3.5 and are scaled relative to the $3a_1$ intensity. As expected, the relative intensities computed for the Mg K_α source in Table 13 compare reasonably well with those obtained experimentally (Rabalais *et al.*, 1974). The orthogonalized plane wave results of Rabalais *et al.* (1975) are presented for comparison and also correctly order the relative intensities. It is interesting to note the larger discrepency between the $1b_1$ and $1b_2$ intensities in our calculations compared to Rabalais *et al.* than in the $2a_1$ and $3a_1$ intensities. Since for X-ray photons the OPW corrections are not expected

Table 13. Relative Photoionization Intensities for Water Excited by Mg K_α (1253.6 eV).

Orbital	FO[a]	$\Sigma^{(2)}(E)$	$\Sigma^{(2)}(E)_{SHIFT} + \Sigma^{(3)}(\infty)$	OPW[b]	Exp.[b]
$2a_1$	4.69	1.32 2.57	4.15	4.50	3.84
$3a_1$	1.00	1.00	1.00	1.00	1.00
$1b_1$	0.62	0.52	0.55	0.18	0.36
$1b_2$	0.40	0.35	0.37	0.09	0.31

[a]Frozen orbital approximation.

[b]Rabalais *et al.* (1974).

Table 14. Relative Photoionization Intensities for Water Excited by He(II) (40.81 eV).

Orbital	FO[a]	$\Sigma^{(2)}(E)$	$\Sigma^{(2)}(E)_{SHIFT} + \Sigma^{(3)}(\infty)$	OPW[b]	Exp.[c]
$2a_1$	0.55	0.28 0.66	0.84	0.26	not observed
$3a_1$	1.00	1.00	1.00	1.00	1.00
$1b_1$	1.16	1.15	1.15	0.86	0.96
$1b_2$	0.83	0.84	0.83	1.10	0.80

[a]Frozen orbital approximation.

[b]Rabalais *et al.* (1975).

[c]Rabalais *et al.* (1974).

to be large, this discrepency is most likely a basis set effect. Our basis contained d-type polarization functions on oxygen as well as p-type polarization functions on the hydrogen atoms, whereas Rabalais et al. have used only a minimal basis.

The relative intensities presented in Table 14 do not correctly match the experimentally observed intensities. This is not particularly surprising owing to the inadequacy of the plane wave approximation at low photon energies. It is more surprising that the OPW results also yield an incorrect ordering of the intensities. The failure of the OPW approximation indicates the necessity for a more accurate photoelectron wavefunction.

Many-electron correlation and relaxation corrections appear negligible in the intensities of both Tables 13 and 14. The deviations between the frozen orbital approximation (FO), the second-order self-energy approximation ($\Sigma^{(2)}(E)$), and the diagonal 2p-h TDA with third-order constant energy diagrams ($\Sigma^{(2)}(E)_{SHIFT} + \Sigma^{(3)}(\infty)$), are small and may be attributed to differences in the photoelectron momenta. Different ionization energies obtained with different decoupling approximations were used to compute the photoelectron momenta from the conservation of total energy

$$|\vec{k}_f| = [2(\omega - \text{I.P.})]^{1/2} \text{ (in atomic units)} , \qquad (5.36)$$

consequently, deviations in the I.P.'s result in deviations in $|\vec{k}_f|$.

The relative intensities computed with the diagonal 2p-h TDA plus third-order constant energy diagrams for the Mg K_α photon source are plotted in Fig. 5. In order to compare the theoretical spectrum to the experimental ESCA (Electron Spectroscopy for Chemical Analysis) spectrum (Siegbahn et al., 1969) which is sketched as an insert, the ionization

Figure 5. A plot of the theoretical ESCA spectrum for the valence ionizations of water. The experimental spectrum of Siegbahn *et al*. (1969) is sketched in the insert.

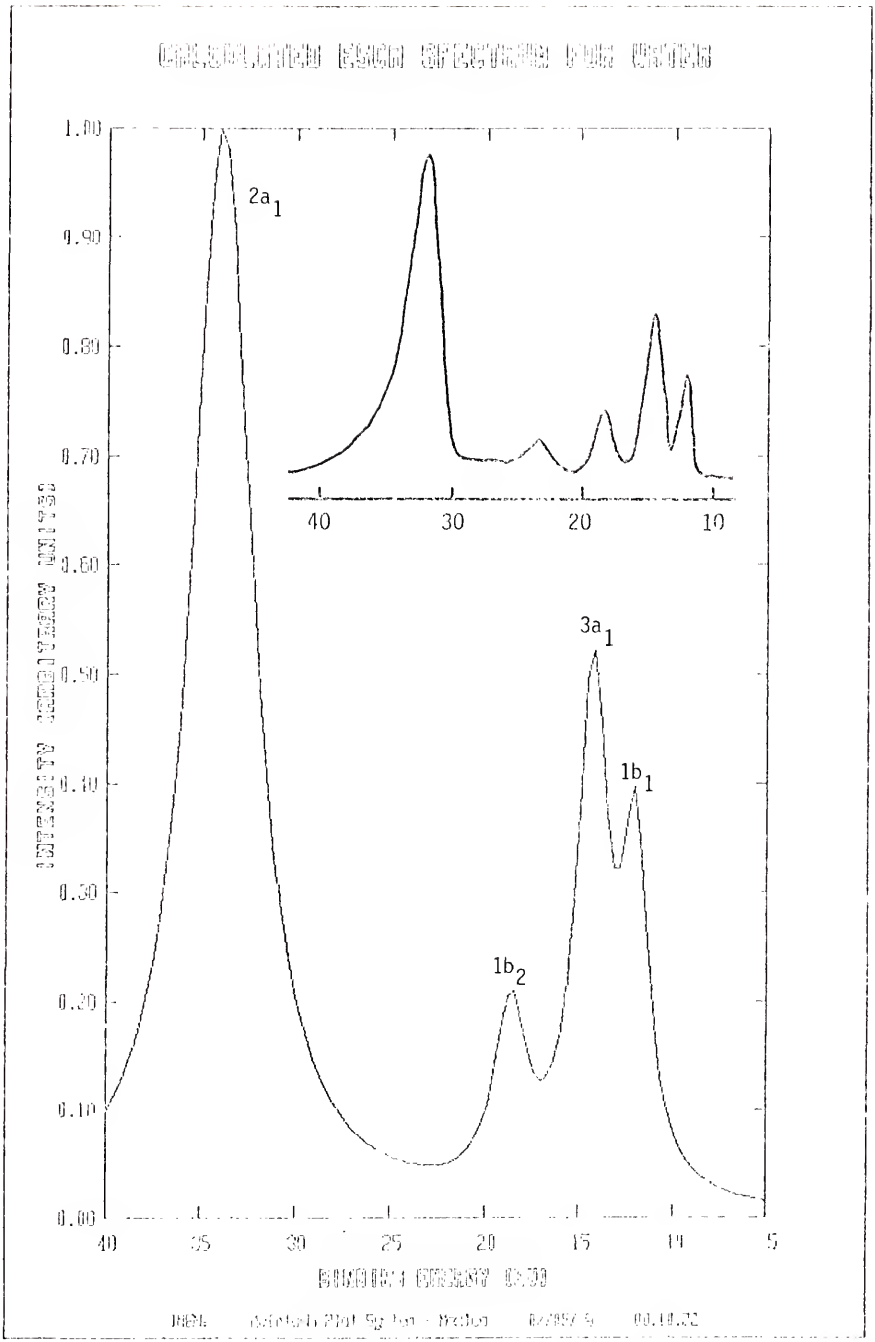
2a1
3a1
1b1
1b2
40
30
20
10
40
35
30
25
20
15
10
5

lines were given a Lorentzian width estimated from the experimental spectrum. The major features of the experimental spectrum are well-reproduced with the exception of the weak peak at approximately 23 eV. This peak has been attributed to the ionization of $2a_1$ electrons by the Mg $K_{\alpha_{3,4}}$ satellite in the photon source (Siegbahn et al., 1969) and therefore should not appear in the theoretical spectrum since it was calculated for a purely monochromatic source.

A recent experimental study of relative photoionization intensities of acetylene with various photon sources (Cavell and Allison, 1978) motivated our examination of this molecule. As preparatory steps to the calculation of relative intensities, Hartree-Fock and electron propagator calculations were performed at the experimental equilibrium geometry, R(C-C) = 2.279 a.u. and R(C-H) = 2.005 a.u. (Buenker et al., 1967), with two different basis sets. The first basis consisted of Huzinaga's 9s,5p primitive basis for carbon and 4s basis (unscaled) for hydrogen (Huzinaga, 1965) contracted with Dunning's coefficients (Dunning, 1970) to 4s,2p on carbon and 2s on hydrogen (see Table 8). The complete molecular basis consisted of 24 contracted Gaussian orbitals and yielded a Hartree-Fock total energy of E(HF) = -76.7948 H. The second basis augmented the first by the addition of a set of d functions on each carbon atom (α_d = 0.60) and a set of p functions on each hydrogen atom (α_p = 0.75). The addition of these diffuse, polarization functions brought the size of the basis to 42 contracted Gaussian orbitals and yielded a Hartree-Fock total energy of E(HF) = -76.8267 H.

Valence ionization energies were computed with the second-order self-energy approximation and the diagonal 2p-h TDA for each basis. The results for the 24 orbital basis are presented in Table 15 and the

Table 15. Valence Ionization Energies for Acetylene (24 CGTO's).

Orbital	Koopmans	$\Sigma^{(2)}(E)$	$\Sigma^{(2)}(E)_{SHIFT}$	Ced.[a]	Exp.[b]
$2\sigma_g$ Shake-up	-	38.29	-	28.9	27.6
$2\sigma_g$	28.42	25.47	26.48	23.9	23.5
$3\sigma_g$	18.55	16.39	17.08	16.4	16.8
$1\pi_u$	11.32	11.20	11.29	10.8	11.4
$2\sigma_u$	20.81	18.21	19.12	18.0	18.7

[a]Cederbaum *et al.* (1978).

[b]Cavell and Allison (1978).

results for the 42 orbital basis appear in Table 16. In each table the full, nondiagonal 2p-h TDA results of Cederbaum et al. (1978) and the experimental results of Cavell and Allison (1978) are included for comparison. In contrast to previous calculations reported here, the ionization energies obtained for acetylene are larger (with the exception of the $1\pi_u$ ionization) than the experimental values. A breakdown in the quasi-particle picture for the $2\sigma_g$ ionization which is evidenced by the shake-up pole may account for the particularly poor results for these ionizations. The off-diagonal 2p-h TDA contributions considerably improve these two ionization energies (Cederbaum et al., 1978), however, the shake-up energy still disagrees with the experimental value by more than an electron volt.

Relative photoionization intensities for acetylene are presented in Table 17 for a Mg K_α photon source and in Table 18 for a He (II) photon source. In both tables the intensities were scaled relative to the $1\pi_u$ intensity. As for water, the intensities corresponding to the Mg K_α source are in reasonable agreement with experimental intensities and show only a slight diminution when correlation and relaxation effects are included. The OPW result of Cavell and Allison (1978) for the $2\sigma_g$ ionization in Table 17 seems unexplicably high, and the $3\sigma_g$ ionization is not observed experimentally (Cavell and Allison, 1978).

The relative intensities for acetylene computed with the He (II) source exhibit better agreement with the experimental results than did the water results. Here, only the relative intensities of the two weakest ionizations, the $2\sigma_g$ and $2\sigma_u$, were reversed. The OPW results predict the correct ordering but attribute a much weaker intensity to the $2\sigma_g$ ionization than is observed experimentally.

Table 16. Valence Ionization Energies for Acetylene (42 CGTO's).

Orbital	Koopmans	$\Sigma^{(2)}(E)$	$\Sigma^{(2)}(E)_{SHIFT}$	Ced.[a]	Exp.[b]
$2\sigma_g$ Shake-up	-	38.20	34.45	28.9	27.6
$2\sigma_g$	28.07	24.56	25.73	23.9	23.5
$3\sigma_g$	18.46	16.56	17.24	16.4	16.8
$1\pi_u$	11.16	11.13	11.24	10.8	11.4
$2\sigma_u$	20.90	no results	19.47	18.0	18.7

[a]Cederbaum *et al.* (1978).

[b]Cavell and Allison (1978).

Table 17. Relative Photoionization Intensities for Acetylene Excited by Mg K_α (1253.6 eV).

Orbital	FO[a]	$\Sigma^{(2)}(E)$	$\Sigma^{(2)}(E)_{SHIFT}$	OPW[b]	Exp.[b]
$2\sigma_g$	18.90	17.75	17.79	26.86	13.3
$3\sigma_g$	0.51	0.48	0.48	0.65	not observed
$1\pi_u$	1.00	1.00	1.00	1.00	1.00
$2\sigma_u$	7.74	-	7.50	11.18	9.5

[a]Frozen orbital approximation.

[b]Cavell and Allison (1978).

Table 18. Relative Photoionization Intensities for Acetylene Excited by He(II) (40.81 eV).

Orbital	FO[a]	$\Sigma^{(2)}(E)$	$\Sigma^{(2)}(E)_{SHIFT}$	OPW[b]	Exp.[b]
$2\sigma_g$	0.45	0.36	0.72	0.09	0.26
$3\sigma_g$	0.45	0.44	0.87	0.77	0.68
$1\pi_u$	1.00	1.00	1.00	1.00	1.00
$2\sigma_u$	0.29	-	0.50	0.41	0.29

[a]Frozen orbital approximation.

[b]Cavell and Allison (1978).

The relative intensities in Table 17 computed with the diagonal 2p-h TDA and Mg K_{α} source have been plotted in Fig. 6. As in Fig. 5, the lines have been given Lorentzian widths and the experimental spectrum appears as an insert. The most striking difference between these two spectra is the absence of the intense shake-up in the theoretical spectrum. Not only was this peak predicted to lie 7 eV higher than the experimental peak in energy, it also yielded a relative intensity several orders of magnitude smaller than the $2\sigma_g$ intensity (at 23.4 eV). The weak experimental peak at about 14.5 eV arises from the ionization of $2\sigma_g$ electrons by Mg $K_{\alpha_{3,4}}$ radiation (Cavell and Allison, 1978) and is absent in the theoretical spectrum. The $3\sigma_g$ peak which should occur at 16.8 eV is not observed experimentally but can be identified as a shoulder on the $2\sigma_u$ peak in the theoretical spectrum.

Figure 7 shows the dependence of the photoionization cross-section on photon energy from 0-200 eV. Over this energy range, ionization from the $1\pi_u$ orbital is predicted to be most probable, and this is verified by the experimental data of Cavell and Allison (1978) obtained at 21.2 eV (He (I)), 40.8 eV (He (II)), and 151.4 eV (Zr M_{ζ}). Another interesting feature of this figure is the slight minimum exhibited by the $2\sigma_g$ curve around 125 eV. Minima of this type in the photoionization cross-section were first predicted by Cooper (1962) and are referred to as Cooper minima. Cooper minima have been observed in the cross-sections for a number of atoms by means of X-ray and ultraviolet absorption spectroscopy (see e.g. Codling, 1976); however, at present there are no photoelectron spectroscopic data of this type owing to the limitation of photon sources which are available. The application of synchrotron radiation to photoelectron spectroscopy should soon offer a means of studying the energy

Figure 6. A plot of the theoretical ESCA spectrum for the valence ionizations of acetylene. The experimental spectrum of Cavell and Allison (1978) is sketched in the insert.

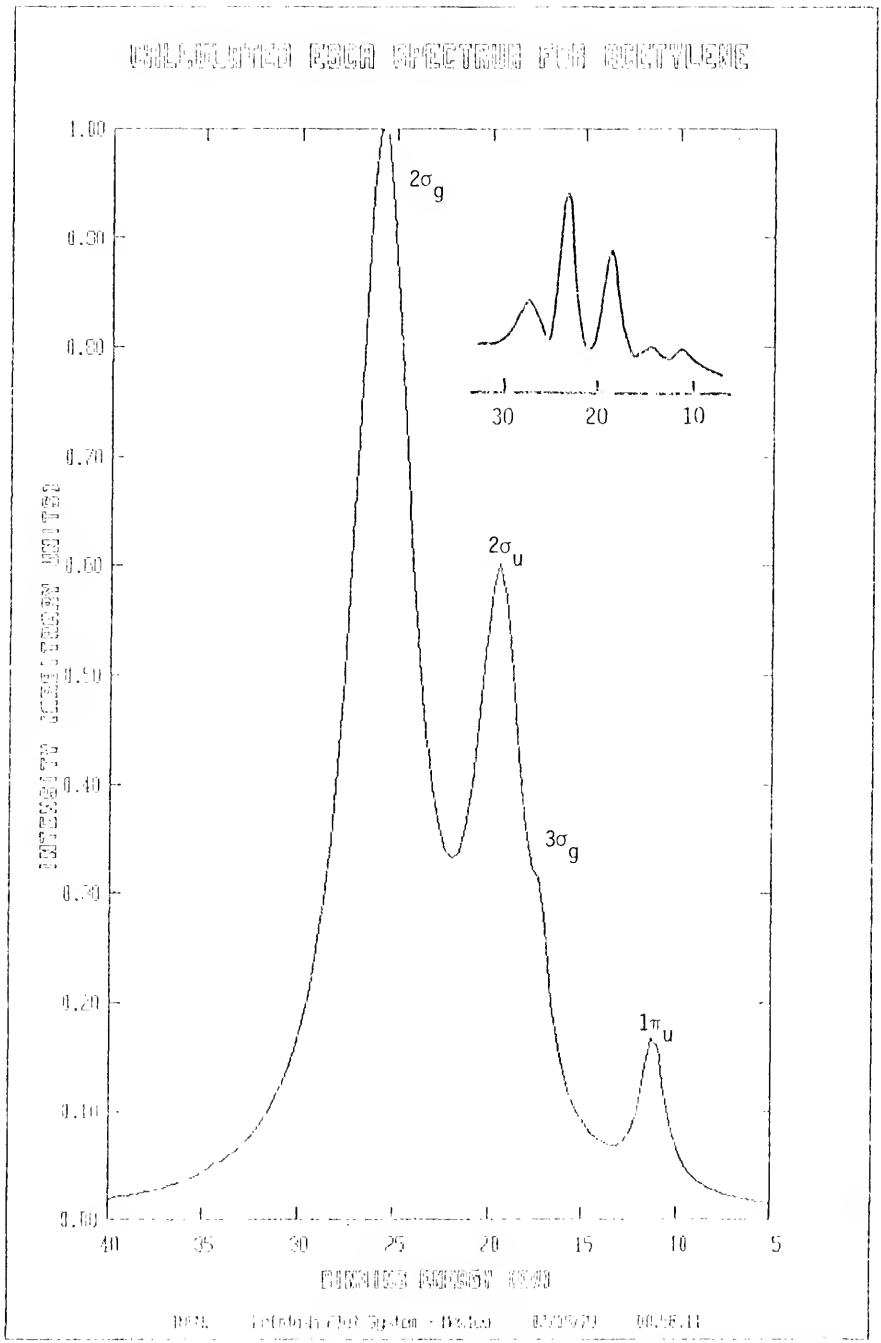
1.00
0.90
0.80
0.70
0.60
0.50
0.40
0.30
0.20
0.10
0.00
40
35
30
25
20
15
10
5
30
20
10
$2\sigma_g$
$2\sigma_u$
$3\sigma_g$
$1\pi_u$

Figure 7. A plot of the photoionization cross-sections versus photon energy for the valence orbitals of acetylene in the region 0-200 eV.

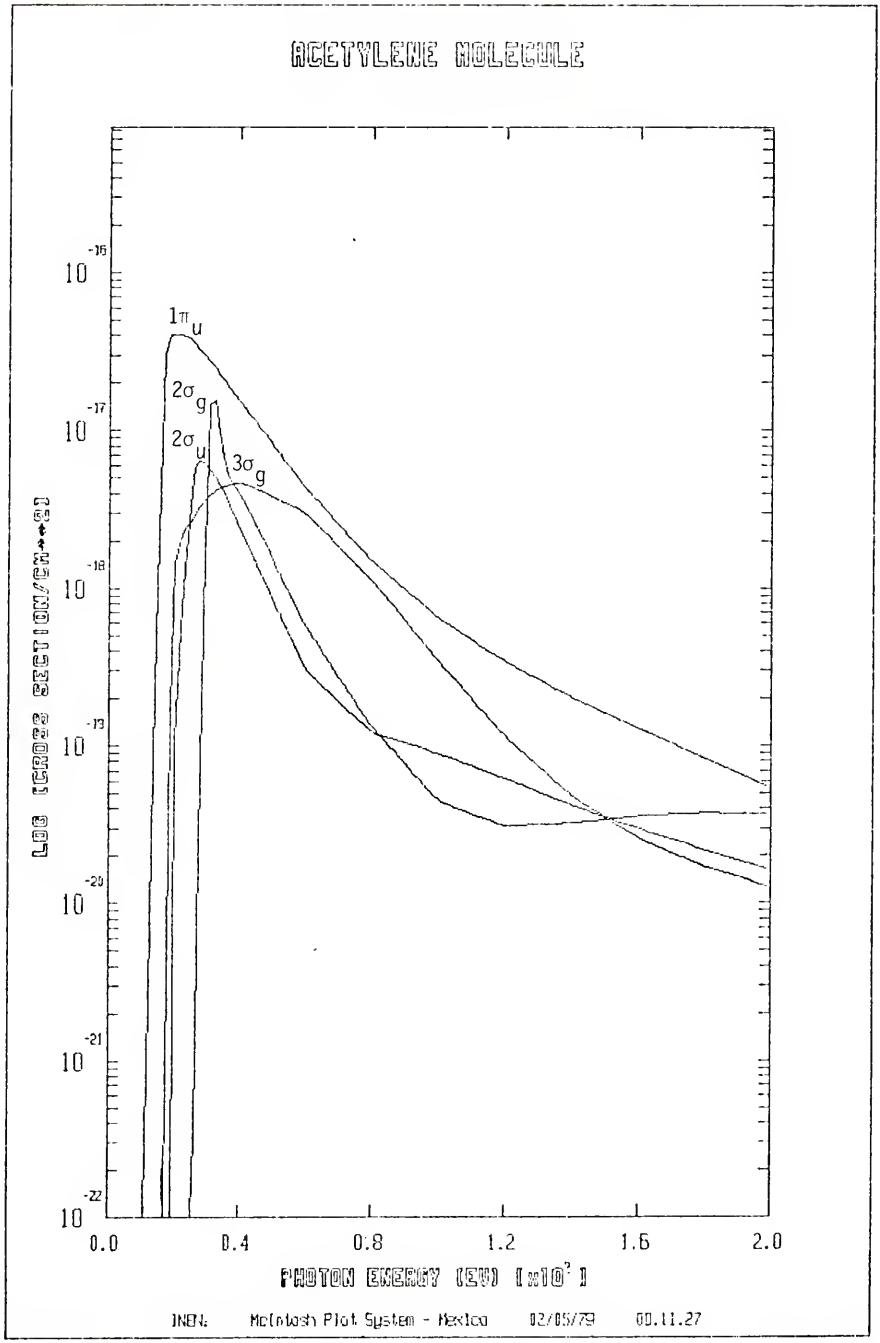
ACETYLENE MOLECULE
$1\pi_u$
$2\sigma_g$
$2\sigma_u$
$3\sigma_g$
LOG [CROSS SECTION/CM**2]
10^{-16}
10^{-17}
10^{-18}
10^{-19}
10^{-20}
10^{-21}
10^{-22}
0.0
0.4
0.8
1.2
1.6
2.0
PHOTON ENERGY (EV) [x10^2]
INEN: McIntosh Plot System - Mexico 02/05/79 00.11.27

dependence of the orbital cross-sections in a continuous energy interval from 0 to about 200 eV (Codling, 1973).

Orbital plots are presented for the $2\sigma_u$, $3\sigma_g$, and $1\pi_u$ Feynman-Dyson amplitudes in Fig. 8. Since the dominant component in each of these amplitudes is the corresponding Hartree-Fock orbital (i.e. $2\sigma_u$, $3\sigma_g$, and $1\pi_u$, respectively) the correlation and relaxation corrections are not readily observable. In order to examine these many-electron contributions more readily, density difference plots between the amplitudes of Fig. 8 and their corresponding Hartree-Fock orbital were made and are presented in Figs. 9-11. Since the Feynman-Dyson amplitudes are not normalized, it is necessary to normalize them before computing the density difference. In all of these plots, the Hartree-Fock density is negative which means any positive distortions imply density enhancement in the propagator amplitude while negative distortions imply density diminution. Figure 9 shows a density diminution in both the C-C and C-H bonding regions with a density enhancement in the anti-bonding region. Figure 10 shows an enhancement in the C-C pi bonding, and Fig. 11 shows an enhancement in the C-H bonding with a slight diminution of anti-bonding character.

It is apparent from the numerical results presented in this section that the calculated relative photoionization intensities, at least within the plane wave approximation, are not very sensitive to improvements in the Feynman-Dyson amplitudes. It is likely that more accurate photoelectron wavefunctions will improve the sensitivity of these quantities but not at the orthogonalized plane wave level. Although the OPW approximation is more justifiable formally, the results of Rabalais et al. (1974) and Cavell and Allison (1978) do not exhibit any marked improvements to the plane wave results in the two molecules studied here. Qualitative

Figure 8. Orbital plots for the $2\sigma_u$, $3\sigma_g$, and $1\pi_u$ Feynman-Dyson amplitudes of acetylene. Approximate scales on the plots are ±0.72 a.u. for $2\sigma_u$, ±0.28 a.u. for $3\sigma_g$, and ±0.29 a.u. for $1\pi_u$.

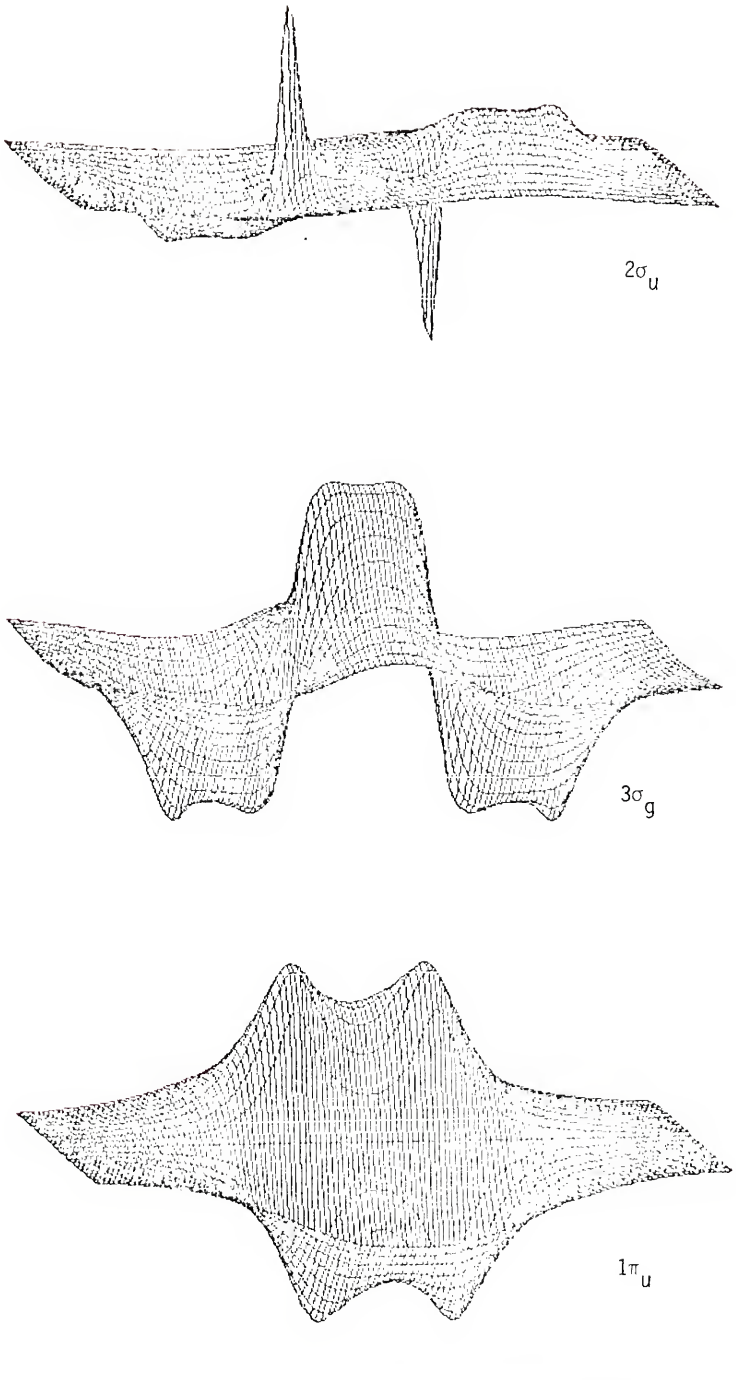
$2\sigma_u$
$3\sigma_g$
$1\pi_u$

Figure 9. A density difference plot between the $3\sigma_g$ Feynman-Dyson amplitude and the $3\sigma_g$ Hartree-Fock orbital of acetylene. Each contour represents a density increment of about 1.5×10^{-4} atomic units.

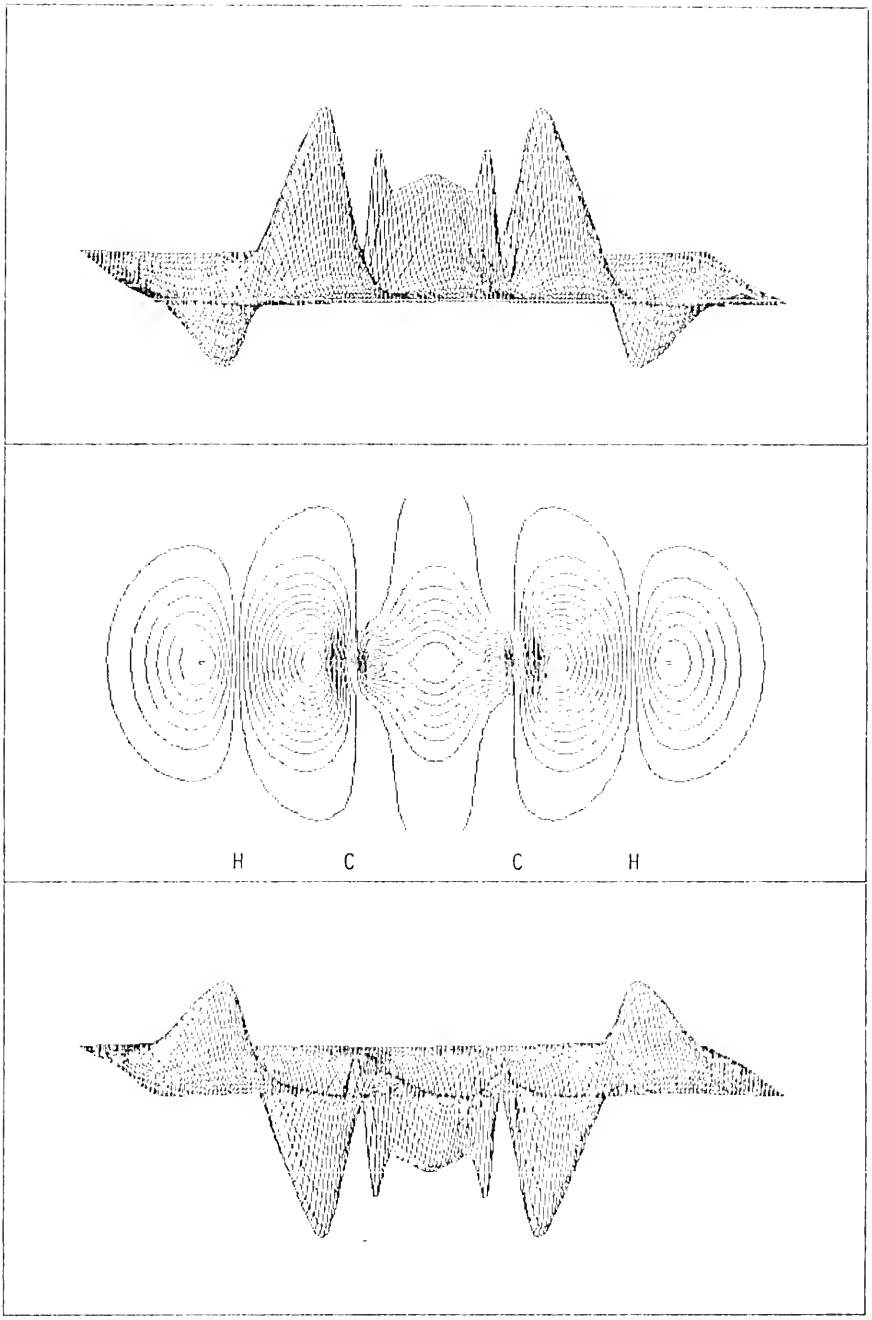
H
C
C
H

Figure 10. A density difference plot between the $1\pi_u$ Feynman-Dyson amplitude and the $1\pi_u$ Hartree-Fock orbital of acetylene. Each contour represents a density increment of about 3.6×10^{-3} atomic units.

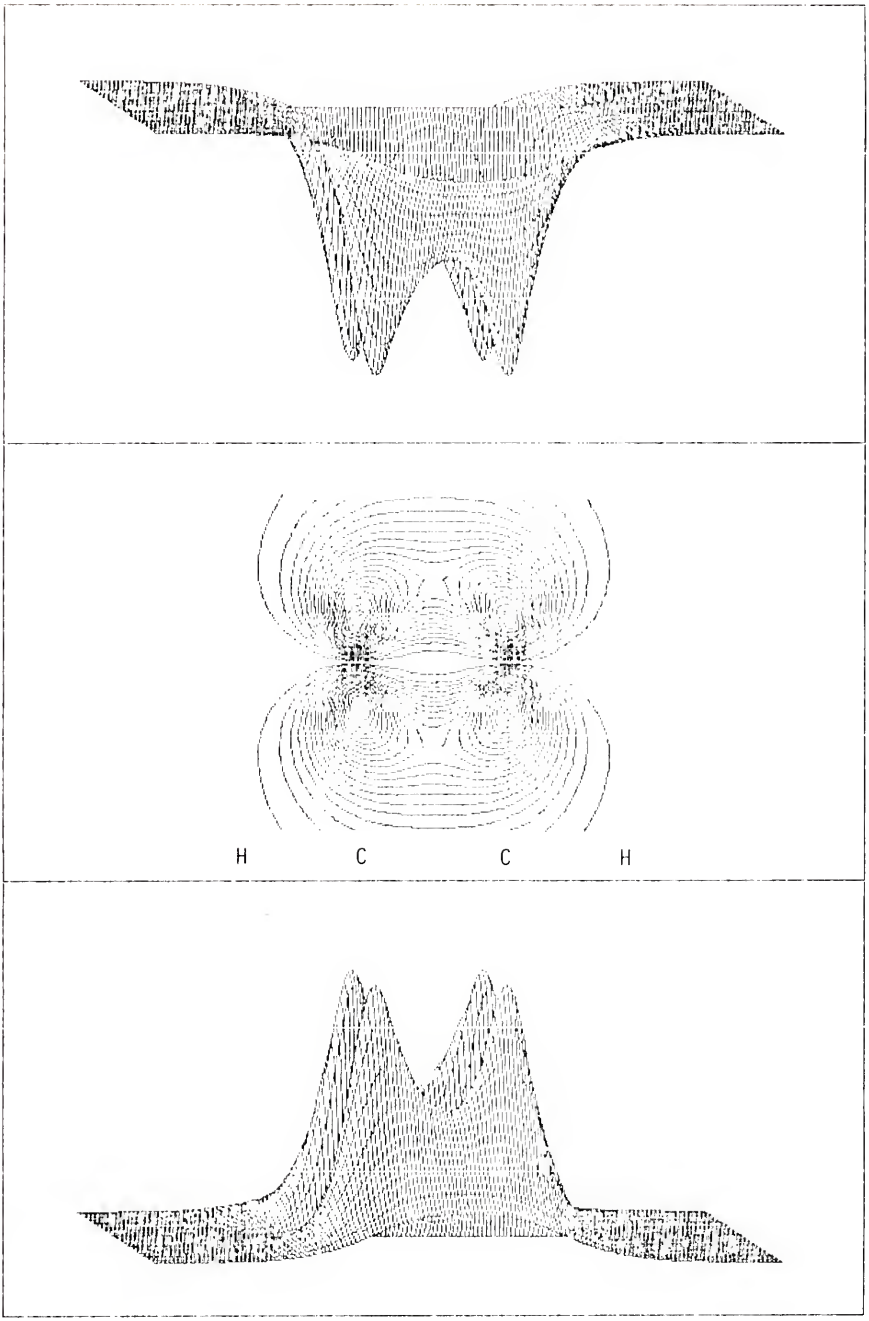
H
C
C
H

Figure 11. A density difference plot between the $2\sigma_u$ Feynman-Dyson amplitude and the $2\sigma_u$ Hartree-Fock orbital of acetylene. Each contour represents a density increment of about 4.4×10^{-4} atomic units.

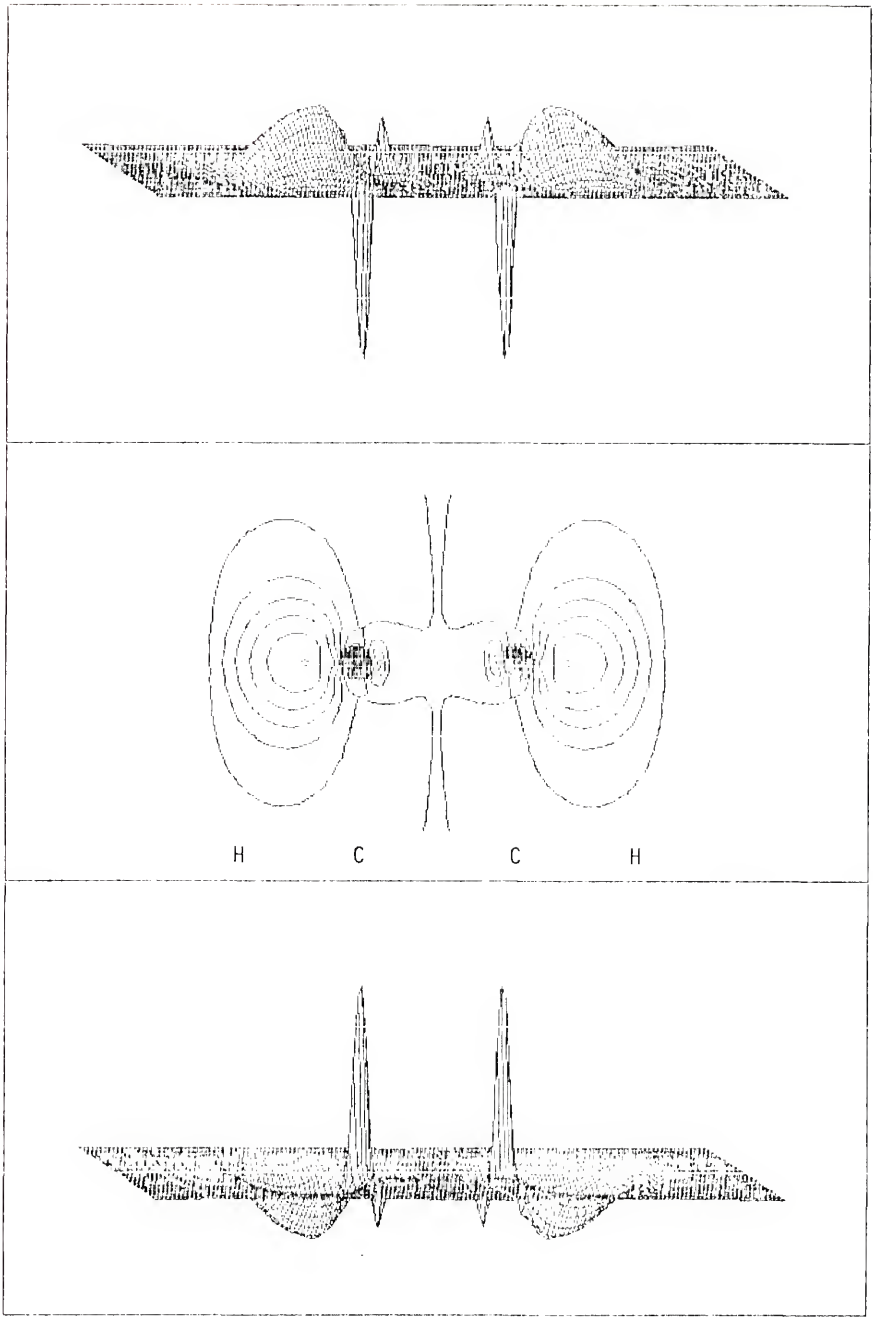
H
C
C
H

changes in the propagator amplitudes may be observed via density difference plots; however, more quantitative comparisons must await other computational applications.

CONCLUSIONS AND EXTENSIONS

The primary objective of this dissertation has been the investigation of alternative decouplings which may allow more accurate calculations of the electron propagator with less computational expenditure than the operator product decouplings. Contrary to previous contentions that decouplings of the propagator equations of motion and choice of reference state averages are interrelated (Oddershede and Jørgensen, 1977), we have demonstrated that they are in fact independent approximations, hence justifying the systematic improvement of one or the other. We have chosen to examine the decoupling approximation while maintaining a Hartree-Fock reference state since these reference states have a simple theoretical representation and are efficiently generated by a number of available computer programs. Since Hartree-Fock reference states ignore electron correlation (by definition), the correlation and relaxation corrections to the electron propagator must be exclusively incorporated through the decoupling approximation.

The superoperator formalism which was originally introduced as a notational convenience has a rich algebraic structure that has been largely unexploited. As we demonstrate in Chapter 3, the superoperator Hamiltonian may be partitioned and a perturbation theory may be developed in the operator space. The perturbation expansion of the superoperator resolvent readily yields the Dyson equation and allows an identification of wave and reaction superoperators. The definition of these auxiliary superoperators elucidates the parallelism between the superoperator

formalism and the diagrammatic expansion method and permits a unified conceptual framework.

When the superoperator resolvent is approximated by an inner projection, various choices of the inner projection manifold which correspond to different decouplings may be viewed as different approximations to the wave superoperator in the following equation (Born and Öhrn, 1977)

$$|\underline{h}) = \hat{W}(E)\ |\underline{a}) \ .$$

In particular, the operator product decoupling corresponds to the choice

$$\hat{W} = \hat{I} + \{a_k^+ a_l\}$$

$$\hat{W} = \hat{I} + \{a_k^+ a_l\} + \{a_k^+ a_l^+ a_m a_n\}$$

. . . ,

the moment conserving decoupling corresponds to

$$\hat{W} = \hat{I} + \hat{H}$$

$$\hat{W} = \hat{I} + \hat{H} + \hat{H}^2$$

. . . ,

and the diagram conserving decoupling of the Pade' type corresponds to

$$\hat{W}(E) = \hat{I} + \hat{T}_0(E)\hat{V}$$

$$\hat{W}(E) = \hat{I} + \hat{T}_0(E)\hat{V}\hat{T}_0(E)\hat{V}$$

. . . .

Alternatively, the superoperator resolvent may be approximated by an outer projection in which case decoupling approximations correspond to various approximations to the reaction (or self-energy) superoperator. Two decouplings of this type which have been presented are the simple

diagram conserving decoupling which corresponds to

$$\hat{t}(E) = \hat{V} + \hat{V}\hat{T}(E)\hat{V}$$

with

$$\hat{T}(E) = \hat{T}_0(E)$$

$$\hat{T}(E) = \hat{T}_0(E) + \hat{T}_0(E)\hat{V}\hat{T}_0(E)$$

. . . ,

and the renormalized decoupling which corresponds to

$$\hat{t}(E) = \hat{V} + \hat{V}\hat{T}(E)\hat{V}$$

with

$$\hat{T}(E) = \hat{T}_0(E) + \hat{T}_0(E)\hat{M}\hat{T}(E)$$

and where $\hat{M}$ is an effective potential obtained by projecting the perturbation superoperator onto a subspace of the full operator space. When this subspace is chosen to consist of simple operator products, this decoupling is formally equivalent to the operator product decoupling, however, other approximations may be envisioned.

Each of the above-mentioned decoupling approximations has been studied in detail computationally and has been evaluated on the basis of a comparison of the propagator poles with experimental ionization energies. The moment conserving decouplings discussed in Chapter 2 were found to yield unacceptably poor numerical results. It is plausible that since the moment matrices involve averages of various powers of the full superoperator Hamiltonian, the moment expansion may not be convergent anywhere in the complex plane. If this is the case, analytic continuation cannot be performed, and the Pade' approximant method will not improve convergence. In any event, it may be generally concluded

that the number of conserved moments is no indication of the accuracy of this decoupling.

A more successful approach is the diagram conserving decouplings presented in Chapter 3. A simple second-order self-energy truncation was found to overcorrect the Hartree-Fock orbital energy estimate of the ionization energy and yielded results that were generally too small. The inclusion of third-order diagrams, particularly rings and ladders, is necessary to obtain reasonable agreement with experiment. Energy shifts resulting from the addition of diffuse, polarization functions to the computational basis were observed to be nearly the same magnitude as the shifts obtained from third-order ring and ladder diagrams, hence care must be taken to insure basis saturation.

The renormalized 2p-h TDA decoupling was found to be the most satisfactory decoupling studied. Although only a diagonal approximation was implemented, principal ionization energies accurate to within an electron volt were generally obtained. Shake-up energies were less accurately described owing to the neglect of ion state relaxation and hole-hole correlation in the 2p-h TDA.

The numerical results of Chapter 5 indicate that the calculation of relative photoionization intensities using a plane wave approximation for the photoelectron is not a sensitive reflection of the quality of the Feynman-Dyson amplitudes. The severity of the plane wave approximation most likely obliterates the many-electron relaxation and correlation corrections. More accurate photoelectron representations such as orthogonalized plane waves or Coulomb waves should afford a more accurate evaluation of the Feynman-Dyson amplitudes, or alternatively, one-electron properties may be computed using the single-particle, reduced density matrix obtained from the spectral density.

There are several other possible extensions of this research that should be mentioned. Most obvious is an application of these decoupling ideas to the polarization propagator. Currently, decouplings of this propagator are based on operator products. The odd or Fermion-like operator products in the electron propagator theory must be replaced by even or Boson-like operator products to account for the particle-conserving nature of the polarization propagator theory, but with this minor modification, the application of the diagram conserving and renormalized decouplings also seems feasible.

More accurate decouplings are still needed for the electron propagator in order to better describe shake-up energies. With this goal in mind, Cederbaum and co-workers have recently implemented the full, non-diagonal 2p-h TDA by exploiting spin and orbital symmetry to reduce the dimension of the 2p-h operator subspace. Preliminary results indicate that this approximation provides some improvement but is still inadequate. The need for higher operator products, particularly quintuple products, has been demonstrated by Bagus and Viinikka (1977) in CI studies and may necessitate the implementation of a 3p-2h renormalization.

Another attractive avenue for extension is a combination of the 2p-h TDA renormalization with the Hamiltonian partitioning of Kurtz and Öhrn. Some work along this line is in progress by Ortiz and Öhrn (1979) and preliminary results are very encouraging. One criticism of this approximation is that if one interprets it as an alternative partitioning of the superoperator Hamiltonian in which the eigenvalues of the unperturbed Hamiltonian correspond to $\Delta E(SCF)$ energies (as in Eq. (3.23)), then the denominators of the self-energy which are obtained from

$$(E\hat{I}-\hat{H}_0')^{-1} \text{ (some operator product)}$$

should also involve $\Delta E(SCF)$ energies. For example, the second-order self-energy denominator would be

$$[E + \Delta E_k(SCF) - \Delta E_l(SCF) - \Delta E_m(SCF)]^{-1} .$$

Since it is probably not feasible to perform $\Delta E(SCF)$ calculations for all doublet (N-1) and (N+1)-electron states, simple approximations to the $\Delta E(SCF)$ energies such as

$$\Delta E_k(SCF) \simeq \varepsilon_k - \sum_{a,p} \frac{\langle ak||pk\rangle\langle pk||ak\rangle}{(\varepsilon_a - \varepsilon_p)}$$

or

$$\Delta E_k(SCF) \simeq \varepsilon_k - \sum_{a,p} \frac{\langle ak||pk\rangle\langle pk||ak\rangle}{(\varepsilon_a - \varepsilon_p) + \langle pa||pa\rangle + \langle pk||pk\rangle - \langle ak||ak\rangle}$$

might be considered.

Finally, the problem of open shell reference states has not been considered here. The retention of a restricted Hartree-Fock reference state in this regard will be a tremendous simplification, and the various spin and orbital symmetry couplings between the reference state and operator manifold may be treated with the theory of tensor operators.

APPENDIX 1

$$\Sigma_{ij}^{(3)}(E) = \frac{1}{4}\sum_{a}\sum_{p}\sum_{q}\sum_{r}\sum_{s}\frac{\langle ia||pq\rangle\langle pq||rs\rangle\langle rs||ja\rangle}{(E+\epsilon_a-\epsilon_r-\epsilon_s)(E+\epsilon_a-\epsilon_p-\epsilon_q)}$$  (A)

$$-\frac{1}{4}\sum_{a}\sum_{b}\sum_{c}\sum_{d}\sum_{p}\frac{\langle ip||ab\rangle\langle ab||cd\rangle\langle cd||jp\rangle}{(E+\epsilon_p-\epsilon_c-\epsilon_d)(E+\epsilon_p-\epsilon_a-\epsilon_b)}$$  (B)

$$-\sum_{a}\sum_{b}\sum_{p}\sum_{q}\sum_{r}\frac{\langle ib||rq\rangle\langle ra||pb\rangle\langle pq||ja\rangle}{(E+\epsilon_a-\epsilon_p-\epsilon_q)(E+\epsilon_b-\epsilon_q-\epsilon_r)}$$  (C)

$$+\sum_{a}\sum_{b}\sum_{c}\sum_{p}\sum_{q}\frac{\langle jq||cb\rangle\langle cp||aq\rangle\langle ab||jp\rangle}{(E+\epsilon_p-\epsilon_a-\epsilon_b)(E+\epsilon_q-\epsilon_b-\epsilon_c)}$$  (D)

$$+\frac{1}{4}\sum_{a}\sum_{b}\sum_{c}\sum_{p}\sum_{q}\frac{\langle ic||ab\rangle\langle ab||pq\rangle\langle pq||jc\rangle}{(E+\epsilon_c-\epsilon_p-\epsilon_q)(\epsilon_a+\epsilon_b-\epsilon_p-\epsilon_q)}$$  (E)

$$+\frac{1}{4}\sum_{a}\sum_{b}\sum_{c}\sum_{p}\sum_{q}\frac{\langle ja||pq\rangle\langle pq||bc\rangle\langle bc||ja\rangle}{(E+\epsilon_a-\epsilon_p-\epsilon_q)(\epsilon_b+\epsilon_c-\epsilon_p-\epsilon_q)}$$  (F)

$$+\frac{1}{4}\sum_{a}\sum_{b}\sum_{p}\sum_{q}\sum_{r}\frac{\langle jp||ab\rangle\langle ab||qr\rangle\langle qr||jp\rangle}{(E+\epsilon_p-\epsilon_a-\epsilon_b)(\epsilon_a+\epsilon_b-\epsilon_q-\epsilon_r)}$$  (G)

$$+\frac{1}{4}\sum_{a}\sum_{b}\sum_{p}\sum_{q}\sum_{r}\frac{\langle jp||qr\rangle\langle qr||ab\rangle\langle ab||jp\rangle}{(E+\epsilon_p-\epsilon_a-\epsilon_b)(\epsilon_a+\epsilon_b-\epsilon_q-\epsilon_r)}$$  (H)

$$-\sum_{a}\sum_{b}\sum_{p}\sum_{q}\sum_{r}\frac{\langle jr||aq\rangle\langle ab||pr\rangle\langle pq||jb\rangle}{(E+\epsilon_b-\epsilon_p-\epsilon_q)(\epsilon_a+\epsilon_b-\epsilon_p-\epsilon_r)}$$  (I)

$$-\sum_{a}\sum_{b}\sum_{p}\sum_{q}\sum_{r}\frac{\langle ib||pr\rangle\langle pq||ab\rangle\langle ar||jq\rangle}{(E+\epsilon_b-\epsilon_p-\epsilon_r)(\epsilon_a+\epsilon_b-\epsilon_p-\epsilon_q)}$$  (J)

$$-\sum_{a}\sum_{b}\sum_{c}\sum_{p}\sum_{q}\frac{\langle jq||ac\rangle\langle ab||pq\rangle\langle pc||jb\rangle}{(E+\epsilon_q-\epsilon_a-\epsilon_c)(\epsilon_a+\epsilon_b-\epsilon_p-\epsilon_q)}$$  (K)

$$-\sum_{a}\sum_{b}\sum_{c}\sum_{p}\sum_{q}\frac{\langle ic\|qb\rangle\langle qp\|\|ac\rangle\langle ab\|\|ip\rangle}{(E+\epsilon_p-\epsilon_a-\epsilon_b)(\epsilon_a+\epsilon_c-\epsilon_p-\epsilon_q)}$$ (L)

$$+\frac{1}{2}\sum_{a}\sum_{b}\sum_{p}\sum_{q}\sum_{r}\frac{\langle ir\|\|jp\rangle\langle ab\|\|rq\rangle\langle pq\|\|ab\rangle}{(\epsilon_a+\epsilon_b-\epsilon_p-\epsilon_q)(\epsilon_a+\epsilon_b-\epsilon_q-\epsilon_r)}$$ (M)

$$-\frac{1}{2}\sum_{a}\sum_{b}\sum_{c}\sum_{p}\sum_{q}\frac{\langle ia\|\|jc\rangle\langle cb\|\|pq\rangle\langle pq\|\|ab\rangle}{(\epsilon_a+\epsilon_b-\epsilon_p-\epsilon_q)(\epsilon_b+\epsilon_c-\epsilon_p-\epsilon_q)}$$ (N)

$$+\frac{1}{2}\sum_{a}\sum_{b}\sum_{p}\sum_{q}\sum_{r}\frac{\langle ip\|\|ja\rangle\langle ab\|\|qr\rangle\langle qr\|\|pb\rangle}{(\epsilon_a+\epsilon_b-\epsilon_q-\epsilon_r)(\epsilon_a-\epsilon_p)}$$ (O)

$$-\frac{1}{2}\sum_{a}\sum_{b}\sum_{c}\sum_{p}\sum_{q}\frac{\langle ip\|\|ja\rangle\langle bc\|\|pq\rangle\langle aq\|\|bc\rangle}{(\epsilon_b+\epsilon_c-\epsilon_p-\epsilon_q)(\epsilon_a-\epsilon_p)}$$ (P)

$$+\frac{1}{2}\sum_{a}\sum_{b}\sum_{p}\sum_{q}\sum_{r}\frac{\langle ia\|\|jr\rangle\langle rb\|\|pq\rangle\langle pq\|\|ab\rangle}{(\epsilon_a+\epsilon_b-\epsilon_p-\epsilon_q)(\epsilon_a-\epsilon_r)}$$ (Q)

$$-\frac{1}{2}\sum_{a}\sum_{b}\sum_{c}\sum_{p}\sum_{q}\frac{\langle ic\|\|jp\rangle\langle pq\|\|ab\rangle\langle ab\|\|cq\rangle}{(\epsilon_a+\epsilon_b-\epsilon_p-\epsilon_q)(\epsilon_c-\epsilon_p)}\,.$$ (R)

APPENDIX 2

$$(\underline{a}|H^3\underline{a})_{ij} = \varepsilon_i^3\delta_{ij}$$

$$+ \sum_{r,s,s'} (\varepsilon_i + \varepsilon_j + \varepsilon_s + \varepsilon_{s'} - \varepsilon_r)\langle ir||ss'\rangle\langle ss'||jr\rangle$$

$$\times [\tfrac{1}{2}\langle n_r\rangle + \tfrac{1}{2}\langle n_s\rangle\langle n_{s'}\rangle - \langle n_r\rangle\langle n_s\rangle]$$

$$+ \sum_{r,s,s',l,l'} \langle ir||ss'\rangle\langle ss'||ll'\rangle\langle ll'||jr\rangle$$

$$\times [\tfrac{1}{4}\langle n_r\rangle - \tfrac{1}{2}\langle n_r\rangle\langle n_l\rangle + \tfrac{1}{2}\langle n_l\rangle\langle n_{l'}\rangle - \tfrac{1}{2}\langle n_r\rangle\langle n_s\rangle$$

$$+ \langle n_r\rangle\langle n_s\rangle\langle n_{l'}\rangle - \langle n_l\rangle\langle n_{l'}\rangle\langle n_s\rangle - \tfrac{1}{4}\langle n_s\rangle\langle n_{s'}\rangle$$

$$+ \tfrac{1}{2}\langle n_s\rangle\langle n_{s'}\rangle\langle n_l\rangle]$$

$$+ \sum_{r,s,s',l,l'} \langle ir||ss'\rangle\langle s'l||rl'\rangle\langle l's||jl\rangle$$

$$\times [2\langle n_l\rangle\langle n_{s'}\rangle + \langle n_r\rangle\langle n_l\rangle\langle n_s\rangle - \langle n_r\rangle\langle n_l\rangle - \langle n_r\rangle\langle n_{l'}\rangle$$

$$+ \langle n_r\rangle\langle n_{l'}\rangle\langle n_{s'}\rangle + 2\langle n_r\rangle\langle n_l\rangle\langle n_{l'}\rangle - \langle n_l\rangle\langle n_{s'}\rangle\langle n_r\rangle$$

$$- \langle n_{l'}\rangle\langle n_s\rangle\langle n_r\rangle - 2\langle n_l\rangle\langle n_{s'}\rangle\langle n_{l'}\rangle - \langle n_l\rangle\langle n_{s'}\rangle\langle n_s\rangle$$

$$+ \langle n_s\rangle\langle n_{l'}\rangle\langle n_{s'}\rangle]$$

$$+ \sum_{r,s,s',l,l'} \langle ir||js\rangle\langle ss'||ll'\rangle\langle ll'||rs'\rangle$$

$$\times [\tfrac{1}{2}\langle n_r\rangle\langle n_{s'}\rangle - \langle n_l\rangle\langle n_{l'}\rangle - \langle n_r\rangle\langle n_{s'}\rangle\langle n_{l'}\rangle$$

$$+ \tfrac{1}{2}\langle n_l\rangle\langle n_{l'}\rangle\langle n_r\rangle + \langle n_l\rangle\langle n_{l'}\rangle\langle n_{s'}\rangle + \tfrac{1}{2}\langle n_s\rangle\langle n_{s'}\rangle$$

$$+ \tfrac{1}{2}\langle n_l\rangle\langle n_{l'}\rangle\langle n_s\rangle - \langle n_s\rangle\langle n_{s'}\rangle\langle n_l\rangle]$$

APPENDIX 3

$$(\underline{a}|\hat{\hat{V}}\hat{\hat{T}}_0(E)\hat{\hat{V}}\hat{\hat{T}}_0(E)\hat{\underline{V}}\underline{a})_{ij}$$

$$= \sum_{r,s,s',l,l'} \frac{\langle ir||ss'\rangle\langle ss'||ll'\rangle\langle ll'||jr\rangle}{(E+\varepsilon_r-\varepsilon_s-\varepsilon_{s'})(E+\varepsilon_r-\varepsilon_l-\varepsilon_{l'})} [\tfrac{1}{4}\langle n_r\rangle - \tfrac{1}{2}\langle n_r\rangle\langle n_l\rangle$$

$$+ \tfrac{1}{4}\langle n_l\rangle\langle n_{l'},\rangle - \tfrac{1}{2}\langle n_r\rangle\langle n_s\rangle + \langle n_r\rangle\langle n_s\rangle\langle n_{l'},\rangle - \tfrac{1}{2}\langle n_l\rangle\langle n_{l'},\rangle\langle n_s\rangle]$$

$$+ \sum_{r,s,s',l,l'} \frac{\langle ir||ss'\rangle\langle ss'||ll'\rangle\langle ll'||jr\rangle}{(E+\varepsilon_r-\varepsilon_s-\varepsilon_{s'})(E-\varepsilon_j+\varepsilon_l+\varepsilon_{l'}-\varepsilon_s-\varepsilon_{s'})} [\tfrac{1}{4}\langle n_l\rangle\langle n_{l'},\rangle$$

$$- \tfrac{1}{4}\langle n_s\rangle\langle n_{s'},\rangle - \tfrac{1}{2}\langle n_l\rangle\langle n_{l'},\rangle\langle n_{s'},\rangle + \tfrac{1}{2}\langle n_s\rangle\langle n_{s'},\rangle\langle n_l\rangle]$$

$$+ \sum_{r,s,s',l,l'} \frac{\langle ir||js\rangle\langle ss'||ll'\rangle\langle ll'||rs'\rangle}{(E-\varepsilon_j+\varepsilon_r-\varepsilon_s)(E-\varepsilon_j+\varepsilon_r+\varepsilon_{s'}-\varepsilon_l-\varepsilon_{l'})} [\tfrac{1}{2}\langle n_r\rangle\langle n_{s'},\rangle$$

$$- \tfrac{1}{2}\langle n_l\rangle\langle n_{l'},\rangle - \langle n_r\rangle\langle n_{s'},\rangle\langle n_{l'},\rangle + \tfrac{1}{2}\langle n_l\rangle\langle n_{l'},\rangle\langle n_r\rangle$$

$$+ \tfrac{1}{2}\langle n_l\rangle\langle n_{l'},\rangle\langle n_{s'},\rangle]$$

$$+ \sum_{r,s,s',l,l'} \frac{\langle ir||js\rangle\langle ss'||ll'\rangle\langle ll'||rs'\rangle}{(E-\varepsilon_j+\varepsilon_r-\varepsilon_s)(E-\varepsilon_j+\varepsilon_l+\varepsilon_{l'}-\varepsilon_s-\varepsilon_{s'})} [\tfrac{1}{2}\langle n_s\rangle\langle n_{s'},\rangle$$

$$- \tfrac{1}{2}\langle n_l\rangle\langle n_{l'},\rangle + \tfrac{1}{2}\langle n_l\rangle\langle n_{l'},\rangle\langle n_{s'},\rangle + \tfrac{1}{2}\langle n_l\rangle\langle n_{l'},\rangle\langle n_s\rangle$$

$$- \langle n_s\rangle\langle n_{s'},\rangle\langle n_l\rangle]$$

$$+ \sum_{r,s,s',l,l'} \frac{\langle ir||ss'\rangle\langle s'l||rl'\rangle\langle l's||jl\rangle}{(E+\varepsilon_r-\varepsilon_s-\varepsilon_{s'})(E+\varepsilon_l-\varepsilon_s-\varepsilon_{l'})} [\langle n_l\rangle\langle n_{s'},\rangle - \langle n_r\rangle\langle n_l\rangle$$

$$+ \langle n_r\rangle\langle n_l\rangle\langle n_s\rangle + \langle n_r\rangle\langle n_l\rangle\langle n_{l'},\rangle - \langle n_{l'},\rangle\langle n_s\rangle\langle n_r\rangle$$

$$- \langle n_l\rangle\langle n_{s'},\rangle\langle n_{l'},\rangle - \langle n_l\rangle\langle n_{s'},\rangle\langle n_s\rangle + \langle n_s\rangle\langle n_{l'},\rangle\langle n_{s'},\rangle]$$

$$+ \sum_{r,s,s',l,l'} \frac{\langle ir||ss'\rangle\langle s'l||rl'\rangle\langle l's||jl\rangle}{(E+\varepsilon_r-\varepsilon_s-\varepsilon_{s'})(E-\varepsilon_j+\varepsilon_r+\varepsilon_{l'}-\varepsilon_{s'}-\varepsilon_l)} [\langle n_l\rangle\langle n_{s'}\rangle$$

$$- \langle n_r\rangle\langle n_{l'}\rangle + \langle n_r\rangle\langle n_{l'}\rangle\langle n_{s'}\rangle + \langle n_r\rangle\langle n_{l'}\rangle\langle n_l\rangle - \langle n_l\rangle\langle n_{s'}\rangle\langle n_r\rangle$$

$$- \langle n_l\rangle\langle n_{s'}\rangle\langle n_{l'}\rangle]$$

BIBLIOGRAPHY

Abdulnur, S. F., Linderberg, J., Öhrn, Y., and Thulstrup, P. W. (1972) Phys. Rev. 6, A889.

Abrikosov, A., Gorkov, L., and Dzyaloshinskii, J. (1965) Quantum Field Theoretical Methods in Statistical Physics, Pergamon Press, Oxford.

Allison, D. A. and Cavell, R. G. (1978) J. Chem. Phys. 68, 593.

Almlöf, J. (1974) Univ. of Stockholm Institute of Physics Report 74-29.

Babu, S. V. and Ratner, M. A. (1972) J. Chem. Phys. 57, 3156.

Bagus, P. S. (1965) Phys. Rev. 139, 619.

Bagus, P. S. and Viinikka, E.-K. (1977) Phys. Rev. A 15, 1486.

Baker, G. A. (1970) in The Pade' Approximant in Theoretical Physics, p. 1, G. A. Baker and J. L. Gammel, Eds., Academic Press, New York.

Baker, G. A. (1975) Essentials of Pade' Approximants, Academic Press, New York.

Banwell, C. N. and Primas, H. (1963) Mol. Phys. 6, 225.

Bartlett, R. J. and Silver, D. M. (1975a) J. Chem. Phys 62, 3258.

Bartlett, R. J. and Silver, D. M. (1975b) Intern. J. Quantum Chem. S9, 183.

Bazley, N. W. (1960) Phys. Rev. 120, 144.

Benedict, W. S., Gailar, N., and Plyler, E. K. (1956) J. Chem. Phys. 24, 1139.

Bethe, H. A. and Salpeter, E. E. (1957) Quantum Mechanics of One- and Two-Electron Atoms, Academic Press, New York.

Born, G. and Öhrn, Y. (1978) Intern. J. Quantum Chem. S12, 143.

Born, G. and Öhrn, Y. (1979) Chem. Phys. Lett. 61, 307

Born, G., Kurtz, H. A., and Öhrn, Y. (1978) J. Chem. Phys. 68, 74.

Brandow, B. H. (1967) Rev. Mod. Phys. 39, 771.

Buenker, R. J., Peyerimhoff, S. D., and Whitten, J. L. (1967) J. Chem. Phys. 46, 2029.

Cade, P. E., Sales, K. D., and Wahl, A. C. (1966) J. Chem. Phys. 44, 1973.

Cavell, R. G. and Allison, D. A. (1978) J. Chem. Phys. 69, 159.

Cederbaum, L. S. (1973a) Theor. Chim. Acta 31, 239.

Cederbaum, L. S. (1973b) Mol. Phys. 26, 1405.

Cederbaum, L. S. (1974) Mol. Phys. 28, 479.

Cederbaum, L. S. (1975) J. Phys. B: Atom. Molec. Phys. 8, 290.

Cederbaum, L. S. (1977) J. Phys. B: Atom. Molec. Phys. 10, L549.

Cederbaum, L. S. and Domcke, W. (1977) in Advances in Chemical Physics, Vol. 36, p. 205, I. Prigogine and S. A. Rice, Eds., John Wiley, New York.

Cederbaum, L. S., Domcke, W., Schirmer, J., von Niessen, W., Diercksen, G. H. F., and Kraemer, W. P. (1978) J. Chem. Phys. 69, 1591.

Cederbaum, L. S., Domcke, W., and von Niessen, W. (1975) Chem. Phys. Lett. 34, 60.

Cederbaum, L. S., Schirmer, J., Domcke, W., von Niessen, W. (1977) J. Phys. B: Atom. Molec. Phys. 10, L549.

Claverie, P., Diner, S., and Malrieu, J. P. (1967) Intern. J. Quantum Chem. 1, 751.

Codling, K. (1973) Rep. Prog. Phys. 36, 541.

Codling, K. (1976) in Photoionization and Other Probes of Many-Electron Interactions, p. 111, F. J. Wuilleumier, Ed., Plenum Press, New York.

Cooper, J. W. (1962) Phys. Rev. 128, 681.

Csanak, Gy., Taylor, H. S., and Yaris, R. (1971) in Advances in Atomic and Molecular Physics, Vol. 7, p. 287, D. R. Bates and I. Esterman, Eds., Academic Press, New York.

Dalgaard, E. and Simons, J. (1977) J. Phys. B: Atom. Molec. Phys. 10, 2767.

Dewar, M. J. S., Komornicki, A., Thiel, W., and Schweig, A. (1975) Chem. Phys. Lett. 31, 286.

Dunning, T. H. (1970) J. Chem. Phys. 53, 2823.

Dunning, T. H. and Hay, P. J. (1977) in Methods of Electronic Structure Theory, p. 1, H. F. Schaefer III, Ed., Plenum Press, New York.

Dyson, F. J. (1949) Phys. Rev. 75, 1736.

Epstein, S. T. (1926) Phys. Rev. 28, 695.

Fetter, A. L. and Walecka, J. D. (1971) Quantum Theory of Many-Particle Systems, McGraw-Hill, New York.

Galitskii, V. (1958) Soviet Phys. - JETP 7, 104.

Gell-Mann, M. and Low, F. (1951) Phys. Rev. 84, 350.

Goldstone, J. (1957) Proc. Phys. Soc. (London) A239, 267.

Goscinski, O. and Brändas, E. (1971) Intern. J. Quantum Chem. 5, 131.

Goscinski, O. and Lukman, B. (1970) Chem. Phys. Lett. 7, 573.

Goscinski, O., Hehenberger, M., Roos, B., and Siegbahn, P. (1975) Chem. Phys. Lett. 33, 427.

Hamburger, H. (1920) Math. Ann. 81, 235.

Hamburger, H. (1921a) Math. Ann. 82, 120.

Hamburger, H. (1921b) Math. Ann. 82, 168.

Harris, F. (1973) Computation Methods of Quantum Chemistry (unpublished).

Hedin, L. and Lundqvist, S. (1969) in Solid State Physics, Advances in Research and Applications, Vol. 23, p. 1, F. Seitz, D. Turnbull, and H. Ehrenreich, Eds., Academic Press, New York.

Herman, M. F., Freed, K. F., Yeager, D. L., and Liu, B. (1978) Eleventh Midwest Theoretical Chemistry Conference, Battelle's Columbus Laboratories.

Herzberg, G. (1955) Diatomic Molecules, 2nd Ed. Van Nostrand, Princeton, New Jersey.

Hood, S. T., Hamnett, A., and Brion, C. E. (1976) Chem. Phys. Lett. 41, 428.

Hugenholtz, N. M. (1957) Physica 23, 481.

Huzinaga, S. (1965) J. Chem. Phys. 42, 1293.

Jolly, W. L. and Schaaf, T. F. (1976) J. Am. Chem. Soc. 98, 3178.

Jørgensen, P. and Simons, J. (1975) J. Chem. Phys. 63, 5302.

Kaijser, P. and Smith, Jr., V. H. (1977) in Advances in Quantum Chemistry, Vol. 10, p. 37, P.-O. Löwdin, Ed., Academic Press, New York.

Kaplan, I. G. and Markin, A. P. (1968) Opt. Spectrosc. 24, 475.

Katrib, A., Debies, T. P., Colton, R. J., Lee, T. H., and Rabalais, J. W. (1973) Chem. Phys. Lett. 22, 196.

Kelly, H. P. (1976) in Photoionization and Other Probes of Many-Electron Interactions, p. 83, F. J. Wuilleumier, Ed., Plenum Press, New York.

Koopmans, T. A. (1933) Physica 1, 104.

Kumar, K. (1962) Perturbation Theory and the Nuclear Many Body Problem, North-Holland, Amsterdam.

Kurtz, H. A. and Öhrn, Y. (1978) J. Chem. Phys. 69, 1162.

Layzer, A. J. (1963) Phys. Rev. 129, 897.

Linderberg, J. and Öhrn, Y. (1967) Chem. Phys. Lett. 1, 295.

Linderberg, J. and Öhrn, Y. (1973) Propagators in Quantum Chemistry, Academic Press, London.

Lohr, Jr., L. L. (1972) in Electron Spectroscopy, p. 245, D. A. Shirley, Ed., North-Holland, Amsterdam.

Löwdin, P.-O. (1962) J. Math. Phys. 3, 969.

Löwdin, P.-O. (1965) Phys. Rev. 139, A357.

Löwdin, P.-O. (1967) in Advances in Quantum Chemistry, Vol. 3, p.324, P.-O. Löwdin, Ed., Academic Press, New York.

Manne, R. (1977) Chem. Phys. Lett. 45, 470.

Marr, G. V. (1967) Photoionization Processes in Gases, Academic Press, London.

Masson, D. (1970) in The Pade' Approximant in Theoretical Physics, p. 197, G. A. Baker and J. L. Gammel, Eds., Academic Press, New York.

Mattuck, R. D. (1967) A Guide to Feynman Diagrams in the Many-Body Problem, McGraw-Hill, New York.

Mittag-Leffler, M. G. (1880) Acta Soc. Scient. Fennicae 10, 273.

Møller, C. and Plesset, M. S. (1934) Phys. Rev. 46, 618.

Morse, P. M. and Feshbach, H. (1953) Methods of Theoretical Physics, McGraw-Hill, New York.

Nehrkorn, C., Purvis, G. D. and Öhrn, Y. (1976) J. Chem. Phys. 64, 1752.

Nesbet, R. K. (1955a) Proc. Roy. Soc. A 230, 312.

Nesbet, R. K. (1955b) Proc. Roy. Soc. A 230, 322.

Nuttall, J. (1967) Phys. Rev. 157, 1312.

Nuttall, J. (1970) in The Pade' Approximant in Theoretical Physics, p. 219, G. A. Baker and J. L. Gammel, Eds., Academic Press, New York.

Nuttall, J. (1973) in Pade' Approximants and Their Applications, p. 29, P. R. Graves-Marris, Ed., Academic Press, New York.

Oddershede, J. and Jørgensen, P. (1977) J. Chem. Phys. 66, 1541.

Oka, T. (1960) J. Phys. Soc. Japan 15, 2274.

Ortiz, J. V. and Öhrn, Y. (1979) unpublished results.

Pade', H. (1892) Ann. Ecole. Nor. 9, 1.

Pickup, B. T. and Goscinski, O. (1973) Mol. Phys. 26, 1013.

Pilar, F. L. (1968) Elementary Quantum Chemistry, McGraw-Hill, New York.

Pines, D. (1961) The Many Body Problem, Benjamin, New York.

Purvis, G. D. (1973) Ph.D. Dissertation, Univ. of Florida.

Purvis, G. D. and Öhrn, Y. (1974) J. Chem. Phys. 60, 4063.

Purvis, G. D. and Öhrn, Y. (1975a) J. Chem. Phys. 62, 2045.

Purvis, G. D. and Öhrn, Y. (1975b) Chem. Phys. Lett. 33, 396.

Rabalais, J. W., Debies, T. P., Berkosky, J. L., Huang, J.-T. J., and Ellison, F. O. (1974) J. Chem. Phys. 61, 516.

Rabalais, J. W., Debies, T. P., Berkosky, J. L., Huang, J.-T. J., and Ellison, F. O. (1975) J. Chem. Phys. 62, 4587.

Redmon, L. T. (1975) Ph.D. Dissertation, Univ. of Florida.

Redmon, L. T. (1977) private communication.

Redmon, L. T., Purvis, G., and Öhrn, Y. (1975) J. Chem. Phys. 63, 5011.

Riesz, F. and Sz.-Nagy, B. (1955) Functional Analysis, Ungar, New York.

Roetti, C. and Clementi, E. (1974) Atomic Data and Nuclear Data Tables, 14, 177.

Rowe, D. J. (1968) Rev. Mod. Phys. 40, 153.

Schirmer, J. and Cederbaum, L. S. (1978) J. Phys. B: Atom. Molec. Phys. 11, 1889.

Schirmer, J., Cederbaum, L. S., Domcke, W., and von Niessen, W. (1977) Chem. Phys. 26, 149.

Schirmer, J., Domcke, W., Cederbaum, L. S., and von Niessen, W. (1978) J. Phys. B: Atom. Molec. Phys. 11, 1901.

Schuck, P., Villars, F., and Ring, P. (1973) Nucl. Phys. A208, 302.

Schweig, A. and Thiel, W. (1974) J. Chem. Phys. 60, 951.

Shavitt, I. (1977) in Methods of Electronic Structure Theory, p. 189, H. F. Schaefer III, Ed., Plenum Press, New York.

Shohat, J. A. and Tamarkin, J. D. (1963) The Problem of Moments, American Mathematical Society, Providence, Rhode Island.

Siegbahn, K., Nordling, C., Johansson, G., Hedman, J., Hedén, P. F., Hamrin, K., Gelius, U., Bergmark, T., Werme, L. O., Manne, R., and Baer, Y. (1969) ESCA Applied to Free Molecules, North-Holland, Amsterdam.

Simons, J. (1976) J. Chem. Phys. 64, 4541.

Simons, J. and Smith, W. D. (1973) J. Chem. Phys. 58, 4899.

Smith, K. (1971) The Calculation of Atomic Collision Processes, Wiley-Interscience, New York.

Steinfeld, J. I. (1974) Molecules and Radiation: An Introduction to Modern Molecular Spectroscopy, Harper and Row, New York.

Stewart, A. L. (1967) in Adv. At. Mol. Phys., Vol. 3, p. 1, D. R. Bates and I. Estermann, Eds., Academic Press, New York.

Stieltjes, T. J. (1894) Ann. Fac. Sci. Toulouse 8, J, 1.

Takagi, K. and Oka, T. (1963) J. Phys. Soc. Japan 18, 1174.

Tchebychev, P. (1874) J. Math. Phys. Appl. 19, 157.

Tuckwell, H. C. (1970) J. Phys. B: Atom. Molec. Phys. 3, 293.

Turner, D. W., Baker, C., Baker, A. D., and Brundle, C. R. (1970) Molecular Photoelectron Spectroscopy, Wiley, New York.

Vorobyev, Yu. V. (1965) Method of Moments in Applied Mathematics, Gordon and Breach, New York.

Wall, H. S. (1948) Analytic Theory of Continued Fractions, Chelsea Publishing Co., Bronx, N.Y.

Wendin, G. (1979) preprint of article to be published in Structure and Bonding, Springer Verlag, Berlin.

Wick, G. C. (1950) Phys. Rev. 80, 268.

Yoshimine, M. (1973) J. Comp. Phys. 11, 449.

Zwanzig, R. (1961) in Lectures in Theoretical Physics, W. E. Brittain, B. W. Downs, and J. Downs, Eds., Vol. 3, p. 106, Interscience, New York.

BIOGRAPHICAL SKETCH

Gregory J. Born was born on July 1, 1951, in Joliet, Illinois. He was raised in Coal City, Illinois, where he attended public schools until his graduation from Coal City High School in May 1969. From September 1969 through June 1973, he attended Southern Illinois University at Carbondale as an Illinois State Scholar and majored in chemistry with math and physics minors. Throughout his senior year, he participated in an undergraduate research program working under the supervision of the late Professor Boris Muslin. After completing his Bachelor of Science degree, Mr. Born enrolled in graduate school at the University of Florida. From September 1973 to June 1976, he was a teaching assistant in the Department of Chemistry. In February 1974, he joined the Quantum Theory Project and has been a research assistant working under the supervision of Professor Yngve Öhrn from June 1976 to the present. During the summer of 1976, Mr. Born attended the Summer School in Quantum Theory held in Uppsala, Sweden, and Dalseter, Norway. He is the co-author of four research publications and has presented several contributed talks at various conferences.

I certify that I have read this study and that in my opinion it conforms to acceptable standards of scholarly presentation and is fully adequate, in scope and quality, as a dissertation for the degree of Doctor of Philosophy.

N. Yngve Öhrn, Chairman
Professor of Chemistry and Physics

I certify that I have read this study and that in my opinion it conforms to acceptable standards of scholarly presentation and is fully adequate, in scope and quality, as a dissertation for the degree of Doctor of Philosophy.

Arthur A. Broyles
Professor of Physics

I certify that I have read this study and that in my opinion it conforms to acceptable standards of scholarly presentation and is fully adequate, in scope and quality, as a dissertation for the degree of Doctor of Philosophy.

David A. Micha
Professor of Chemistry and Physics

I certify that I have read this study and that in my opinion it conforms to acceptable standards of scholarly presentation and is fully adequate, in scope and quality, as a dissertation for the degree of Doctor of Philosophy.

Willis B. Person
Professor of Chemistry

I certify that I have read this study and that in my opinion it conforms to acceptable standards of scholarly presentation and is fully adequate, in scope and quality, as a dissertation for the degree of Doctor of Philosophy.

John R. Sabin
Professor of Physics and Chemistry

This dissertation was submitted to the Graduate Faculty of the Department of Chemistry in the College of Liberal Arts and Sciences and to the Graduate Council, and was accepted as partial fulfillment of the requirements for the degree of Doctor of Philosophy.

June 1979

_____

Dean, Graduate School